EXAMINATION OF THE REGULATION OF BIOFILM-SPECIFIC ANTIBIOTIC RESISTANCE GENES IN *PSEUDOMONAS AERUGINOSA*

By

Jean-Paul Nadeau

A thesis submitted to The Faculty of Graduate and Postdoctoral Studies in partial fulfillment of the requirements for the M.Sc. degree in Microbiology and Immunology

Department of Biochemistry, Microbiology and Immunology

Faculty of Medicine

University of Ottawa

ABSTRACT

Upon contact with a surface, the bacterium *Pseudomonas aeruginosa* forms a bacterial community encased in an exopolysaccaride matrix. One difference between this structure, known as a biofilm, and free-swimming cells is its ability to be 10 to 1,000 times more resistant to antibiotics. This increased resistance is partially due to the presence of six biofilm-specific antibiotic resistance genes. Three of these genes, *ndvB,* PA1874-77 and *tssC1* have been characterized in terms of their role in antibiotic resistance, while the other three have not been fully characterized. However, all six genes are more highly expressed in biofilm cells as compared to planktonic cells and contribute to a biofilm-specific antibiotic resistance phenotype. Previous *in silico* analysis found a 22 base pair consensus sequence upstream in the promoters of all six biofilm-specific antibiotic resistance genes. It is hypothesized that this motif controls the biofilm-specific expression of these genes.

Results from a DNA-affinity chromatography experiment suggest that several proteins from a biofilm extract bound the 22bp motif of *ndvB* and PA1874-77. However, one major band was consistently binding the 22bp motif. It is predicted that the regulatory protein that binds to the 22bp motif will play a prominent role in conferring a biofilm-specific antibiotic resistance phenotype. This protein was identified as a putative transcriptional regulator. Further experimentation using this protein in the binding reaction found that this interaction may not be specific to the 22bp motif and further investigation is warranted. A second separate but related research goal was to analyze temporal expression of *ndvB* using promoter-fluorescent protein constructs. The reason for this study was to examine the effects of heterogeneity within

biofilms on expression of biofilm-specific antibiotic resistance genes. Using fluorescence microscopy it was found that planktonically, *ndvB* begins to be expressed at an OD_{600} of 2.0, an OD_{600} that corresponds to early stationary phase. In biofilms *ndvB* expression begins following monolayer formation. These initial discoveries have highlighted the usefulness of this experimental system and laid the groundwork for a more comprehensive study of spatial and temporal expression of all six biofilm-specific antibiotic resistance genes in *Pseudomonas aeruginosa.*

ACKNOWLEDGEMENTS

The work presented in this thesis could not have been completed without the help of numerous individuals. I would like to thank:

- Dr. Thien-Fah Mah, for being an outstanding supervisor.
- My TAC members, Dr. Laura Trinkle-Mulcahy and Dr. Sandra Ramirez for their guidance and critical analysis of my work.
- Li Zhang, for all of her help with the technical aspects of experiments that were completed in the lab.
- Sylvain Lanouette (and the Couture Lab), for their help with anything and everything related to the creation of recombinant proteins.
- Dr. Aaron Hinz, for his support during my first year in the lab.
- Delphine Chamousset, for her help with the western blot.
- Dr. Valerie Greco-Stewart, for her help with cloning using the pET30a vector.
- Dr. Nicole Forbes, for being there to discuss all aspects of my degree.
- My friends at BMIGSA, for their support.
- Fay Draper, for her help with the administrative side of my degree and with my professional development.

Last but not least, I would like to thank my immediate family for their support during the entirety of my work. Thank you.

LIST OF ABBREVIATIONS

ACB	affinity chromatography buffer
ALI	air-liquid interface
bp	base pair
BSA	bovine serum albumin
CF	cystic fibrosis
CFU	colony forming unit
ddH_20	double distilled water
dNTPs	deoxyribonucleic acids
eDNA	extracellular deoxyribonucleic acid
EMSA	electrophoretic mobility shift assay
EPS	exopolysaccharide
GFP	green fluorescent protein
HEPES	4-(2-hydroxyethyl)-1-piperazineethanesulfonic acid
HIS	histidine
IPTG	isopropyl β-d-1-thiogalactopyranoside
LB	luria bertani
M63	m63 salts
MBC	minimal bacteriodical concentration
MCS	multiple cloning site
MEME	multiple E_m for motif elicitation
OD_{600}	optical density at absorbance of 600nm
oligo	oligonucleotide
PA	*Pseudomonas aeruginosa*
PBS	phosphate buffered saline
PCR	polymerase chain reaction
PMSF	phenylmethanesulfonylfluoride
qPCR	quantitative real-time polymerase chain reaction
SDS	sodium dodecyl sulfate
T3SS	type III secretion system
T6SS	type VI secretion system
TSS	transcription start site
wt	wild type

TABLE OF CONTENTS

LIST OF TABLES

LIST OF FIGURES

CHAPTER 1. INTRODUCTION

1.1 Biofilms

1.1.1 General

Upon contact with a surface, individual bacterial cells known as planktonic cells can form a community called a biofilm. Biofilms are ubiquitous across prokaryotes including both bacterial and archaeal lineages (22, 43). Observances of biofilms in the environment via fossil records date back as far as 3.5 billion years (114). Although biofilms have been around for a very long time, only in the past century have we begun to acknowledge their increasing importance in the modern world.

In the natural environment, cell growth within biofilms provides protection from sudden changes in environmental conditions such as pH, temperature, nutrient and waste levels which may threaten the cells (9). Biofilm cells are characterized by a unique phenotypic profile that confers this enhanced protection. In the bacterium *Pseudomonas aeruginosa* for example, this unique phenotypic profile includes upregulation of alginate and other EPS synthesis genes, antibiotic resistance genes as well as quorum sensing genes (76). The study of biofilms including the biofilm development cycle as well as antibiotic resistance in biofilms is most commonly studied in *P. aeruginosa*. The study of biofilms is important as they are the major cause of persistent bacterial infections across the prokaryotic world (24, 117). Some prominent biofilm-based infections are found in the lungs of CF patients, in the middle ear and on medical implants (21, 24).

1.1.2 Biofilm matrix

The exopolysaccharide (EPS) matrix accounts for approximately 90% of the biomass in biofilms and plays a very significant role in the overall biofilm phenotype (20, 35). It contains a unique, diverse set of high molecular weight polysaccharides as well as smaller quantities of proteins, lipids, and DNA that create a very viscous environment that surrounds cells that are part of the biofilm. The EPS matrix reduces flowing velocities through and around the biofilm leading to protection from liquid shearing forces as well as preventing penetration of antibiotics (14, 24). The exact composition of the biofilm matrix depends on both overall gene expression of the bacterial cells in the biofilm as well as the collection of environmental signals present. Although traditional research has been focused on polysaccharides and proteins, recent studies have determined that other components of the matrix, notably extracellular DNA and cell debris may play an important role in biofilm physiology (113, 115).

In *P. aeruginosa* biofilms, alginate is the predominant EPS, and strains that overproduce alginate are called mucoid strains (46). Alginate is composed of β-1,4 linked chains of L-guluronic and D-mannuronic acid monomers (34). The overproduction of alginate is commonly found in clinical strains of *P. aeruginosa* and has been linked to increased virulence (49). The EPS matrix also contains polysaccharides encoded by the *psl* and *pel* loci. Although the structure of the *pel*-encoded polysaccharides remains undefined, they have been shown to be required for development of mature biofilm structure, and promote adherence and aggregation of individual bacterial cells (2, 36). The *pel*-encoded polysaccharides are expressed at higher levels in PA14 biofilms which results in stronger biofilms than PA01 (36). The *psl* locus codes for the production of a polysaccharide chain

consisting of D-mannose, D-glucose and L-rhamnose (16). These polysaccharides allow for initial attachment to surfaces, provide protection from the innate immune system and provide structural stability to the biofilm as a whole (16, 70).

Extracellular DNA (eDNA) has also been found to be part of the EPS matrix of many biofilms and has been reported to be involved in cell-to-cell communication in addition to playing a role in the structure and antibiotic resistance properties of the biofilm (2, 71, 115).

Dead bacterial cells found in the EPS matrix have also been shown to be important for biofilm physiology. A select group of *P. aeruginosa* genes derived from the Pf1 prophage present inside the *P. aeruginosa* genome have been shown to be linked to induction of cell death within microcolonies which allows for differentiation as well as dispersal of subpopulations of cells, a critical component of the biofilm development cycle (113).

1.1.3 Pseudomonas aeruginosa

P. aeruginosa is an aerobic, gram negative rod-shaped bacterium that is found commonly in soil and water throughout the environment (117). *P. aeruginosa* is part of the proteobacteria phylum, the largest and most diverse phylum which includes over 500 genera including *Escherichia coli* and *Neisseria gonorrhoeae* (17, 117). Although ubiquitous in the environment, *P. aeruginosa* poses a threat due to the presence of ideal environmental conditions for growth of *P. aerguinosa* biofilms inside the human host, especially in immunocompromised individuals (73). *P. aeruginosa* was chosen as a model organism for biofilm growth and development because of its relevance to human infections, but also because it was already a well studied planktonic model due to its basic nutritional and

environmental requirements (40, 117). As a result, a significant amount of the genome has been characterized and a genome database has been developed (118).

The standard laboratory strain that is used is *P. aeruginosa* PA01. However UCBPP-PA14 (PA14), a strain that is more relevant to study due to its increased virulence in a variety of model infection systems is currently used in our lab (45, 84). PA14 was isolated from a patient with severe burns and consequently the use of PA14 in the lab will hopefully yield results most relevant to the strains found during human infection (84). The increase in virulence is derived from the presence of virulence genes that are mostly present on the PAPI-1 pathogenicity island (45). This results in a slightly larger PA14 genome size (6.54 million base pairs versus 6.26 million base pairs) compared to PA01 (105). The common method of annotation of *P. aeruginosa* genes is by writing PA followed by the four digit gene number. It is important to note that this "PA number" is then used to describe orthologous genes present in other *P. aeruginosa* strains, even though they may have their own strain ID. The PA01 strain identification numbers will be used for the entirety of the thesis to describe the genes regardless of the strain in which they are from.

1.1.4 Biofilm development cycle

A model of biofilm development was first presented by O'Toole *et al* at the turn of the millennium (Figure 1) (76). It describes the changes that are observable through microscopy to *P. aeruginosa* cells as they attach to a surface and form a biofilm and focuses on the stages of biofilm development (76). Numerous genes have been identified that play a role in biofilm formation. These are designated *sad* (surface attachment deficient) genes.

Study of individual *sad* mutants led to the discovery that each one was responsible for some aspect of biofilm formation (76). The first step in the biofilm development cycle occurs when cells reversibly attach to a surface. This is known as initial attachment. The *sadB* gene was identified as important for the transition from reversible to irreversible attachment to the surface, the second stage in biofilm development (17, 68). A *sadB* deletion mutant will only reversibly attach to the surface which arrests the biofilm development cycle. The third stage of the biofilm development cycle is microcolony formation. This stage is characterized by the presence of larger aggregations of cells which can be seen under phase-contrast microscopy. The presence of macrocolonies (large, three-dimensional aggregations of bacteria), indicates that the biofilm has reached the fourth stage of development, macrocolony formation. The final stage of the biofilm development cycle (spread) has also been studied. Spreading is characterized by swarming dispersal and seeding of inner macrocolony cells, leaving behind a hollow inner core (68, 93).

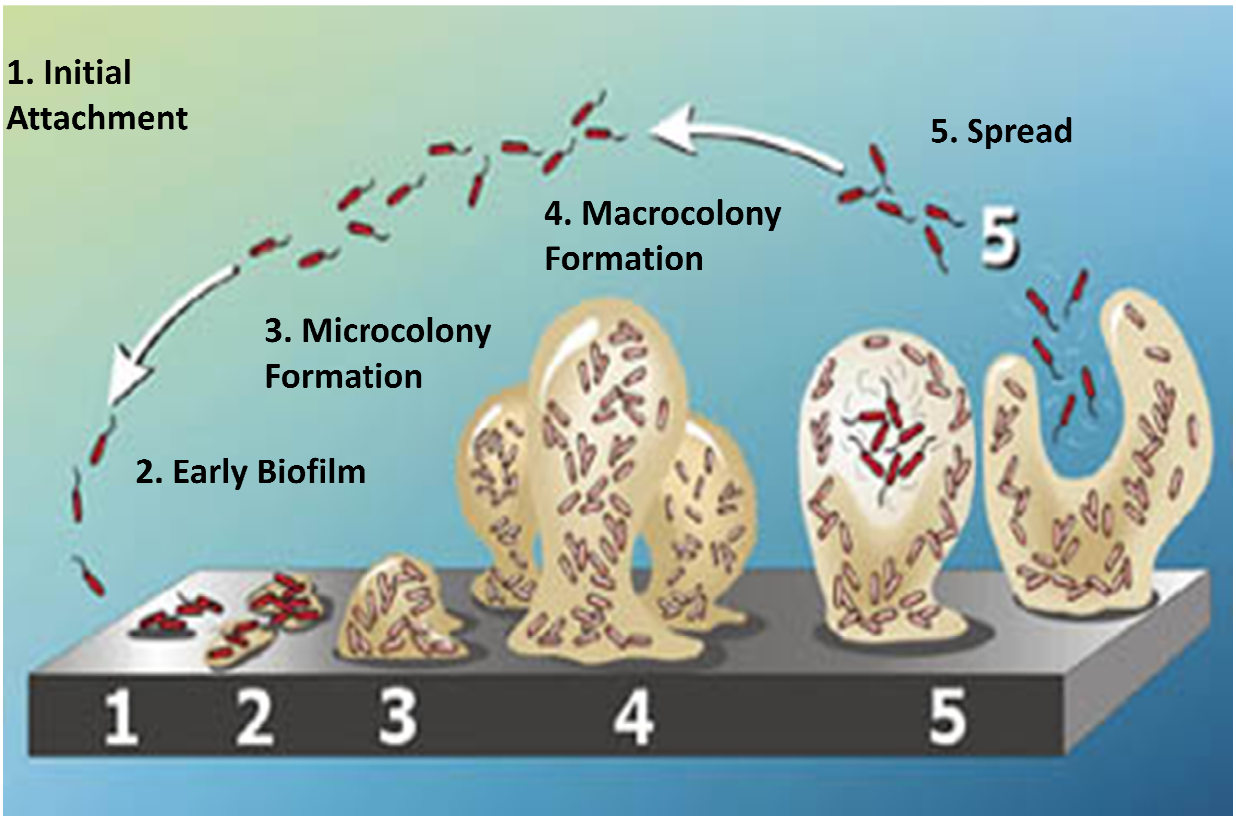

Figure 1: Biofilm Development Cycle. Stages of the biofilm development cycle as described by O'Toole *et al* (76). 1. Initial attachment. (2) Irreversible attachment. (3) Microcolony formation. (4). Macrocolony formation. (5) Spread

1.1.5 Biofilm heterogeneity

Regions within developed biofilms vary significantly in their gene expression profiles (77, 100). This is due to the heterogeneity in metabolic substrates, intermediaries and products found inside well developed biofilms (102). Typically, substrates are found at higher concentrations further away from the core of the biofilm, whereas products are found at higher concentrations near the core of the biofilm. This simple phenomenon is explained in an analysis of the reaction-diffusion model for diffusion in biofilms (103). Due to the accumulation of meatbolic products at the core of the biofilm, it has been well established that inner macrocolony cells exhibit very slow growth (58). Localized gene expression measurements found that expression of housekeeping genes (such as *acpP*) was more abundant in the upper layers of macrocolonies confirming the slow growth inside this area of the biofilm (62).

Microscale gradients in biofilms have been established for over ten important chemicals including carbon dioxide, chlorine, hydrogen peroxide as well as pH (25-28, 61, 86). The totality of these analyses confirmed the finding that substrates were found at higher concentrations at the edges of the biofilm, whereas the opposite trend was found for metabolic products. Approximately 60% of inner macrocolony cells grown under extremely low oxygen conditions (a metabolic substrate) and are at a stage of arrested growth because of these poor conditions and high levels of waste products. The opposite occurs at the edges of the biofilm which have been shown to be metabolically active (102). The key point is that bacterial cells respond to these local differences in chemical gradients which results in a unique transcriptome based on where the cells are located in the biofilm.

1.2 Antibiotic resistance

It is widely known that cells within biofilms are much less sensitive to antibiotics than individual planktonic cells (23, 73). One of the key aspects of biofilm-specific antibiotic resistance is that there are multiple mechanisms that contribute to the overall antibiotic resistance profile of a particular biofilm. The number and variety of species of bacteria present and thus the chemical signals produced, the environment in which the biofilm is found as well as the particular antibiotic that may be present all affect the phenotype of the biofilm. All of these factors must be taken into account when determining the collection of antibiotic resistance abilities of a particular biofilm as they influence the expression of genes that may confer antibiotic resistance (62). These mechanisms add an additional level of resistance to intrinsic resistance mechanisms that are well described in planktonic cells.

1.2.1 EPS matrix

One of the most widespread mechanisms of initial resistance in biofilms is the presence of the thick EPS matrix. This matrix acts as a protective barrier that can prevent the penetration of some antibiotics to the cell surface, and especially to deep within the biofilm (14, 27, 50). Recent findings have linked the structural role of certain components of the EPS to antibiotic resistance. In *P.aeruginosa*, the glucose polysaccharide encoded by *pel* has been shown to play a role in antibiotic resistance to aminoglycosides (20). eDNA has also been found to be a cation chelator and has shown to be involved in antibiotic resistance to some antibiotics (71).

1.2.2 Drug indifference

Due to the slow growth of cells within macrocolonies, a subset of cells present in biofilms become unresponsive to antibiotic treatment due to their reduced growth rates (59). These cells are termed drug indifferent cells. These dormant cells are naturally resistant due to the fact that antibiotics typically work through interference with bacterial growth strategies (protein translation, DNA replication etc). Thus, slow growing, nutrient deprived cells are less likely to be affected (4). Interestingly, Evans *et al* found that *P. aeruginosa* biofilms were more susceptible to a DNA replication inhibitor (ciprofloxacin) than planktonic cells, but that slow growth rate only accounted for some of the difference in susceptibility between these two phenotypes suggesting that more than one factor is responsible for this effect (33)**.** It is also known that the amount by which the intrinsic slow growth rate of cells within biofilm affects antibiotic resistance is dependent on the specific class of antibiotic used (15).

1.2.3 *rpo* general stress response

Although there is much variance when comparing individual microarray studies looking at global transcription in biofilm, there are still some genes that are identified as differentially expressed more consistently than others. One of those genes is *rpoS. rpoS* codes for the sigma subunit of RNA polymerase, and has been shown to increase expression of many biofilm development genes resulting in more robust biofilms (41). *rpoS* deleted strains of bacteria are much less virulent than their wild type counterparts (108). Although the mechanism of resistance due to increased *rpoS* expression remains unclear, *rpoS* may

play a role in increasing antibiotic resistance in biofilms due to its wide variety of downstream targets (41).

1.2.4 Persister cells

In addition to the mechanisms described above, the concept of persistence may also describe the antibiotic tolerance of a cell in both planktonic and biofilm cells. It is well established in the bacteriology community that although treating a logarithmic phase culture with antibiotics will significantly reduce the numbers of bacteria, it does not eliminate every cell (39). The reason for this is due to the presence of persisters, which are a subset of cells that at any given moment are not actively growing (53). There is still debate about the origin of persister cells. One popular hypothesis claims that cells in the process of repairing damaged DNA are not actively dividing and that they may be tolerant at that moment in their life cycle (42). The mechanism of resistance of persister cells differs from that of drug indifferent cells in the mechanism that is driving this tolerance. Persister cells are present in very small numbers in both starved as well as well nourished planktonic and biofilms cultures. Indifferent cells arise due to severe nutrient limitations present within macrocolonies and thus can comprise a majority of cells within this region of the biofilm (59).

1.3 Biofilm-specific antibiotic resistance

Although the mechanisms above contribute towards antibiotic resistance in biofilms the totality of the mechanisms described above account for only a part of the antibiotic resistance ability of biofilms (65). There is also evidence that specific genetic loci may confer biofilm-specific antibiotic resistance mechanisms. In order to identify specific genes that are

important for biofilm-specific antibiotic resistance, Mah *et al* took a genetic approach by assaying approximately 4,000 random *P. aeruginosa* PA14 transposon insertion mutants for decreased biofilm specific antibiotic resistance (64). These mutants could still produce biofilms and had equivalent levels of planktonic resistance; however they were more sensitive to antibiotics when growing in a biofilm. In total there were six mutants that were identified in the screen. Determination of the genes that showed the desired phenotype has laid the ground work for a series of experiments characterizing the genes that were affected. qPCR results has found that all six genes identified in the screen are more highly expressed in biofilms as compared to logarithmic-phase planktonic cells and confer a variety of independent mechanisms of resistance (64, 126, 127)

Mah *et al* showed that the transposon in one of the mutants disrupted *ndvB,* a gene that encodes a glucosyltransferase that is responsible for the production of cyclic glucans. The glucans have been shown to bind and sequester antibiotics in the periplasm (64) (Figure 2). More specifically, it was found that the glucans bound tobramycin. This observation was confirmed by Sadovskaya et al who elucidated the NMR structure of the *ndvB*-encoded glucans as well as characterized the interaction between the glucans and a similar aminoglycoside antibitiotic, kanamycin (91). *ndvB* has also been shown to be involved in the expression of ethanol oxidation genes. Further study revealed that these genes are linked to biofilm-specific antibiotic resistance (10). The *ndvB* transposon-insertion mutant had a similar biofilm thickness, surface area as well as overall biomass as compared to wild type which confirms that the transposon did not disrupt the structure of the biofilm. Additionally, *ndvB is* expressed at higher levels in biofilm as compared to logarithmic phase planktonic

cells further confirming its role as biofilm-specific (Figure 3). What remains to be known is how *ndvB* is regulated as well as how its expression is affected by heterogeneity in biofilms, two questions that will be addressed at length in this thesis.

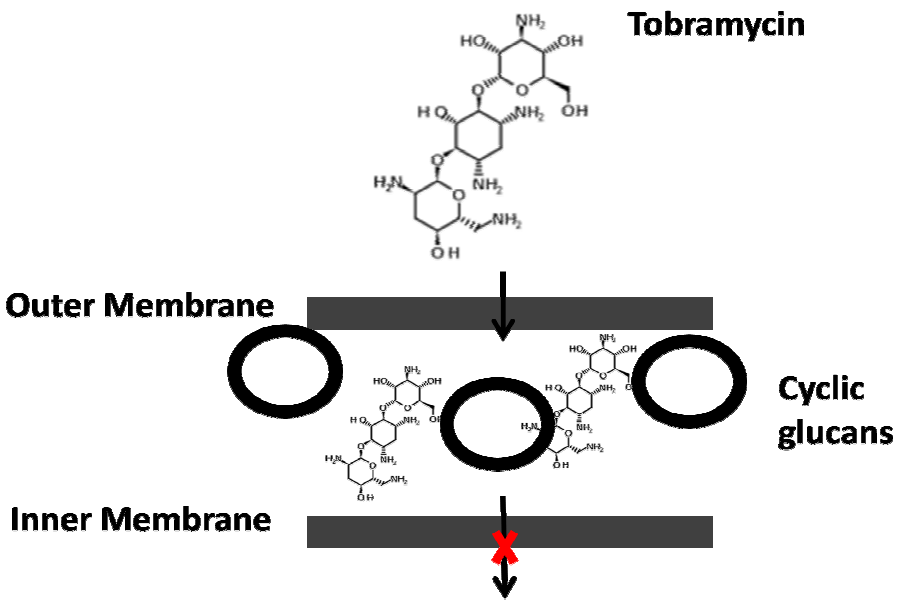

Figure 2: A model of the proposed mechanism of *ndvB*; sequestering of antibiotics in the periplasm by cyclic glucans.

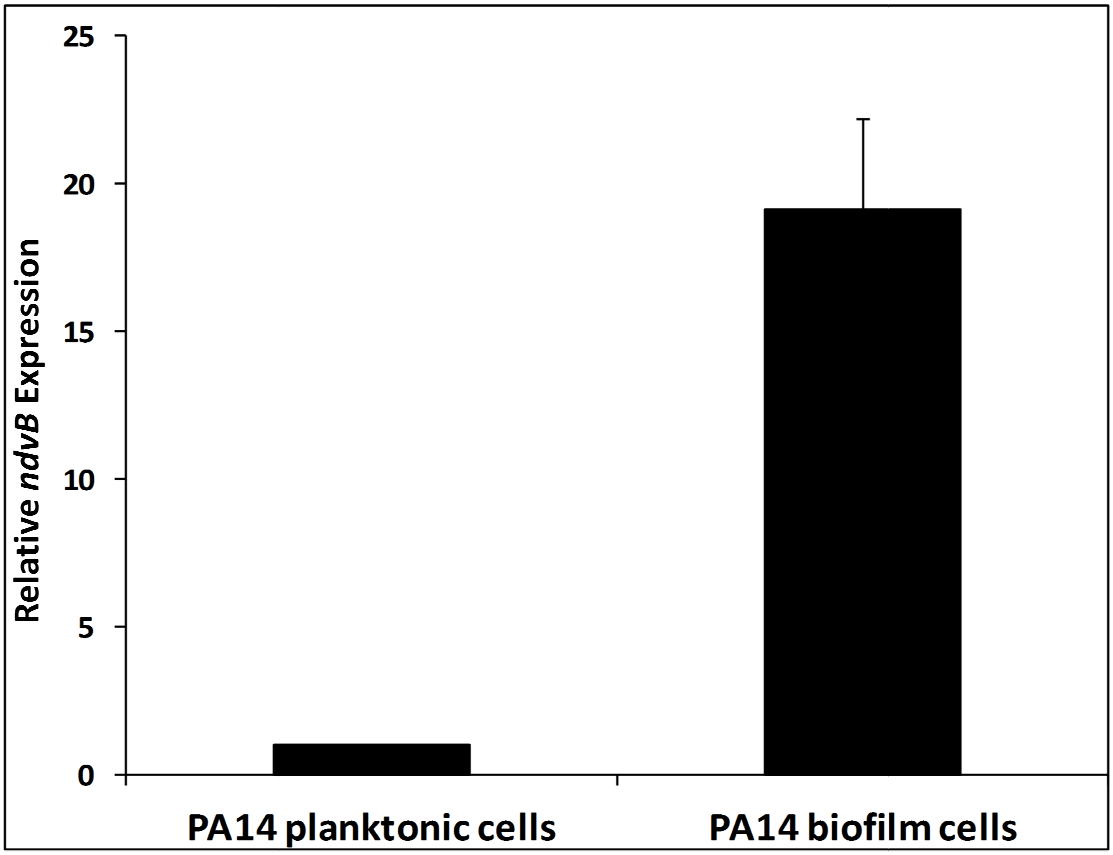

Figure 3: *ndvB* is expressed at higher levels in biofilm cells as compared to logarithmic phase planktonic cells. qPCR was performed using cDNA from logarithmically grown planktonic PA14 cells (left) and biofilm cells in M63-arginine (right). cDNA was quantified using SYBR-green. Biofilms were grown using the colony biofilm assay for 48 hours (Section 2.2.1.1). *rpoD* was used as a reference standard. Standard error bars are shown (10)

The second locus to be characterized was PA1874-77. The transposon insertion mutant of PA1874 was identified in the screen, and consequently the entire operon was selected for study (64, 127). Analysis of the genes in the operon found that its components had significant similarities to parts of well-characterized ABC and RND efflux pumps leading Mah et al to study the role of the operon in the efflux of antibiotics (60, 127). They found that the operon is involved in the efflux of multiple classes of antibiotics and is more highly expressed in biofilms (127). Individual analysis of the four genes within the operon found that only PA1875-77 showed an antibiotic resistance phenotype whereas PA1874 did not (98). Additionally, they showed that doubly deleted *ndvB* and PA1874-77 strains resulted in a mutant that was more sensitive to antibiotics that either mutant alone indicating separate mechanisms of resistance at these genetic loci (64).

The third locus to be characterized was *tssC1*, a component of a newly described type six secretion system (T6SS) (126). T6SS are widely known for the delivery of toxins from pathogenic bacteria to their hosts (87, 126). However, Zhang et al show a novel role for T6SS in biofilm-specific antibiotic resistance to multiple classes of antibiotics through assessing the sensitivity of a *tssC1* deletion to a set of antibiotics. It has been proposed that an uncharacterized effector of the T6SS is responsible for this antibiotic resistance phenotype (126).

The transposons from the other three mutants identified in the screen were examined to determine the genetic loci that were affected by the transposon insertion. Two of the genes (*PA2070, PA5033*) that were found encode proteins with unknown function

(118). Whereas, the third gene found in the screen (PA0757) was part of a two-component system. These genes were more highly expressed in biofilms as compared to logarithmic-phase planktonic cells, confer independent mechanisms of resistance and show biofilm-specific antibiotic resistance phenotypes (64, 125, 127)

To date, research in the lab suggests that each of the six genetic loci identified in the original screen represents a different mechanism of antibiotic resistance (64, 125-127). This was found not only through initial characterization of three of the six genes but also by comparing the susceptibility of double mutants to a set of antibiotics. Results found that double mutants of *ndvB* and PA1874-77 as well as *ndvB* and PA0756-0757 were doubly sensitive to tobramycin and gentamycin suggesting that these genes code for independent mechanisms (125, 127).

Very recently, research in the lab has found that these genes may be important *in vivo* through experiments using a *C.elegans* slow killing model. In this type of experiment, *C.elegans* was plated onto bacterial lawns containing E.coli (normal food), PA14 wild type (kills *C.elegans*) or PA14 wt containing a deletion mutant of one of the biofilm-specific antibiotic resistance genes. Following incubation, the amount of viable *C.elegans* was counted to determine the persistence of each bacterial strain in *C.elegans*. All six biofilm-specific antibiotic resistance gene deletion mutants were attenuated in their ability to survive in the host indicating that they play a role in persistence in an in vivo model system (125). This attenuation effect is hypothesized to occur due to the presence of antimicrobial compounds from the innate immune system and the lack of expression of individual biofilm-

specific antibiotic resistance genes in the deletion mutants that would normally protect the biofilm cells against these antimicrobial compounds (125). These findings show that biofilm-specific antibiotic resistance genes are important for persistence *in vivo*.

1.4 Biofilms and stationary phase planktonic cells

Cells in planktonically-grown cultures progress through typical phases (117). The first phase consists of the lag phase which occurs after inoculation of the culture and is characterized by slow growth as the cells adjust to the new environment. The second phase is logarithmic growth which occurs when nutrient levels are high and waste levels are low. In this phase, cells are in a state of rapid, continuous division where OD_{600} increases rapidly (117). Due to this increase in cell number, waste products begin to accumulate and nutrient levels decrease. The rate of cell growth begins to slow down and eventually the culture reaches a growth rate of zero, known as the stationary phase. Under further incubation, the cell density decreases as the rate of cell death continues to increase (117).

Recent evidence suggests that stationary phase planktonic cells have gene expression profiles more similar to biofilm cells as opposed to logarithmic cells (5). Many groups have compared gene expression of *P. aeruginosa* cells in these three states (planktonic-logarithmic, planktonic- stationary and biofilm) and found much closer levels of gene expression between biofilms and stationary phase planktonic cells as compared to logarithmic planktonic cells (5).

The six biofilm-specific antibiotic resistance genes were called *biofilm*-specific because of their phenotypes as described by their initial discovery in Mah et al's transposon-

insertion mutant screen (64). The six mutants all grew well as wild-type, could grow biofilms and had equivalent levels of planktonic resistance, but when grown in biofilms were more sensitive to a set of antibiotics. Additionally, all six biofilm-specific antibiotic resistance genes are more highly expressed in stationary-phase planktonic cells and biofilms as compared to logarithmic-phase planktonic cells (same trend as Figure 3) (125). This led us to examine if these six genes are regulated by cell density and/or respond to quorum sensing. Despite the fact that none of the six have been identified in screens looking for quorum-sensed genes, cell density will be examined as a possible avenue of biofilm-specific antibiotic resistance gene expression (94, 111, 116).

My thesis is split into two data chapters each focused on the analysis of two separate but related research questions. The focus of the first chapter (chapter 2) is dedicated to the study of a newly discovered DNA motif present in the putative promoters of the six biofilm-specific antibiotic resistance genes found by the transposon-insertion screen. A previous post-doctoral fellow used an *in silico* program called MEME to identify the strong 22bp motif (Figure 4) (7). The 22bp motif is found between 26 to approximately 200 bases upstream of the transcriptional start site in five of the six biofilm-specific antibiotic resistance genes. It is hypothesized that the expression of the six biofilm specific antibiotic resistance genetic loci is controlled by a protein that binds to this motif. An affinity chromatography based approach was used and a protein was identified that bound to the 22bp consensus motif. Direct binding of this protein to the motif was analyzed by creating a His-tagged version of the protein and repeating the affinity chromatography experiment with pure protein.

Figure 4: A 22 base pair motif was identified in the promoter regions of the biofilm specific antibiotic resistance genes. Analysis was performed by Sine Svenningen using MEME (7). Height of the letters indicates certainty of that particular base pair at each position in the motif. No consensus was found at base pair 16.

The second data chapter (chapter 3) examines spatial and temporal expression of one of the biofilm-specific antibiotic resistance genes, *ndvB*. Due to the heterogeneous nature of biofilms (Section 1.1.5), it is hypothesized that expression of *ndvB* will vary spatially and temporally. Fluorescent proteins were used as reporters to indirectly measure promoter activity through the creation of promoter-fluorescent protein constructs. A previously created *ndvB*p-GFP construct was used to analyze temporal expression of *ndvB* in both stationary phase planktonic cells as well as in biofilms. The study of spatial and temporal gene expression of biofilm antibiotic resistance genes is a new approach for not only the lab but for the scientific community. To my knowledge, there are no published papers that examine spatial and temporal expression of antibiotic resistance genes in biofilms. The results in this chapter are exciting but at the same time only preliminary and a lengthy discussion of future experiments as well as improvements to the current approach will be included.

CHAPTER 2. DISCOVERY OF A POTENTIAL REGULATOR OF BIOFILM SPECIFIC ANTIBIOTIC RESISTANCE IN *PSEUDOMONAS AERUGINOSA*

2.1 Introduction

2.1.1 Overview

As described in chapter 1, six biofilm-specific antibiotic resistance genes were identified in a screen by Mah *et al* (64). Since this original screen, three of the six genes have been characterized, while three more are currently being characterized (64, 125-127). Together, all six biofilm-specific antibiotic resistance genes are expressed at higher levels in biofilms as compared to logarithmic-phase planktonic cells (64, 125, 127). The fact that each of the six genes is expressed at high levels in biofilms but not in logarithmic-phase planktonic cells (Figure 4) suggests that these genes may be regulated by a common regulatory mechanism. In order to assess this possibility a previous post-doctoral fellow in the lab, Sine Lo Svenningsen studied the predicted promoters of the six biofilm-specific antibiotic resistance genes. The results from this study identified a 22bp DNA motif present in the predicted promoters from these six genes. The binding of an unknown protein to this regulatory element may be responsible for the increased expression of the six biofilm-specific antibiotic resistance genes in biofilms. The goal of this chapter was to identify proteins that bind to the 22bp motif and confirm that they interact directly.

2.1.2 Identification of a DNA motif

An in-silico approach was used to discover the 22bp motif. The input sequence into MEME was the region of DNA upstream of the transcriptional start site (TSS) from the six

biofilm-specific antibiotic resistance genes. The program that was used was called MEME (Multiple Em for Motif Elignment) (7). MEME used this data to create a probability-based matrix that described the likelihood of having one of the four bases at each position in comparison to the other sets of imputed data (7). The output of this analysis was the most relevant consensus motifs based on a derivative of the p-value but for multiple sets of data. This was called the E-value. The MEME analysis retrieved one significant motif found in the upstream region of all six biofilm-specific antibiotic resistance genes, and a total of 18 times in upstream regions in the entire *P. aeruginosa* genome (unpublished data- Sine Lo Svenningsen). This motif was 22 bases long (Figure 4). Based on the strength of the consensus motif found using MEME and the low number of hits of the motif in the genome as a whole, this motif was selected for use in the identification of a DNA-binding protein that may play a role in regulating biofilm-specific antibiotic resistance.

2.1.3 Activation in biofilms cells versus repression in planktonic cells.

In this chapter, an analysis of proteins that bind the 22bp motif found using MEME will be done in an attempt to explain the increased expression of these genes in biofilms. However, the increased level of expression of these antibiotic-resistance genes in biofilm cells could be the result of either activation in biofilms, or repression in planktonic cells. In order to determine which of these two scenarios was more likely, previous studies using a chromosomal deletion of the 22bp motif from *ndvB* was analyzed. qPCR experiments using this deletion mutant suggested that the biofilm-specific antibiotic resistance genes are more likely activated in biofilm cells as opposed to repressed in planktonic cells. This is supported by the finding that *ndvB* expression was low in the *ndvB* 22bp motif deletion mutant in

biofilms, whereas typically *ndvB* is more highly expressed in biofilms (64). In the deletion mutant, it is hypothesized that a potential activator binding the 22bp motif can no longer bind and induce expression of *ndvB*, which explains low ndvB expression.

If there was a repressor of the biofilm-specific antibiotic resistance genes in planktonic cells, one would expect *ndvB* expression to be higher in the 22bp motif deletion in planktonic cells as the repressor would not have a binding site. However, planktonic *ndvB* expression is relatively unchanged between the 22bp deletion mutant and wt indicating that it is not binding the motif in planktonic cells (unpublished data- Li Zhang). This finding helped narrow the focus of the experimental protocol to analysis of biofilm extract for an activator of biofilm-specific antibiotic resistance.

2.1.4 Regulation of gene expression in bacteria

Typically, bacterial promoters contain a core promoter which includes a -10 region and a -35 region upstream of the TSS (117). These are highly conserved sequences that act as binding locations for the σ subunit of RNA polymerase (44). Besides the core promoter, there are additional nucleotides that act as binding sites for other subunits of RNA polymerase or for a number of transcription factors (32). These sites are generally found anywhere from 35 to over 1000 bases upstream of the TSS (90). Some of these sites are referred to as an UP element which is a binding site for the C-terminal domain of the alpha subunit of RNA polymerase, thus playing a direct role in transcription (13). The strongest of UP elements' are usually found within 100 bases of the TSS and can increase promoter activity over 300 fold (32). UP elements are also usually A-T rich (~90%) (32).

Regulation of gene expression is a very complex process, with approximately 8% of the *P. aeruginosa* genome coding predicted regulatory proteins (118). This equals over 400 regulatory proteins in the PA01 genome (105). Although most binding sites for these regulatory proteins in *E.coli* and *P. aeruginosa* are within 65 bases of the TSS, they have been shown to be up to 350 or more bases upstream of the TSS. For example, Huang et al discovered an OmpR binding site over 350 bases upstream of the TSS to which OmpR bound and interacted with proteins bound at 50 bases upstream of the TSS (51). They found that this strong protein interaction bent the DNA into a loop which repressed *ompF* transcription.

It is hypothesized that the 22bp motif may act as a binding site for an unknown activator of biofilm-specific antibiotic resistance. Binding of this unknown protein to the motif may increase the likelihood that RNA polymerase will bind to the core promoter and begin transcription, just as OmpR was able to influence transcription by binding to an upstream regulatory element (51).

2.1.5 22bp Motif

The 22bp motif consensus is located between 20 to 500 bases upstream of the TSS in the promoters of the six biofilm-specific antibiotic resistance genes (Table 1). Although there is significant variability in the location of the motif with respect to the TSS, this is not uncommon, as is shown with the discovery of binding sites for OmpR (51). The 22bp motif of *ndvB* was shown in reference to their TSS and predicted -10 and -35 core promoter (Figure 5).

Table 1: 22bp motif in the putative promoters of the six biofilm-specific antibiotic resistance genes.

22bp motif (PA01 gene number)	22bp motif (PA14 gene number)	Sense	Distance upstream from TSS (bp)	Sequence
1874-1877	40230-40260	_	1181*	GCTTCGCGGGATGCCCGGCGAT
1163	49360	+	191	GAATCGCGGATTGCCGCGCGCA
5033	66540	+	26	GTGTCCAGGGATGTCCGTCGAG
2070	37730	+	45	GGCCGGCCGGATGCCGGCCGCA
0756-0757	54510	-	86	GGATTGCTGAAAGCCTGGCGAA
0082-0084	00990-01010	+	143	GCCTTGCGGCATGCCACAAGAA

* 423 bp in PA01 and is + sense

ndvB

TGTTCATCCACCTGCATCACCAACCACCTCTGAAACCGAATCGCGGATTGCCGCGCGCATTA
TAAAAAGCCGCGGCCGCCGCGTCGCCTGCGTTCTTACGGCTCGTCGCGCAGGCCGGACTA
GACTTGCAACAGACCCGCCGGCCCGGCGCC**TGTACA**CCCCGGGGGGTGCGG**GGTAGCAT**
GCGCCGCCCCGTGTTCAGCGAAACATCCGGAACCTGGTTTCATCTCT**ATG**

Figure 5: The putative promoter of *ndvB* showing the 22bp motif in comparison to the core promoter and TSS. The 22 bp motif is underlined. The predicted-10, -35 and the TSS are in bold.

As not a lot is known about the promoters of the biofilm-specific antibiotic resistance genes, it is possible that there is a novel regulatory site that influences transcription of these genes that has not yet been identified. For example, a novel *P. aeruginosa* regulator that bound to the DNA sequence approximately 50 bases upstream of the TSS that activated expression of type three secretion system effectors (54). Consequently, the discovery of a novel proximal control element in *P. aeruginosa* is quite possible and may explain why the biofilm-specific antibiotic resistance genes are upregulated in biofilms.

Based on the low E-value (section 2.4.1) of the 22bp motif found in MEME and the fact that all six genes are more highly expressed in biofilms, the initial goal of my project was to use the 22bp motif consensus to identify a regulator of biofilm-specific antibiotic resistance genes in *P.aeruginosa*. Amongst the different methods to assess DNA-protein interactions, DNA-affinity chromatography was used mainly due to the fact that there was expertise in the lab. Affinity chromatography was also cost-effective, and has been used successfully to identify novel DNA-protein interactions in numerous occasions (18, 79, 80, 99, 121, 124). A schematic depicting the main steps involved in the affinity chromatography experiment is presented (Figure 6).

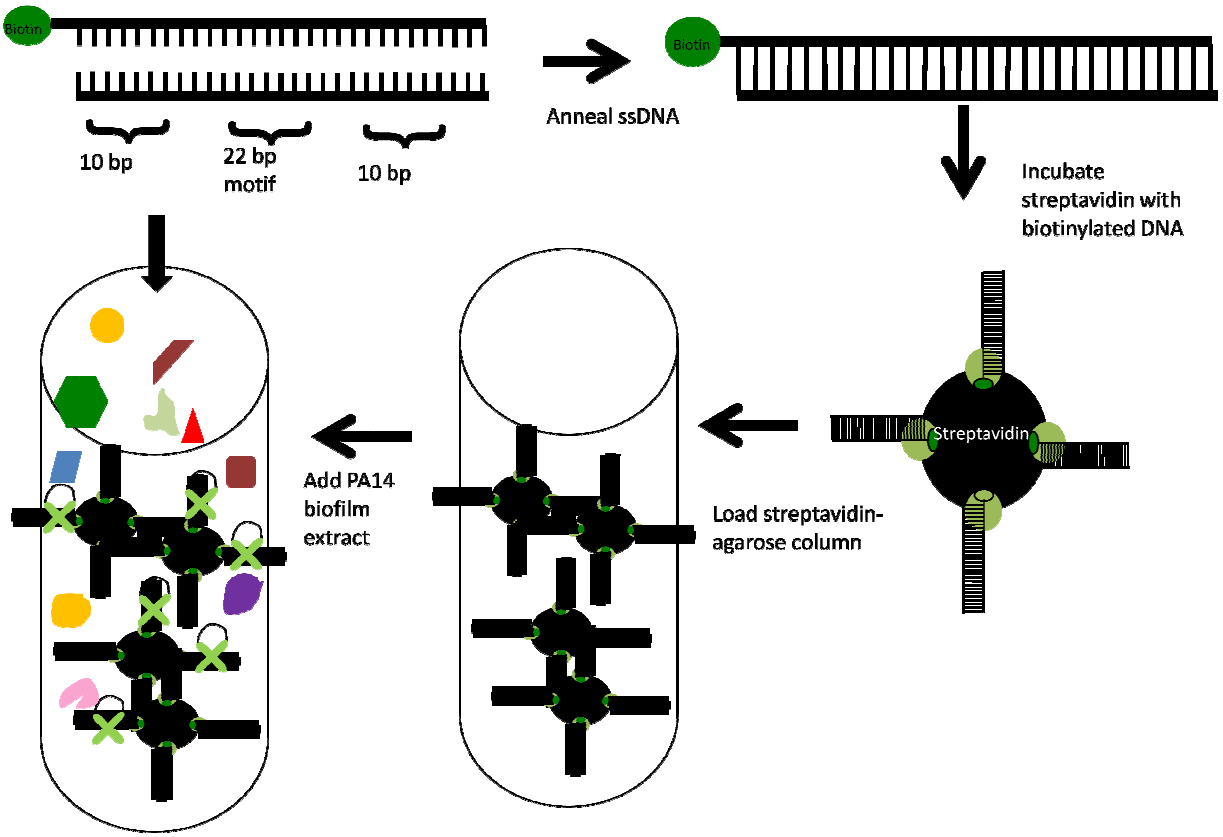

Figure 6: Overview of affinity chromatography methodology. Coloured symbols are meant to represent hypothetical proteins found in biofilm extract. Green crosses represent a protein from biofilm extract that has affinity for the 22bp motif.

2.2 Materials and methods

Table 2: Bacterial strains and plasmids used in Chapter 2

Strains, plasmids	Stock location	Relevant Characteristics	Source
E.coli			
DH5α	JPP5		
S17-1	JPP6		
c41s	TFM		Baezinger Lab
BL21 Rosetta	JPP30	ClorR	Couture Lab, Novagen
P.aeruginosa PA14	JPP1		(64)
Plasmids			
pQE30	JPP23	Expression vector, AmpR, His tag	
pHisparallel	JPP34	Expression vecgtor, AmpR, His tag	Couture Lab
pET30a	JPP35	Expression vector, KnR, His tag	Ramirez-Arcos Lab

2.2.1 Affinity chromatography pull down and identification of DNA binding proteins

2.2.1.1 Preparation of PA14 Biofilm Extract

PA14 biofilm cells were grown using a colony biofilm assay. This method is much simpler than other biofilm growth methods and produces cells with similar phenotypes to biofilms grown using more complex methods (112). To grow a colony biofilm, overnight cultures of PA14 wt were grown and 100µL of the cultures were inoculated into 5ul circular colonies onto 1xM63 plates. The plates were incubated for 16 hours at 37°C, followed by incubation at room temperature for 24 hours. The biofilms were removed from the agar plate surface by gently pipetting 1xM63 liquid media multiple times over the biofilms. The resuspended biofilm cells were collected into 1.5mL microcentrifuge tubes and spun down at 4,000 rpm for 5 minutes. Cell pellets were resuspended in 2mL of 0.8M NaCl affinity chromatography buffer (ACB) (78).

Cell lysates were prepared in a high concentration of NaCl in order to elute most of the DNA-binding proteins off chromosomal DNA (124). 10µL of 100X Bacterial Protease Inhibitor (BioLynx) was added per mL of suspended cells solution. Lyzozyme was added as necessary to help in the breakdown of the cell wall (1mg/mL) Cells were sonicated six times in 10 second pulses. The lysates were centrifuged at 20,000 rpm in 1.5mL microcentrifuge tubes for 15 minutes at 4°C. The collected supernatants were then dialyzed into 0.1M NaCl ACB for a minimum of 4 hours, switching the buffer once midway through. The dialyzed cell supernatants were mixed with glycerol to a final concentration of 35%. Salmon sperm DNA (ssDNA) was added to a final concentration of 0.05 mg/mL in order to bind the abundant

ssDNA binding proteins and reduce non-specific interactions during the affinity chromatography experiment. 2µL of 1M $MgCl_2$ was also added to the extract. The extracts were either immediately loaded onto the affinity column or stored at -20 °C.

2.2.1.2 Preparation of streptavidin-agarose slurry

6% beaded straptavidin agarose (Invitrogen) was used as the column. 200uL of the streptavidin-agarose slurry was pipetted into 1.5mL microcentrifuge tubes per column. The slurry was added to 40mL of 0.1M NaCl ACB, spun down and resuspended in 1mL 0.1M NaCl ACB and a final concentration of 500 µg/mL of BSA in 1.5mL microcentrifuge tubes. The tubes were incubated on a rotating wheel for 5 minutes at 4°C. They were then briefly centrifuged and the buffer was replaced with 1.5 M NaCl ACB in order to remove BSA proteins. Tubes were once again incubated for 5 minutes at 4°C, briefly centrifuged and resuspended in 300uL of 0.1M NaCl ACB.

2.2.1.3 Preparation of biotinylated oligos

Individual single stranded oligonucleotides representing the 22bp motifs from the PA1874-77 and *ndvB* promoters were designed so that the 22bp motifs were flanked on each side by 10bp of DNA chosen at random in order to prevent steric interactions with biotin. The forward oligonucleotides were biotinylated, while the complementary reverse oligonucleotides were not (Figure 6). Both the forward and reverse oligonucleotides were diluted to a concentration of 400pmol/µL and mixed together at a 1:1 molar ratio. The forward and reverse oligonucleotides were annealed in a thermocycler. The oligos were first heated at 95°C for 5 minutes, decreasing by 1°C every minute to 4°C. Annealed oligos were

stored at 4°C. The main differences were in the length of the nucleotides placed between the motif and biotin as well as the number of 22bp motifs present on one oligonucleotide. In the end, AFFCHRO-F/R 8, 9 and 10 were used for the identification of PA0564.

Table 3: Description of the oligonucleotides used for affinity chromatography

Name	Description	Sequence (5' to 3')	Direction
MOTIF-AFFROCHRO	PA1874-77 motif with 10bp flanking sequence	Biotin-GCTAGTTGCAGCTTCGCGGGATGCCCGGCCATGTGCGAGTAA	Forward
MOTIF-AFFROCHRO		Reverse complement of above	Reverse
MOTIF-AFFROCHRO-F2 (PAGE)	PA1874-77 motif x2 with 15bp flanking sequence	Biotin-GGATAGACCAGCTAGTTGCACGTAGGCTTCGCGGGATGCCCGGCGATGTGCGAGTAATTTATGCTTCGCGGGATGCCCGG	Forward
MOTIF-AFFROCHRO-R (PAGE)		Reverse complement of above (minus 10bp beside biotin)	Reverse
AFFCHRO-F3/4 (HPLC)	PA1874-77 motif with 14bp flanking sequence	BiotinGGATAGCTAGTTGCACGTAGCTTCGCGGGATGCCCGGCGATGTGCGAGTAATTTA	Forward
AFFCHRO-R3 (HPLC)		Reverse complement of above (minus 5bp bedide biotin)	Reverse
AFFROCHRO-F6	Negative control motif with 10 bp flanking sequence	Biotin-GATGCGTAGTTTGCATAATTCGTTAGATTAGGTTGTCCATCC	Forward
AFFROCHRO-R6		Reverse complement of above	Reverse
AFFROCHRO-F7	Negative control motif with 10bp flanking sequence	Biotin-GATGCGTAGTTTGCATAATTCGTTAGATTAGGTTGTCCATCC	Forward
AFFROCHRO-R7		Reverse complement of above	Reverse
AFFROCHRO-F8	*ndvB* motif with 10bp flanking sequence	Biotin-GATGCGTAGTGAATCGCGGATTGCCGCGCGCATTGTCCATCC	Forward
AFFROCHRO-R8		Reverse complement of above	Reverse
AFFROCHRO-F9	PA1874-77 motif with 10bp flanking sequence	Biotin-GATGCGTAGTCGTTCGCGGGATGCCCGGCGATTTGTCCATCC	Forward
AFFROCHRO-R9		Reverse complement of above	Reverse
AFFROCHRO-F10	Negative control motif with 10bp flanking sequence	Biotin-GATGCGTAGTTTGCATAATTCGTTAGATTGGGTTGTCCATCC	Forward
AFFROCHRO-R10		Reverse complement of above	Reverse

2.2.1.4 Affinity Chromatography:

The prepared resin (in 300uL 0.1M NaCl ACB) was incubated with each individual annealed biotinylated oligo (40µL of 400pmol/µL) for 15 minutes at 4°C on a rotating wheel. Following incubation, the oligonucleotide-bound resin was briefly spun down in a centrifuge and washed with 1.5M NaCl ACB twice to remove unannealed oligonucleotides. After the final wash, the oligo-bound resin was resuspended in 1.5M NaCl ACB. Glass beads (Sigma) were loaded into the column (a standard 200µL pipette tip) up to the 10µL mark. The oligo-bound streptavidin-agarose resin (already blocked with BSA) was loaded onto the column up to the 50µL mark (40µL of resin). 1.5M NaCl ACB was run through the column to equilibrate it. The oligo-bound resin was resuspended one time by pipetting the buffer in the column up and down. Once settled (as seen in Figure 7), the column was washed with 10 x column volumes (total 500 µL) of 1.5M NaCl ACB. Following this wash, the column was washed with 10 column volumes (total 500uL) of 0.1 M NaCl ACB. 250uL of PA14 biofilm cell extract was loaded onto the column and incubated at 4°C for 1.5 hours. The PA14 biofilm extract slowly moved through the column over the span of 1.5 hours. When the extract had completely run through the column, the column was washed with 10 column volumes of 0.1M NaCl ACB (low salt wash). 50uL of 1.5M NaCl ACB was added to the column to elute proteins from the extract that had bound to the column (high salt elution). A final elution with 0.1% SDS to clear the column was performed (SDS).

A

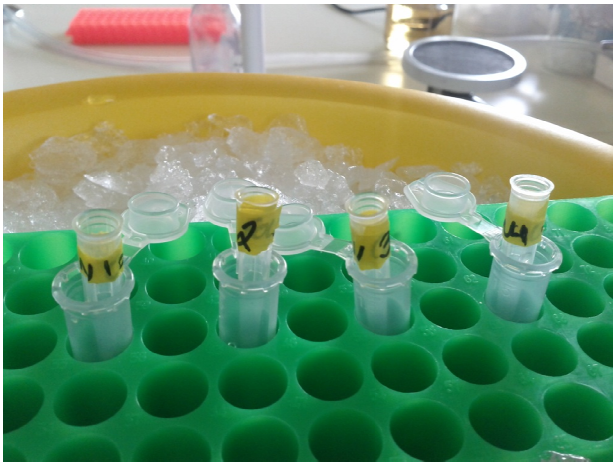

B

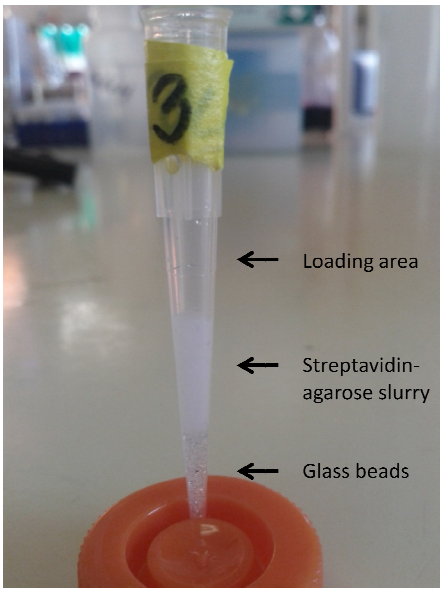

Figure 7: Set-up of Affinity Chromatography. (A) Columns were kept on ice during the affinity chromatography. (B). Close-up of the column showing the layers. The glass beads were present on the bottom of the column followed by the strepavidin agarose slurry.

Fractions that were collected and analyzed by SDS-PAGE electrophoresis included the flow through (extract), low salt wash, high salt elution, and SDS elution. The collected fractions were kept on ice and mixed in a 4:1 ratio with 5x SDS-PAGE loading buffer and immediately heated to 95°C for 4 minutes. The remaining elutes were kept at -20°C after being mixed with glycerol to a final concentration of 35%. All buffers were kept at 4°C, and columns were kept on ice during washing.

2.2.1.5 SDS-PAGE

10% SDS-PAGE gels consisting of both a stacking and resolving gel were made. The resolving gel contained 4mL ddH20, 3.33mL acrylamide, 2.5 mL of 1.5M Tris pH 8.8, 100uL 10% SDS, 100µL 10% ammonium persulfate and 5µL TEMED. These components were mixed in an erlenmeyer flask and poured into an SDS-PAGE holding cassette (BioRad) by a Pasteur pipette. The gel was immediately covered by a thin layer of 0.1% SDS to facilitate polymerization of the gel. Gels were allowed to solidify for 45 minutes. Following polymerization, the 0.1% SDS layer was washed off and the tops of the gels were quickly rinsed with ddH20. The stacking gel which consisted of 3.1mL ddH20, 670µL acrylamide, 1.25mL 0.5M Tris pH6.8, 50µL 10% SDS, 25µL 10% ammonium persulfate and 5µL TEMED was prepared and poured over the resolving gel. Combs were placed at the surface of the gel and the gel was left to polymerize for 45 minutes. Once polymerized, the gels were loaded into the gel electrophoresis apparatus and immersed in 1X SDS-PAGE running buffer. Gels were run at 110V until the dye front reached the end of the gel.

2.2.1.6 Silver stain

After running the SDS-PAGE, gels were fixed for at least one hour in a 10% acetic acid, 40% methanol solution on a shaker at room temperature. Following fixing, the gels were washed for 10 minutes in 30% ethanol three times. Following the wash, the gels were incubated in a 1.3mM solution of sodium thiosulfate for 1 minute. The gels were washed with ddH_20 for 20 seconds three times. Following the wash the gels were incubated with a 0.1M solution of silver nitrate for 20 minutes. Following this incubation, the gels were washed with ddH_20 for 20 seconds three times. The wash was removed and the gels were incubated with a develop solution (6g of sodium carbonate, 100µL formaldehyde, and 5mL of sodium thiosulfate) for up to 10 minutes until the appropriate level of staining was completed. To stop the developing, the gels were incubated in a 0.5% solution of glycine.

2.2.1.7 Digestion and mass spectrophotometry analysis

In-gel digestion and mass spectrometry analysis were performed at the Ottawa Institute of Systems Biology (OISB) proteomics resource centre. The LTQ mass spectrophotometer (Thermo Fisher) was used.

2.2.2 Protein induction

2.2.2.1 PCR of PA0564

PCR was used to amplify the open reading frame of PA0564 for cloning. PA14 genomic DNA was first isolated using a genomic DNA isolation kit (Invitrogen). It was then PCR amplified using primers PA0564-pET30-F-1 and PA0564-pET30-R-1 (Table 4). The PCR master mix consisted of the following components in 50uL final reaction volume: 2uL PA14

genomic DNA, 6µL Band Sharpener, 2µL 10mM dNTPs, 2µL forward primer (10pmol/µL), 2µL reverse primer (10pmol/ µL), 4.5µL DMSO, 10µL 10X buffer and 1.5µL TAQ. All components were from Feldan. The PCR was run in the MyCycler thermocycler (Bio-Rad) with the following reaction conditions: an initial denaturation at 95°C for 3 minutes followed by 30 cycles of denaturation at 95°C for 30 seconds, annealing at 74°C for 30 seconds and extension at 72°C for 2 minutes. A final extension was run for 10 minutes following the cycles. PCR products were run on a 1.0% DNA agarose gel to verify amplicon size. PCR products were purified using a PCR purification kit (Invitrogen).

2.2.2.2 Cloning of PA0564 into pET30

The purified PA0564 PCR product and pET30a vector were digested with NcoI and XbaI at 37°C for 1.5 hours. Digests were performed in duplicate in 25 µL final volume consisting of 2.5uL buffer, 1uL NcoI, 1uL Xbal and 8uL DNA. Following digestion, the duplicate reactions were combined, PCR purified (Invitrogen), and eluted in 30uL. Duplicates were performed and elution was in a small volume in order to maximize the DNA content of the samples prior to ligation. Samples were run on a 1.0% DNA agarose gel prior to ligation to visualize the DNA and confirm the digestion. Ligations were performed at both a 1:1 and 4:1 vector to insert ratio at 16°C for 20 hours in 15µL final volume consisting of 4 µL ligase buffer, 1.5uL T7 ligase, 1uL PA0564 fragment, and 8uL pET30a vector. Ligations were diluted 5:1 in ddH_20 and 10uL of the diluted ligation mix was added to 100uL competent DH5α cells and this mixture was incubated for 30 minutes on ice. The cells were heat shocked for 90 seconds at 42°C and then put back on ice. The cells were added to 800uL LB and incubated

on a shaker at 37°C for 75 minutes. 150uL of the incubated broth was plated on 50µg/mL kanamycin and placed at 37°C for 16 hours to allow for colony growth.

In order to check for correct clones, individual colonies were numbered and used to inoculate overnight cultures with LB+50µg/mL kanamycin and as template DNA in a colony PCR reaction. This method of growing overnight cultures with antibiotic (along with subsequent miniprep, and digest) as well as using the same colony in a PCR reaction with primers specific for the insert allowed for careful, efficient screening of transformants by two different methods. The colony PCR reaction consisted of initial denaturation at 95°C (10 min) followed by 30 cycles of denaturation at 95°C (30 sec), annealing at 67°C (1min) and extension at 72°C (3 min). The PCR products were run on a 1% agarose gel. Transformants that gave both a positive colony PCR result and a 900bp fragment in the digestion reaction continued in the process. Minipreps of these transformants were PCR purified (Invitrogen) and their A_{260} was taken to calculate DNA concentration. DNA from several positive clones was sent for sequencing using T7 promoter and terminator primers (StemCore- OHRI) until a positive clone was found. Positive clones were transformed into c41s and BL21 Rosetta *E.coli* and screened using the same method as above. Both BL21 Rosetta and c41s strains were made competent through the calcium–chloride method (Molecular Cloning).

2.2.2.3 Protein Induction

Protein expression was completed in BL21 Rosetta *E.coli* cells. In order to check for appropriate induction conditions, a 1:100 subculture of an overnight culture containing pET30a-PA0564 was grown to an OD_{600} of 0.5 on a shaker at 37°C. Cultures were induced

with 0.1mM and 0.5mM IPTG for 3 more hours, and then pelleted. Cell pellets were vortexed with 100µl of H_20 and 25µl of 5x sample buffer. The samples were heated at 100°C for 5 minutes and then loaded onto an SDS-PAGE gel. The gels were Coomassie stained to visualize the protein bands

The solubility of the induced His-PA0564 protein was first verified before large-scale production. Induced cultures were split into 8 eppendorf tubes and spun down at 5000 rpm for 5 minutes at 4˚C. The supernatant was removed, and cell pellets were vortexed with different buffers to test for the best conditions for solubility (Buffer 1: 50mM Na_2PO_4 pH7.0, 500mM NaCl. Buffer 2: 50mM Na_2PO_4 pH7.0, 100mM NaCl. Buffer 3: 50mM Na_2PO_4 pH7.0, 100mM NaCl, 10% glycerol. Buffer 4: 50mM Tris pH8.0, 100mM NaCl. Buffer 5: 50mM Tris pH8.0, 100mM NaCl, 10% glycerol. Buffer 6: citrate pH 6.0, 100mM Nacl. Buffer 7: 50mM Tris pH9.0, 100mM NaCl.) BugBuster© Master Mix (Novagen) was used as a detergent for maximum recovery of soluble proteins. Solutions were supplemented with 4 µg/mL of lyzozyme (Sigma) to assist in bacterial cell wall breakdown. Following vortexing, tubes were placed on a rotating wheel at 4˚C for 20 minutes. 20 µL (whole cell fraction) was removed, and the remaining 80uL was spun down at 13,000 rpm for 5 minutes at 4˚C to collect the soluble fraction. Both the soluble and whole cell fractions were subjected to SDS-PAGE to confirm solubility of the recombinant protein.

For large scale induction, a 25mL overnight culture was grown in appropriate antibiotic. Two 500mL LB cultures were inoculated with the appropriate culture and grown to an OD_{600} of 0.5 and then induced with 0.1mM IPTG for 3 hours at 37˚C on a shaker. The

cells were spun down for 30 minutes at 3000 rpm at 4˚C. Pelleted cells were vortexed in 100mL of Buffer 6 (50mM citrate, pH6.3, 250mM NaCl), lyzozyme (4 µg/mL) and sonicated 3 pulses x 1 minute on ice. Sonicated cells were spun down at 16,000 rpm for 30 minutes at 4˚C. Cell supernatants were incubated with rinsed TALON resin (ClonTech) for purification and eluted with 50mM citrate pH6.3, 250mM NaCl, 0.5M Imidazole. Purified recombinant protein was dialyzed overnight into 50mM citrate pH 6.3, 250mM NaCl and concentrated using an ultracentrifuge concentrator (Amicon). Concentrated proteins were flash frozen by immersing in liquid nitrogen. Concentrates were run on a 10% SDS-PAGE gel (as described above) to examine the level of purity.

2.2.2.4 Coomassie Staining

After running the SDS-PAGE, gels were fixed in a 45% methanol/10% acetic acid solution for one hour. They were then stained in a 0.1% Coomassie blue, 40% methanol, 10% acetic acid solution for approximately one hour. Gels were destained in a 45% methanol, 10% acetic acid solution and then soaked in 5% acetic acid following the destain. Stained gels were soaked in a 10% glycerol, 90% ethanol solution for drying and then were placed between two layers of plastic and dried overnight.

2.2.2.5 Induction Strains:

c41s is a popular strain used for induction of recombinant proteins in *E.coli* due to its ability to express a wider variety of proteins including proteins that may be toxic in *E.coli*, and proteins that are induced at low levels(69). Miroux et al (1996) tested expression of 7 membrane and 10 soluble proteins in BL21 and c41s and confirmed the higher expression in

c41s without toxic effects. The uncharacterized mutations of C41(DE3) and C43(DE3) occurred by a spontaneous process, followed by a phenotypic selection based on the ability to survive after inducing the expression of a toxic recombinant protein(69).

BL21 Rosetta strain is a derivative of BL21 *E.coli*, a strain specifically adapted for protein induction due to the loss of *lon* and *ompT* proteases (81). BL21 Rosetta adds an additional benefit in that it contains a chloramphenicol-marked plasmid encoding genes for six tRNAs which allows for expression of a wider variety of proteins. DE3 indicates that the strain contains a chromosomal copy of the T7 RNA polymerase (81). pLysS indicates that the strain contains a plasmid that encodes T7 lysozyme which inhibits T7 polymerase. This allows for suppression of expression and thus stabilization of pET recombinants that contain insert (107, 128).

Table 4: Primers used in Chapter 2

Name	Sequence (5' to 3')	Direction	Usage
pQE30_PA0564SEQR	ACCGAGCGTTCTGAACAAAT	Reverse	Sequencing clones
pQE30_PA0564SEQF	GCGGATAACAATTTCACACAG	Forward	Sequencing clones
PA0564clon-F	GCAAGCTTTCAGCGAGCGGAG TCGGCCT	Forward	Cloning PA0564 into pQE30 (HindIII)
PA0564clon-R	CGAGTCTATGGACCCACTCGA CCGGCT	Reverse	Cloning PA0564 into pQE30 (SacI)
PA0564clon-F2	GCGAATTCTGATGGACCCACT CGACCGGCT	Forward	Cloning PA0564 into pHis (EcoRI)
PA0564clon-R2	CGTCTAGCATCAGCGAGCGGA GTCGGCCT	Reverse	Cloning PA0564 into pHis (XbaI)
pHIS-PA0564SEQ-R	CCCCAAGGGGTTATGCTAGC	Reverse	Sequencing clones
pHIS-PA0564SEQ-F	TCCCGCGAAATTAATACGAC	Forward	Sequencing clones
PA0564-clon-R3	CATGTCGACTCAGCGAGCGGA GTCGGCCT	Reverse	Cloning PA0564 into pHis (SalI)
PA0564-clon-R-5	GCTCGAGTCAGCGAGCGGAG TCGGCCT	Reverse	Cloning PA0564 into pHis (SacI)
PA0564clon-F-6	GCCCATGGTATGGACCCACTC GACCGGCT	Forward	Cloning PA0564 into pHis (NcoI)
PA0564-pET30-F-1	GCTCCATGGTCATGGACCCAC TCGACCGG	Reverse	Cloning PA0564 into pET30a (NcoI)
PA0564-pET30-R-1	CATCTCGAGTCAGCGAGCGGA GTCGGC	Forward	Cloning PA0564 into pET30a (XbaI)

2.3 Results

2.3.1 Identification of proteins that bind the 22bp motif consensus

The overall goal of this chapter was to identify proteins with affinity to the 22bp motif. An overview of the steps of this chapter is presented in Figure 8. The 22bp PA1874-77 motif was selected to be used in the first affinity chromatography experiment as it was closest in sequence to the consensus motif (Figure 4). Initial affinity chromatography experiments revealed that only a single candidate protein (PA4232) was binding to the PA1874-77 22bp motif (data not shown). Mass spectrometry analysis identified this protein as Ssb, single-stranded DNA-binding protein. This result suggested one of two possibilities; that Ssb was non-specifically binding single stranded DNA that was present in the column, or that it had affinity for the PA1874-77 22bp motif. Further experimentation revealed that Ssb was binding single stranded DNA and not binding the 22bp motif (data not shown). Continuous optimization and the inclusion of a single stranded negative control motif resulted in the discovery of a 33kDa protein binding the PA1874-77 motif.

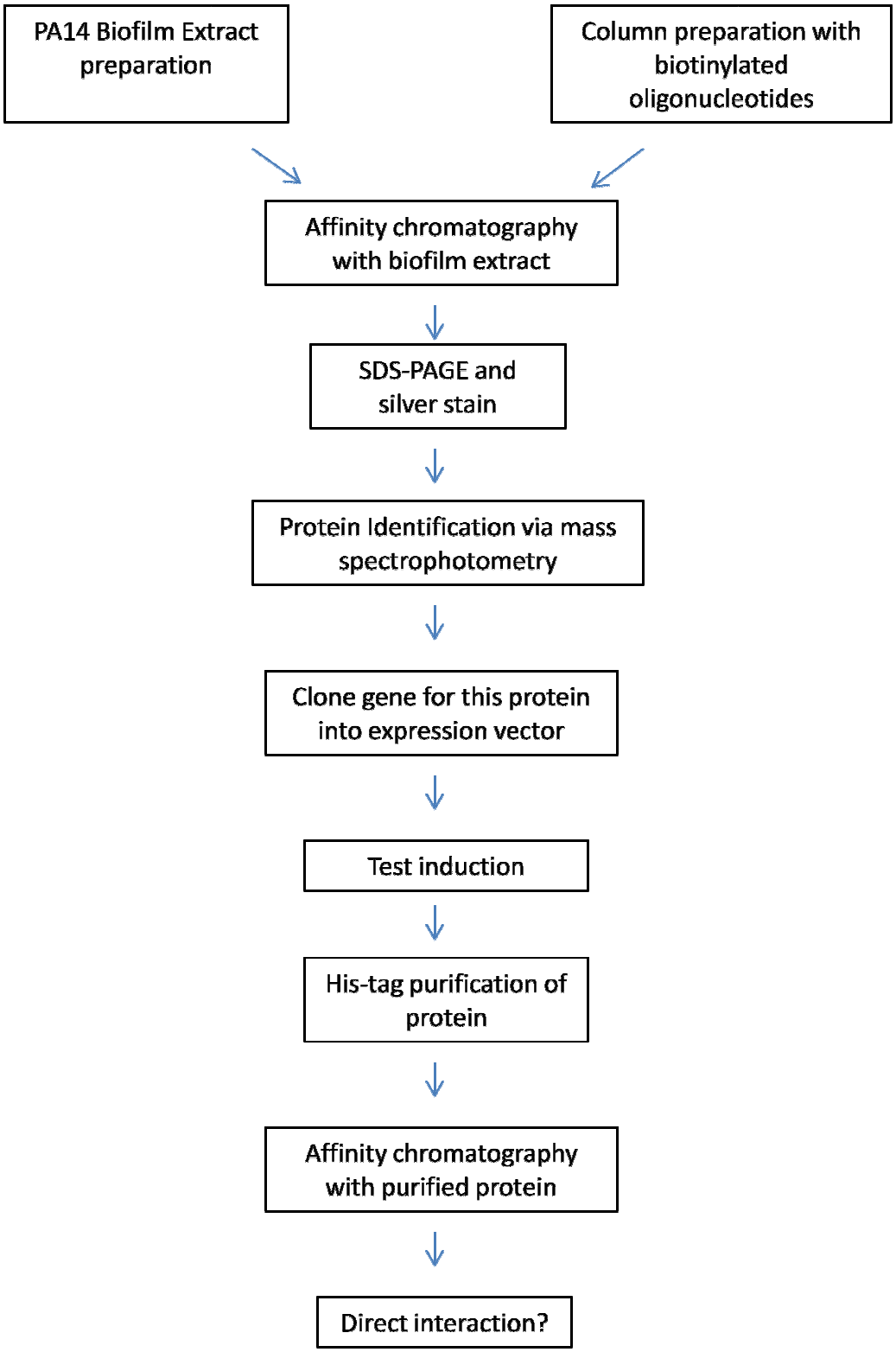

Figure 8: Overview of Chapter 2

The silver stained protein gels containing the fractions from the affinity chromatography experiment discovering a 33kDa protein are shown in The flow through and low salt washes are shown for the affinity chromatography experiment shown in Figure 9, but not for the remainder of affinity chromatography experiments in this chapter due to repetition in the results obtained. The flow through fractions always showed that the biofilm extract was not degraded, and that the amount loaded did not vary between columns in the same experiment (Figure 9A, lanes 2-4). Analysis of the low salt washes confirmed that there were no eluted proteins prior to addition of the high ionic strength buffer in each experiment. Initial affinity chromatography experiments were run with columns containing 1x (15 nmol) and 4x (60 nmol) biotinylated motifs. In Figure 9, Figure 10, and Figure 11, the eluates from these two columns were shown as replicates as there were minimal differences in the proteins eluted between the two.

Analysis of the high salt eluates from the PA1874-77 22bp motif columns (Figure 9B) revealed approximately 10 proteins that were found to be consistently binding to the PA1874-77 22bp motif. This experiment was repeated in order to confirm this observation (Figure 9C). Results from this experiment suggest that the most consistent, as well as the most intense band was at 33kDa. This band was selected for future study.

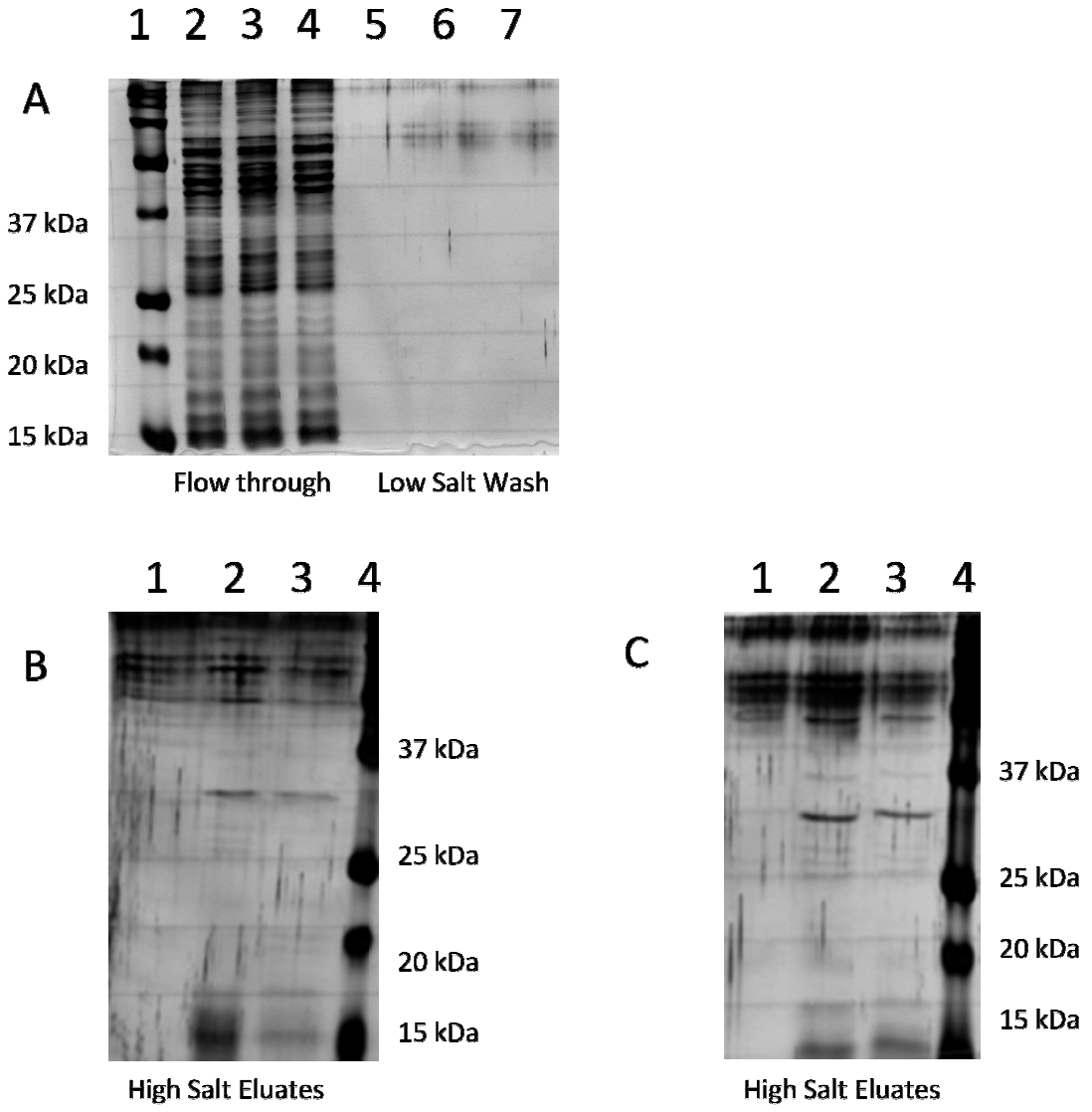

Figure 9: A 33kDa protein is binding the PA1874-77 22bp motif. Silver-stained SDS-PAGE gels containing elution fractions from three separate affinity chromatography columns. (A) Flow through showing un-degraded PA14 biofilm extract that was loaded onto each column. Low salt washes showing that there were no eluted proteins prior to addition of the high salt buffer. Ladder (lane1), no DNA negative control (lane 2), PA1874-77 22bp motif (lanes 3 and 4), no DNA negative control (lane 5), PA1874-77 22bp motif (lanes 6 and 7). (B) Proteins eluted from the addition of a high salt buffer to the columns. The most prominent band on this gel was at 33 kDa. No DNA negative control (lane 1), PA1874-77 22bp motif (lanes 2 and 3), ladder (lane 4). (C) Proteins eluted from the addition of a high salt buffer to duplicate columns to (B). DNA in each column was the same as in (B). Once again, a band at 33 kDa was the most prominent.

The next step was to confirm that the 33kDa protein was able to bind a motif from the promoter of a different biofilm-specific antibiotic resistance gene in order to confirm the specificity of the interaction. An affinity chromatography experiment was performed using *ndvB* 22bp motif instead of the PA1874-77 22bp motif as the DNA in the column. The high salt eluates from the columns containing the *ndvB* motif showed the same major band at 33kDa along with several minor bands (Figure 10). A comparison of the bands in the high salt elutes from the PA1874-77 and *ndvB* motifs revealed that the 33kDa protein was the most abundant and most consistent band being eluted (Figure 9, Figure 10)

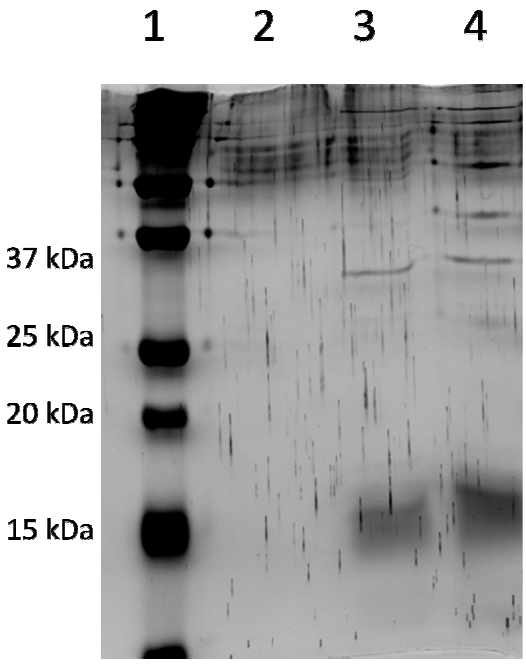

Figure 10: The 33kDa protein is eluted from the *ndvB* motif. Silver-stained SDS-PAGE gel showing the high salt eluates from three separate affinity chromatography experiments. Ladder (lane 1) no DNA negative control (lane 2), *ndvB* 22bp motif (lanes 3 and 4). A band at 33 kDa is visible in lane 3 and 4.

Due to some inconsistencies in running the SDS-PAGE and the silver staining procedure, it was still unclear if the band present at 33kDa was the same in the high salt elutes from both the PA1874-77 and *ndvB* motifs as these were run on separate gels. Although it was not possible to be certain of the identity of each protein without mass spectrometry, running the high salt eluates from the affinity chromatography experiments using the 22bp motifs from PA1874-77 and *ndvB* on the same gel helped minimize differences in running separate gels. Therefore, the eluates from both the *ndvB* and PA1874-77 22-bp motifs (duplicate experiments of each) were run together on a single gel along with high salt eluate from the affinity chromatography experiment using single stranded biotinylated *ndvB* DNA negative control (Figure 11). This gel showed that the 33kDa band present in the high salt elutes from both the *ndvB* and PA1874-77 22bp motif appears to run at the same location. The two 33kDa bands eluted from the *ndvB* motif were pooled (lanes 6 and 7) and sent for in-gel digestion and subsequent analysis via mass spectrometry (Figure 11).

Further analysis of the silver stained gel revealed other bands binding as was mentioned previously. Figure 11 reveals that many of these bands were also binding the single stranded DNA control (lane 10) and were not analyzed. For example, the band at approximately 15kDa that was found in all of the eluates appears to be also be present in the single stranded negative control DNA, although the resolution at the bottom of the gel is not ideal. Regardless, the band present at 33kDa is not only the strongest, but is also the only band that is clearly not present in the eluate from the negative control motif.

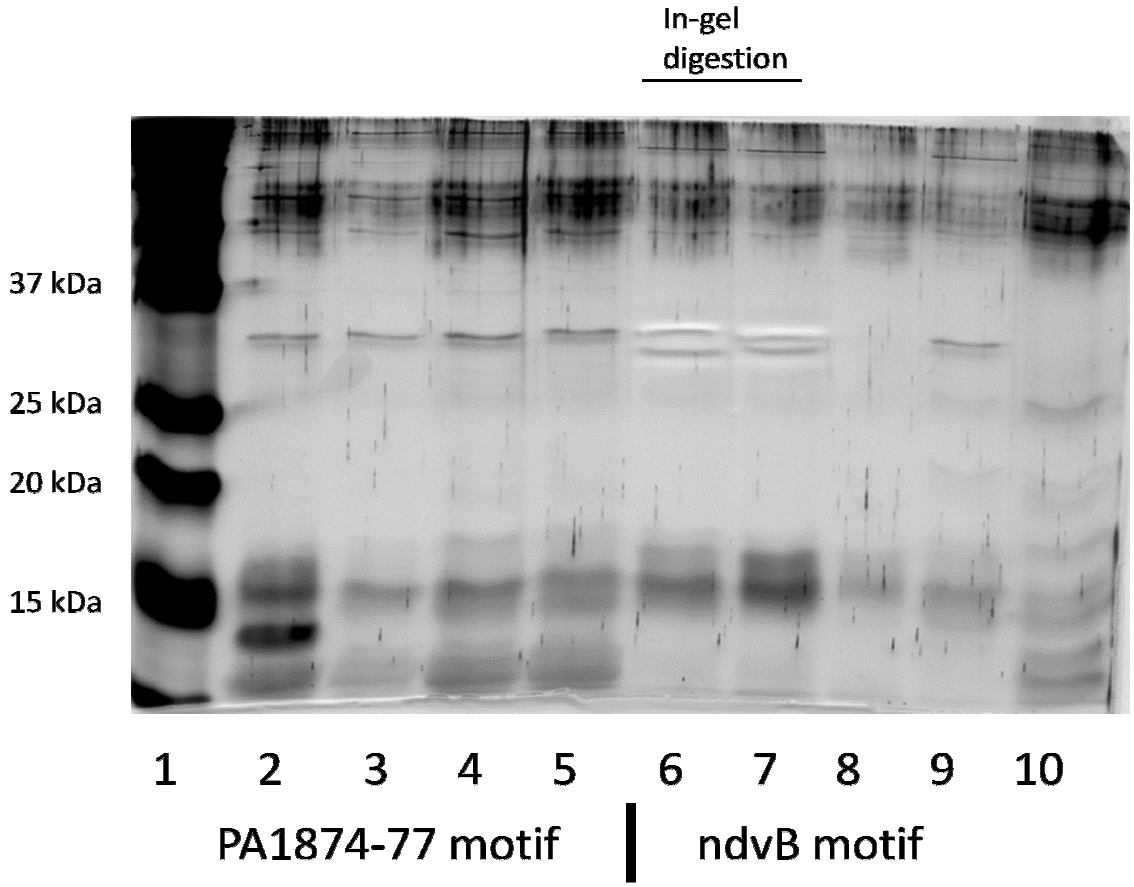

Figure 11: A 33kDa protein is binding the PA1874-77 and ndvB 22bp motifs. Silver-stained SDS-PAGE gel containing the high salt elutes from Figure 9(PA1874-77 22bp motif) and Figure 10 (*ndvB* 22bp motif) as well as the high salt elutes from duplicate columns containing the *ndvB* 22bp motif. Ladder (lane 1), PA1874-77 22bp motif (lanes 2-5) (Figure 9B and C), *ndvB* motif (lanes 6-7) (Figure 10), high salt eluates from a duplicate experiment using *ndvB* 22 motif (lane 8 and 9), single stranded biotinylated oligo negative control (lane 10). The 33kDa band appears to be running to the same location in the gel and the two bands that eluted from the *ndvB* motif were digested and sent for mass spectrometry.

The digested band from Figure 11 was identified as PA0564 using mass spectrometry with a p-value of <0.05. This protein is a putative transcriptional regulator based on in silico data (119). Due to the fact that PA0564 had affinity for the 22bp motifs from the promoter regions of two different genes and was a probable transcriptional regulator, it was cloned into an expression vector in order to create a His-tagged version of the protein. This His-tagged protein was used in an affinity chromatography experiment to assay for a direct interaction between PA0564 and the 22bp motif.

2.3.2 PA0564 is cloned into pET30a and induced in c41s *E.coli* cells

Following unsuccessful induction of PA0564 in pQE30 and unsuccessful cloning of PA0564 into pHisparallel2, a different His-tagged vector (pET30a) was chosen for cloning of PA0564 (Figure 12A). Cloning was successful, and the new plasmid (PA0564-pET30) was transformed into DH5α, BL21 Rosetta and c41s *E.coli* cells (Figure 12A). However, sequencing revealed a missense mutation in the gene, which explained the truncated protein found when looking at Coomassie stained SDS-PAGE gels of induced protein (data not shown). Eventually, a positive clone was found that expressed a protein of 33kDa (Figure 12B). This successful cloning result was also verified by sequencing.

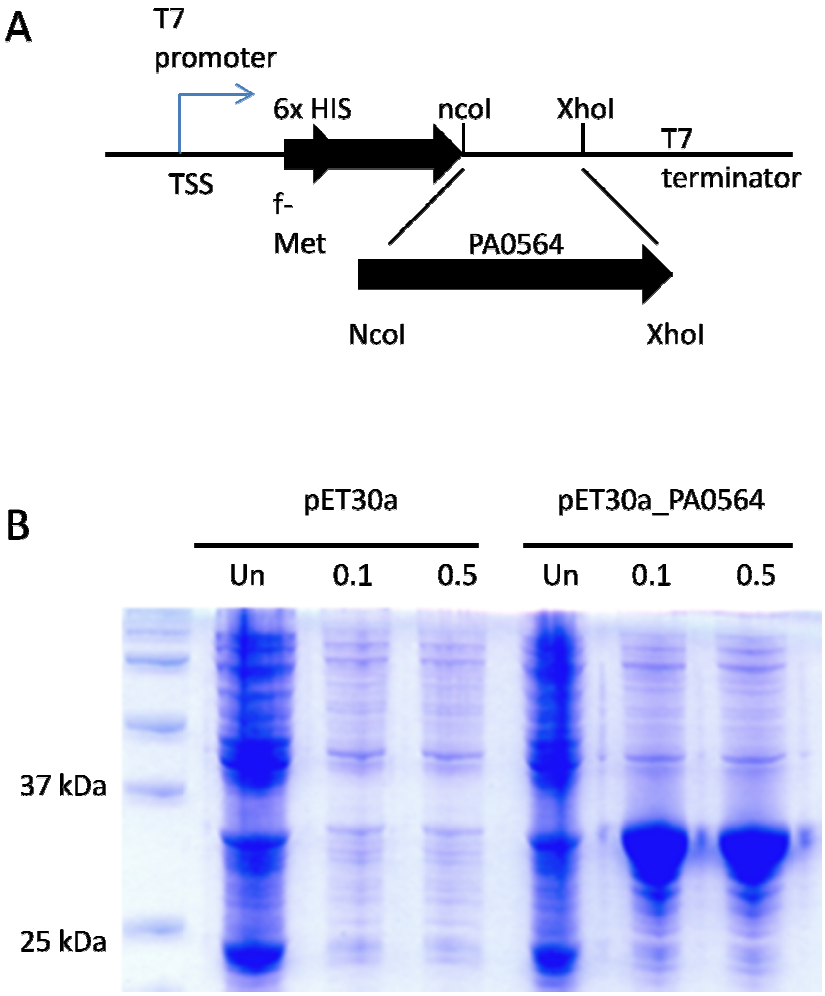

Figure 12: PA0564 is cloned into pET30a and induced in *E.coli* BL21 Rosetta. (A) pET30a MCS. PA0564 was cloned using NcoI and XhoI. (B) Coomassie-stained SDS-PAGE gel showing induced PA0564 at 33kDa in pET30-PA0564 but not in pET30a.
un= uninduced. 0.1= 0.1mM IPTG. 0.5 = 0.5 mM IPTG.

Following confirmation of successful cloning, an assortment of buffers were used during purification in order to determine the conditions in which His-PA0564 was most soluble. Induction in BL21 Rosetta *E.coli* cells revealed that most of the protein was present in the insoluble fraction (Figure 13A). Induction in c4ls *E.coli* cells showed what appears to be a slightly larger fraction of His-PA0564 in the soluble fraction when using a low ionic strength, low pH buffer (Figure 13B, lane 4). It was difficult to determine how much PA0564 was in the soluble fraction as there was a band present in uninduced c41s cells at around the same size. However, it was determined that even though only a small amount of protein may be soluble (Figure 13B, lane 4), these conditions could be used in a large scale purification in order to purify a sufficient quantity of protein.

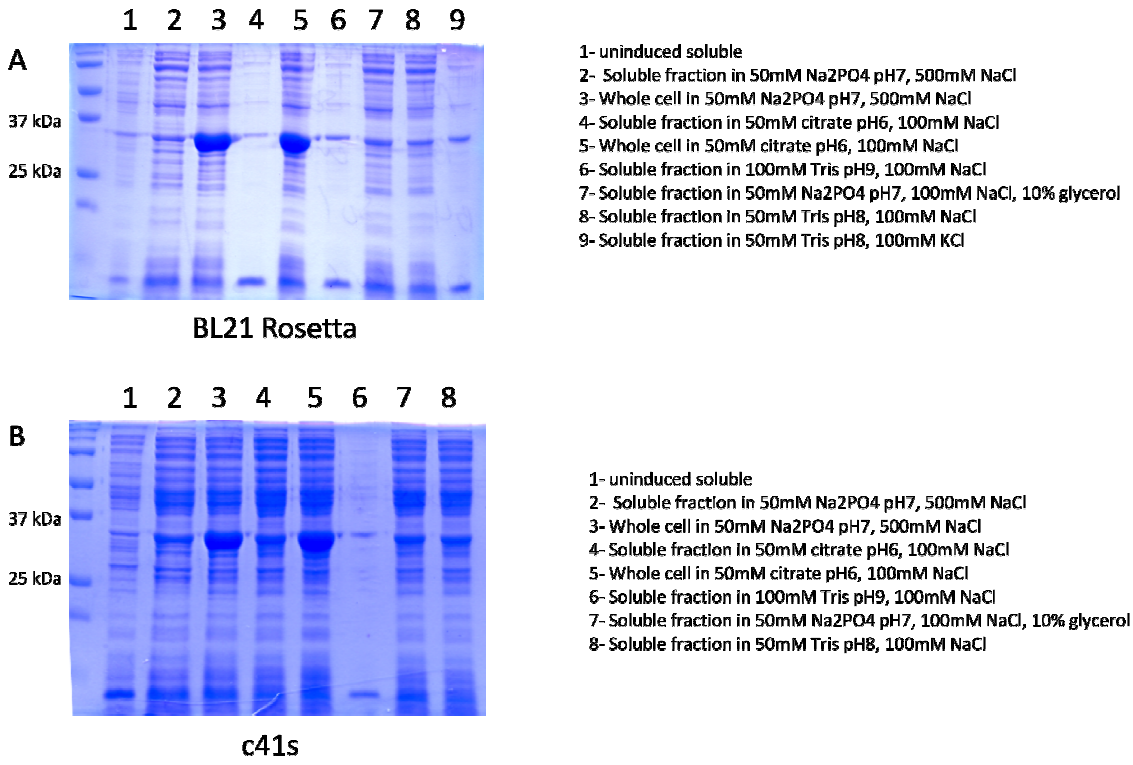

Figure 13: PA0564 purification using various buffers in order to optimize purification conditions. Coomassie-stained SDS-PAGE gel showing whole cell protein and solubilised protein under various buffer conditions in BL21 Rosetta *E.coli* cells (A) and c41s *E.coli* cells (B). The conditions used in (B) lane 4 appear to produce the largest quantity of soluble PA0564.

2.3.3 PA0564 is purified using TALON affinity resin

His-PA0564 was induced with IPTG and purified in 50mM citrate pH6, 100 mM NaCl (Figure 13B, lane 4). A small-scale purification using TALON resin revealed that a significant amount of PA0564 was eluted from the resin (Figure 14, lane 4). However, numerous attempts to repeat this purification were not successful and a sufficient quantity of pure His-PA0564 was not collected.

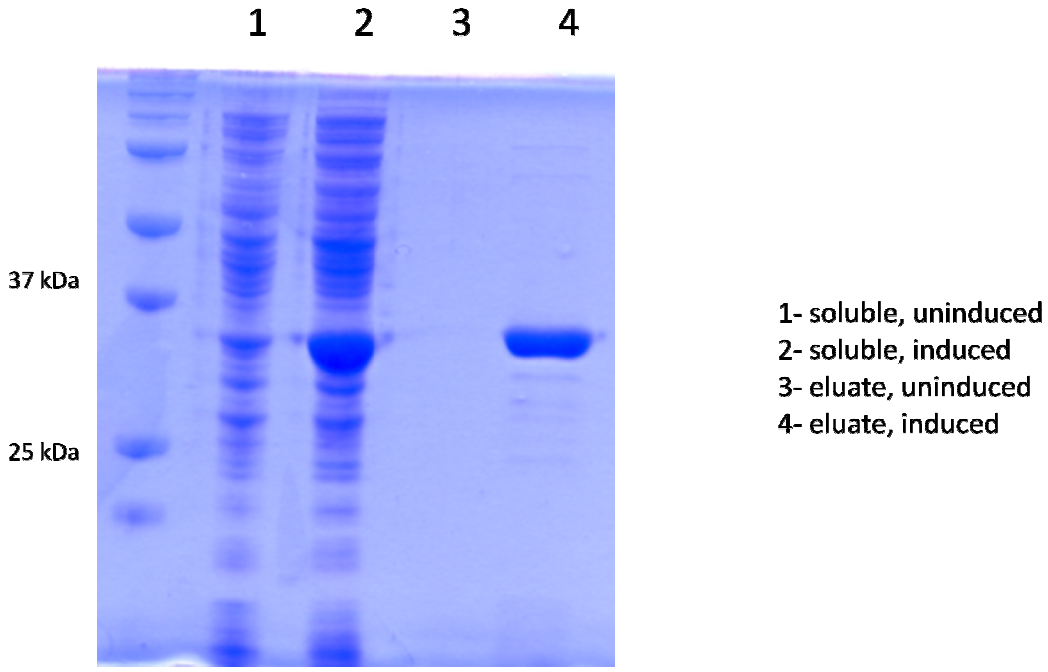

Figure 14: PA0564 is purified using TALON resin. Coomassie-stained SDS-PAGE gel showing fractions following protein purification using TALON resin. A band at 33 kDa is eluted from the TALON resin using 0.5M imidazole and is shown in lane 4.

Throughout the numerous attempts to purify the protein, it was determined that PA0564 requires very specific buffer conditions during the purification in order to remain stable. Through experimentation with an assortment of buffers, it was determined that His-PA0564 was most stable and highly soluble in high ionic strength buffers (> 500mM NaCl), but that purification using the TALON resin under these conditions was not optimal (see discussion) (Figure 15, lane 5).

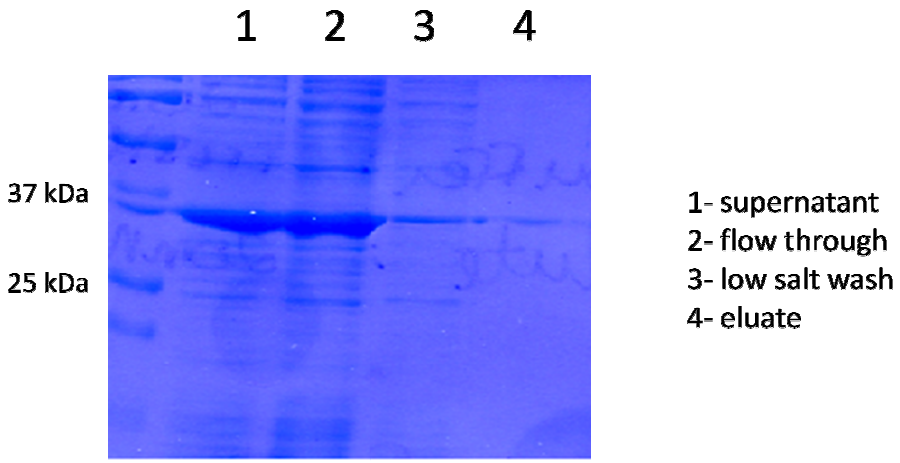

Figure 15: PA0564 is most soluble in high ionic strength buffers but could not be purified. Coomassie-stained SDS-PAGE gel showing the fractions following purification using TALON resin. There is a large amount of PA0564 present in the supernatant prior to purification (lane 1). However, the majority of it does not bind the resin as is shown by the large amount of protein in the flow through (lane 2)

An experiment was designed where His-PA0564 was purified under high ionic strength conditions to maximize solubility. It was then dialyzed from this buffer into a lower ionic strength buffer that is more compatible with the TALON resin. However, the results of this experiment were not successful (data not shown).

Due to that fact that attempts to purify His-PA0564 by collecting large quantities of soluble protein under high ionic strength conditions and subsequent dialysis to a lower ionic strength buffer for purification were unsuccessful, His-PA0564 was induced and purified in moderate (250mM NaCl) ionic strength conditions. Under these conditions a lower quantity of PA0564 was solubilised due to the reduced ionic strength of the buffer. However, this buffer was compatible with the TALON resin for the purification step. Overall, very careful attention was paid to the preparation of buffers for purification. The eluates collected following TALON resin purification from c41s and BL21 Rosetta *E.coli* (Figure 16A, lanes 4 and 8) were pooled prior to dialysis to increase overall protein yield. Following many unsuccessful purification attempts, PA0564 was finally purified, concentrated and successfully stored (Figure 16, lane 3).

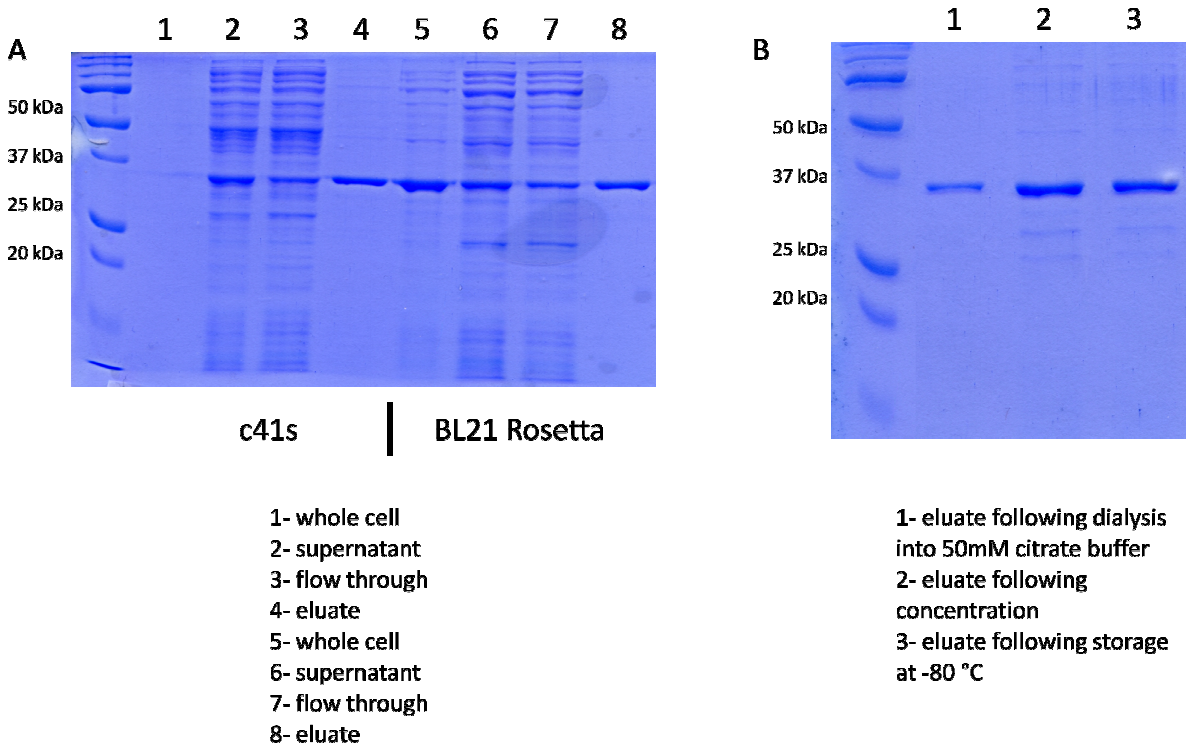

Figure 16: PA0564 is purified, concentrated, and stored at -80°C. Coomassie-stained SDS-PAGE gels containing fractions from the purification of PA0564. (A) Eluates from purification using both c41s and BL21 Rosetta *E.coli.* Lanes 4 and 8 were pooled, dialyzed and ran in (B) lane 1, concentrated (B) lane 2 and stored at -80°C (B) lane 3.

In order to confirm a direct interaction between PA0564 and the 22bp consensus motif, affinity chromatography was performed using purified His-PA0564 from Figure 16B, lane 3. The methodology and conditions for affinity chromatography that was used was identical to the original affinity chromatography that identified PA0564 as binding the 22bp motif from total PA14 biofilm extract. A silver stain of purified PA0564 is shown in Figure 17A. The experiment found that PA0564 bound to the *ndvB* motif (Figure 17B, lane 3), but also bound to the negative control motif (Figure 17B, lane 2). The negative control motif was double stranded and biotinylated and was used as a control for non-specific interactions (Table 3) PA0564 did not bind a negative control column containing no DNA (Figure 17). These results suggest that His-PA0564 is binding non-specifically to double stranded DNA.

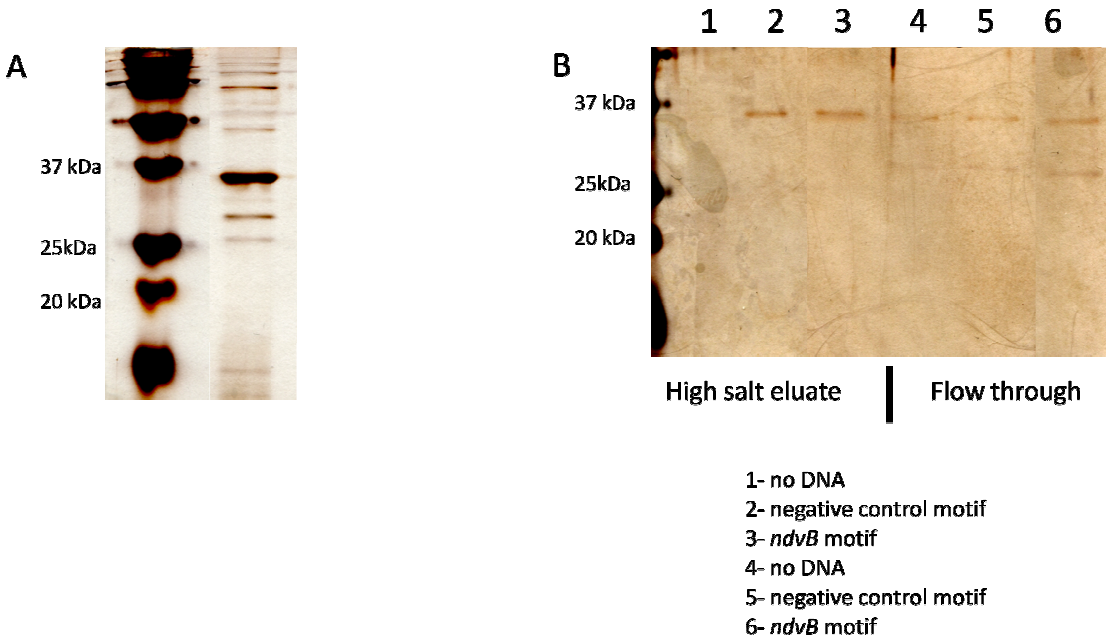

Figure 17: PA0564 binds to both the ndvB and negative control 22bp motif. (A) Silver-stained SDS-PAGE gel showing purified PA0564. (B) Silver-stained SDS-PAGE gel showing the fractions from three affinity chromatography columns. A band at 33 kDa representing PA0564 was present in the high salt elutes from both the negative control motif (lane 2) and the *ndvB* motif (lane 3).

2.4 Discussion

In this chapter, it was shown that a putative transcriptional regulator was binding the 22bp motif from two different biofilm-specific antibiotic resistance genes. Although this discovery was novel and contributes data to a future paper describing the possibility of a regulator of biofilm-specific antibiotic resistance, the specificity of its interaction to the motif remains in question and consequently additional experiments are required to confirm this interaction. The results from this chapter will be discussed herein, in addition to optimization and troubleshooting that occurred at each step in the progress of the experimental work.

2.4.1 MEME

The consensus 22bp motif was found by imputing promoter regions from other genes that contain a known motif into MEME and using the E-value to compare the strength of these motifs to the 22bp motif to determine its significance. For example, the upstream sequences for *qrr1*, *qrr2*, *qrr3* and *qrr4*, four genes that were worked on previously by Sine were imputed into MEME to see how efficiently it could find a known motif, the binding site for sigma-54. MEME identified the known motif with an E-value of 5.4×10^{-3}. Additionally, an E-value of 1.4×10^{2} was found for a previously studied, less conserved motif present that acts as a binding site for LuxO (unpublished data- Sine Lo Svenningsen). The E-value for the 22bp motif consensus was 9.1×10^{1}. This motif's E-value indicates that it is slightly more conserved than the LuxO binding site previously described but not as strong as the sigma-54 binding site. This data confirmed that the 22bp motif is a good candidate to be a regulatory sequence for tandem expression of biofilm-specific antibiotic resistance genes.

2.4.2 Affinity Chromatography

The affinity chromatography experiment and subsequent analysis of the fractions represented in Figure 9, Figure 10 and Figure 11 revealed that a 33kDa protein was binding the *ndvB* and PA1874-77 22-base pair motifs. The band representing the 33kDa protein was cut out of the gel and sent for mass spectrometry. Mass spectrometry matched three polypeptides from the sample to a single protein, PA0564. However, there were other bands present in the eluates that were visible in the silver stain that were not analyzed, but not without appropriate reasoning. Many of the bands that were present were very small (< 15kDa), are out of the range of the typical size of prokaryotic transcription factors (117). In addition, there was significant variation in the bands present in the eluates between duplicate experiments using the same conditions. Finally, many of the proteins smaller than 15 kDa, were being eluted from the single stranded oligo negative control suggesting that they were not specifically binding the double stranded motif. In contrast, PA0564 was consistently found to be present in the eluates from experiments with both the *ndvB* and *PA1874-77* 22bp motifs and as a result was chosen for cloning into the His-tagged vector in order to be studied further. Alternatively, the affinity chromatography with biofilm extract could have been repeated paying special attention to smaller molecular weight proteins binding the column in order to assure that no specific DNA-protein interactions were left unanalyzed.

Although PA0564 was found to bind two different motifs, when *P. aeruginosa* biofilm extract was loaded onto the DNA affinity columns, it was not confirmed whether or not it binds the 22bp motifs from the four other biofilm-specific antibiotic resistance genes. For the

purposes of this thesis, it was decided that using two of the motifs to verify binding of PA0564 was sufficient evidence to clone the gene into a His-tagged vector for analysis of a direct interaction to the 22bp motif consensus.

In order to assay for a direct interaction, purified His-PA0564 was created. Although it is referred to as purified protein, analysis of the Coomassie stained SDS-PAGE gel containing the prepared, frozen elutes reveals that there were other proteins present, albeit in smaller quantities (Figure 16B, lane 3). As a result, it is possible that there is not a direct interaction between PA0564 and the 22bp motif due to the fact that one of the less abundant proteins in the purified PA0564 fraction is acting as an intermediary for this interaction. In order to confirm a direct interaction, purification of PA0564 would need to be repeated paying special attention to non-specific interactions during the purification in to order to create pure PA0564. However, the level of purity was considered sufficient for the experiments using purified PA0564 in this chapter.

The affinity chromatography experiment using His-PA0564 (Figure 17B) revealed that although the protein may be directly binding the 22bp motif, it may also be directly binding any double stranded DNA (Figure 17B, lane 2 and 3). The negative control motif (double stranded) had been used previously in affinity chromatography experiments alongside the *ndvB* and PA1874-77 22bp motifs in order to ensure specificity of the interaction between binding factors out of extract and the 22bp motif. These experiments showed that at times the 33kDa protein bound the negative control motif while at other times it did not, indicating that the conditions for this interaction were very important (data not shown). However, it

was found that PA0564 bound to the *ndvB* and PA1874-77 22bp motif consistently. It was determined from these results that there was sufficient evidence to continue analysis of PA0564 and that the use of His-tagged PA0564 would better determine the specificity of the interaction of PA0564 to the 22bp motif.

In the end, it was found that the interaction between PA0564 and the 22bp motif is likely non-specific due to the interaction between His-PA0564 and the negative control motif (Figure 17B). In order to confirm that this interaction is non-specific, the affinity chromatography experiment should be repeated but with additional negative controls. For example, in addition to the *ndvB* and PA1874-77 motifs, three or more negative control motifs (containing a random sequence of DNA) should be included. Consistent binding between PA0564 and all of the negative control motifs would indicate that PA0564 is non-specifically binding double-stranded DNA. As consistency between experiments was a concern, the running of more than one negative control column would make it easier to determine the specificity of the binding of PA0564 to the 22bp motif consensus.

An alternative method to assay for DNA-protein interactions would be to use an electrophoretic mobility shift assay (EMSA). As there have been difficulties with replicating results as well as specificity between PA0564 and the 22bp motif, the use of a different experimental model would help to decide whether or not PA0564 is important in biofilm-specific antibiotic resistance.

2.4.3 AraC transcription factors

Following the initial identification of PA0564 from affinity chromatography, the protein was analyzed in silico using the *Pseudomonas* genome database (120). PA0564 was predicted to be a transcriptional regulator due to a conserved AraC DNA-binding motif shown to be involved in transcriptional regulation in gram negative bacteria (118). In addition, the collection of protein structural prediction databases listed on the genome database predicted three transcriptional activation domains and no repression domains, consistent with the hypothesis that this protein is acting as an activator in biofilms and not as a repressor in planktonic cells (118).

Transcriptional regulation via AraC-like proteins in *P. aeruginosa* is not a novel concept. AraC-like transcription factors have been found to play significant roles in the regulation of many type three secretion systems (T3SS) through interaction via their AraC-like structure (123). AraC transcriptional activators are characterized by two helix-turn-helix DNA binding motifs (66). In addition to this domain, many AraC proteins contain an N-terminal ligand binding domain that has been found to interact with low molecular weight proteins that act as ligands and can activate transcription (83).

2.4.4 Optimization of the affinity chromatography experiment

In order to determine proteins that have affinity for the 22bp motif, an affinity chromatography-based approach was used to assess potential binding interactions. In comparison to the more common use of DNA-protein interaction methods such as affinity chromatography to isolate and purify known proteins, this procedure was used to isolate and

purify an unknown protein. Consequently, optimization of binding conditions to a specific protein was not possible. Alternatively, binding conditions were initially used in which a large proportion of proteins were stable in order to increase the chances that a binding factor would bind the motif (52) (see Table 5, column 2). Mass spectrometry of the band present in the eluate of the affinity chromatography experiment under these conditions identified the protein as single-stranded DNA binding protein (PA4232), a protein which as its name suggests, binds single stranded DNA non-specifically. Further analysis of the interaction found that it is most likely that PA4232 was not binding the motif, but was actually binding single stranded biotinylated oligo that was in the column.

Once it was determined that the interaction between PA4233 was most likely non-specific (due to the presence of single stranded DNA in the column) the conditions were manipulated individually in order to create a more favorable environment for DNA-protein interactions. In addition to optimizing for an unknown protein, the protocol itself was optimized as it was the first time that such a protocol had been used in the lab. The experimental protocol that was used was created by myself and comprised of parts of past experimental protocols from my supervisor as well as numerous sources that used affinity chromatography in a similar manner (18, 52, 79, 99, 121). There was no established protocol for the experiment that was designed, and as a result various sources were used in order to create a novel protocol. This required additional time and optimization. Table 5 describes some of the parameters of the affinity chromatography experiment that were adjusted through the troubleshooting steps in order to achieve optimal conditions for binding of proteins to the 22bp motif in vitro.

Some important parameters that needed to be varied include the preparation and concentration of proteins in the biofilm extract, the amount of biotinylated oligos added to the column, oligo design as well as the blocking of non-specific interactions. It was found that the concentration of proteins in the extract was important in determining the outcome of the binding interaction. The interaction between DNA-binding proteins and their targets has been studied extensively (85, 89). An important aspect of this interaction is the amount of free protein versus free DNA targets. Every binding factor has a unique binding curve and as a result a unique K_D that describes the equilibrium between bound and unbound DNA (89). Understanding the relationship between protein concentration and the amount of binding sites was important in order to optimize the amount of protein for the amount of available targets on the column. Oversaturation of the column with protein would result in forcing DNA-protein interactions that would not naturally occur.

Other important parameters of the affinity chromatography had to do with the streptavidin-agarose column. In order to reduce protein degradation, column preparation, binding and elution in the column was completed at 4°C. This was one of the major changes between some of the older attempts that did not purify any protein, and successful attempts that found PA0564. In order to add the appropriate amount of DNA to saturate the column, the total amount of available binding sites on the column was calculated. In order to prevent proteins from binding single stranded DNA that may be present on the column, oligos were annealed in a thermocycler at equivalent concentrations. This reduced the amount of single stranded DNA that might be present on the column. Additionally, sheared single stranded

DNA was added to the protein extract to allow for non-specific proteins to bind the single stranded DNA and reduce interaction to the 22-bp motif.

The design of the oligonucleotides was also a critical component of the affinity chromatography experiment. PA0564 was successfully purified using AFFROCHOM 8 and 9, which were designed with ten base pairs added on each side of the motif to minimize the possibility of steric hinderance. However, prior to this successful experiment other oligos were designed and used. These included the addition of a second motif, as well as the addition of more bases adjacent to the 22bp motif (Figure 18)

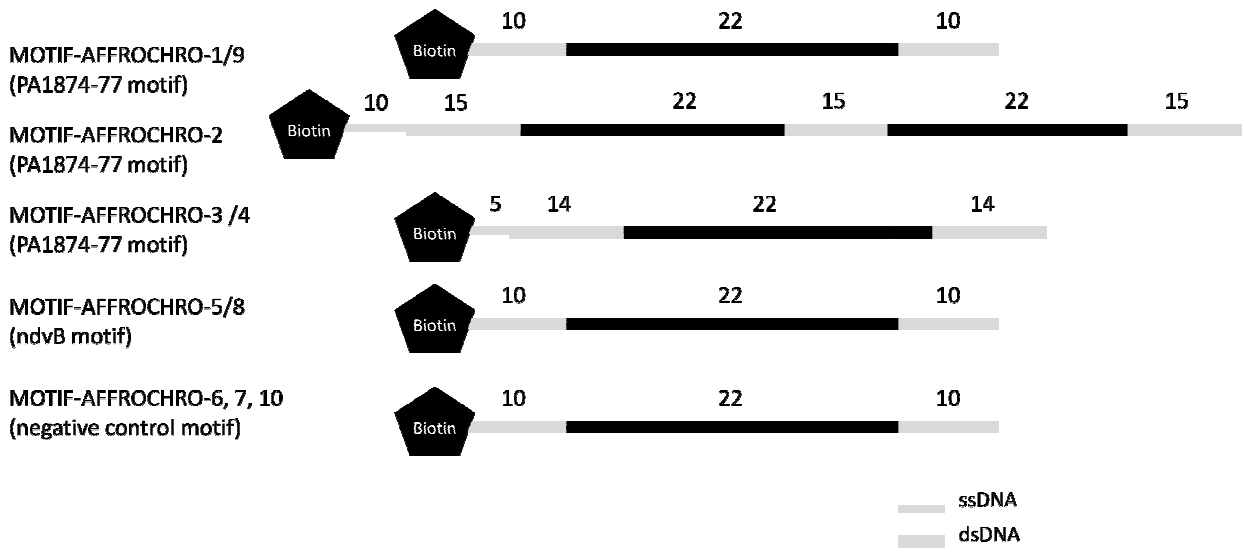

Figure 18: Construction of oligonucleotides containing the 22bp motif for affinity chromatography

In order to reduce non-specificity on the column, bovine serum albumin (BSA) was added to the streptavidin-agarose slurry before the binding reaction to block non-specific protein sites. Sheared salmon sperm DNA was also added to some experiments to block non-specific nucleic acid binding sites. The majority of protocols surveyed suggested <0.1M NaCl for washing and 1.0M NaCl elution during the affinity chromatography (18, 52). Due to the small volume of elution for my column (40µl), it was necessary to increase the concentration of NaCl for elution in order to assure that the actual concentration present in the column would be sufficient for elution.

In addition to optimization of the pull-down experiment, the choice of buffer was also important. Since we did not know the identity of the protein being pulled-down, a general buffer in which wide assortment of proteins are stable was chosen. The buffer that was chosen was affinity chromatography buffer (ACB) due to the fact that many proteins are stable and also due to the success my supervisor had using this buffer for protein purifications (63). This buffer was similar in composition to the buffers used by other groups that also purified transcription factors from bacterial extract (18, 80, 99). It was additionally important to use a buffer with high ionic strength due to the fact that PA0564 is a transcription factor and has affinity for chromosomal DNA. Use of a low ionic strength buffer would significantly reduce the amount of transcription factors available for binding to the column as they would have affinity for their binding sites on chromosomal DNA (124).

The totality of the changes listed above in addition to other changes that were not discussed resulted in the discovery of PA0564 binding to the 22bp motif consensus. The specific parameters used in the identification of PA4232 and PA0564 are listed in Table 5.

Table 5: Specific parameters used in Affinity chromatography for the purification of PA0564 and PA4232

Parameter	PA0564	PA4232 (Initial conditions)
pH (buffer)	6.7	7.0
BSA (blocking)	Added to column	Added to column
Carrier DNA	Added to biofilm extract	Added to column
DNA amount added to column	250pmol/µL x 40µL loaded / column	5 pmol/µL x 20µL loaded / column
Oligo Identity (Figure 18)	AFFROCHROM 8/9/10	AFFROCHROM 3/4
Protein Extract Preparation	Colony Biofilm assay (2.2.1.1)	Colony Biofilm assay (2.2.1.1)
Protein Extract Concentration	1.0 mg/mL	0.4 mg/mL
Elution conditions	1.5M NaCl ACB	2.0M NaCl ACB
Protease Inhibition	Protease Inhibitor Cocktail	PMSF
Binding Time/ Temperature	2 hours, 4°C	30 minutes, 22°C
Cofactors	5mM MgCl2	5mM MgCl2

It became apparent during the affinity chromatography experiments using purified PA0564 that the ionic strength of the buffer was very important. Through experimentation with different buffers and protocols, it became clear that the solubility of induced protein was greatly increased under high ionic strength conditions. This makes sense as high ionic strength conditions disturbs protein-DNA interactions and releases the most amount of protein during cell purification. However, the use of high ionic strength buffers during the cell preparation stage made it difficult to purify using the TALON resin as the eluates did not contain the desired protein (19). When low ionic strength conditions were used, the solubility was low, and purification would yield a small amount of protein. In the end, the perfect conditions were found that balanced solubility during cell preparation and a low enough ionic strength buffer to allow for His-tag- cobalt interaction on the resin.

2.4.5 Troubleshooting with cloning/ induction

In addition to the optimization that occurred with the affinity chromatography, significant troubleshooting was completed in order to create a His-tagged PA0564. In the end, cloning was completed with three different His-tagged vectors. However, a successfully cloned and induced PA0564 could only be completed with pET30a which was used for the production of pure PA0564.

2.4.5.1 Cloning of PA0564 in pQE30

Once PA0564 was identified as binding the 22bp motif of both *ndvB* and PA1874-77, it was cloned into a His-tagged expression vector (pQE30 from Qiagen) for eventual

expression and purification. Following confirmation of successful cloning through PCR and restriction digests, the new plasmid was transformed into BL21 Rosetta, DH5α and c41s *E.coli* cells. Numerous attempts at inducing PA0564 were unsuccessful, and it was suggested to try cloning the gene in a different vector.

2.4.5.2 Cloning of PA0564 into pHisparallel2

PA0564 was then cloned into a His-tagged vector (pHisparallel2) in order to try and induce protein expression. PA0564 cloning was confirmed by PCR and restriction digests. PA0564 was transformed into BL21 Rosetta, DH5α and c41s *E.coli* cells. Initial induction of PA0564 was not successful. pHisparallel2_PA0564 was sequenced which revealed that the gene had not been cloned in properly. More clones were sequenced, which revealed negative results. It was at this point that pET30a was chosen for the cloning of PA0564, which eventually resulted in the creation of a successful construct.

2.4.6 Final thoughts

Taken together, the concepts discussed suggest that a protein that binds the 22bp motif from the *ndvB* and PA1874-77 promoter was identified, but that this interaction may not be specific. Therefore, this regulator needs to be studied more extensively in order to determine its specificity for the 22bp motif consensus, keeping in mind the importance of binding conditions in this interaction. The potential outcomes following determination of a specific reaction between PA0564 and this motif may be large. Targeting a regulator that has many downstream effectors is a very important approach to the treatment of biofilm-based antibiotic resistance in the future. The Mah lab has shown that individually assessing biofilm-

specific mechanisms of antibiotic resistance does not fully explain the importance of these genes. Biofilm-specific antibiotic resistance assays using deletion mutants of individual genes usually only shows a two- to four- fold difference in sensitivity between the wild type and the deletion mutant depending on the antibiotic (125, 127). This is in contrast to similar sensitivity testing done with deletion mutants of planktonic mechanisms where the difference in sensitivity may be as high as 50 to 100 fold or more (64). Potentially, a deletion mutant of a regulator of biofilm-specific antibiotic may be able to show a similar sensitivity profile to that found in planktonic cells, where a large increase in sensitivity to a panel of antibiotics occurs. Not only will this have important implications in understanding antibiotic resistance, but it will also have an impact on the status of biofilm-driven antibiotic resistance in the field as a whole.

The diversity of antibiotic resistance mechanisms in biofilms makes it difficult to approach potential methods to treat biofilm-based diseases. Targeting the regulator of biofilm-specific antibiotic resistance genes has the potential to transform our understanding and treatment of antibiotic resistance in biofilms. The results laid out in this chapter are just the very beginning of an investigation into how the biofilm-specific antibiotic resistance genes studied in the lab are regulated. Following confirmation that PA0564 (or another yet to be discovered protein) binds to the 22bp motif, the next step is to confirm that a deletion mutant of this gene has an effect on antibiotic resistance through the use of antibiotic resistance assays and qPCR. These critical experiments will determine how important of a role the regulator plays in triggering expression of the six biofilm-specific antibiotic resistance genes. It is expected that deletion of PA0564 may have drastic effects on

antibiotic resistance in biofilms as there will be cessation of activation of all 6 independent mechanisms of antibiotic resistance in biofilms. A large drop in resistance of the deletion mutant to antibiotics will open the door for a numerous experiments to not only determine the mechanism of activation but also to quantify the resistance effects based on the antibiotic class that is used in order to pinpoint particular antibiotics that may be of use to the treatment of *P. aeruginosa* biofilm infections. It will also be important to discover methods to upregulate the expression of the regulatory protein.

Upon confirming that the protein has the ability to regulate antibiotic resistance, it should be established that it binds to all six 22bp motifs through either affinity chromatography or EMSA experiments. Successful binding to other motifs and the finding of a strong antibiotic sensitivity phenotype in the deletion mutant would certainly confirm the importance of this finding and lay down the rationale for future studies on the mechanism of action of it as an activator of biofilm-specific antibiotic resistance.

CHAPTER 3. TEMPORAL AND SPATIAL GENE EXPRESSION OF BIOFILM-SPECIFIC ANTIBIOTIC RESISTANCE GENES IN *PSEUDOMONAS AERUGINOSA*

3.1 Introduction

3.1.1 Heterogeneity in biofilms

The goal of the experiments described in this chapter is to examine the usefulness of promoter-fluorescent protein constructs in the analysis of spatial and temporal gene expression in biofilms. The rationale for this chapter comes from the difficulties in studying gene expression within regions of cells, especially within biofilms. Biofilms are unique in that there are numerous microgradients of nutrients and waste products that create a diversity of chemical environments within the biofilm itself (102, 104). This diversity of chemical environments has effects on gene expression of regions of cells depending on where they are located in the biofilm. The result is differences in gene expression between cells depending on their exact location in the biofilm. Thus, analysis of gene expression from the whole biofilm does not accurately represent gene expression of individual cells within a biofilm, and simply represents the average pattern of expression. The use of promoter-fluorescent protein constructs allows for the study of gene expression within small regions of cells, a technique that is useful to resolve the heterogeneity of the biofilm.

Commonly used techniques to analyze gene expression such as qPCR negates the unique heterogeneity present within biofilms. Another method to study gene expression in biofilms is the use of a DNA microarray. However, previous studies have identified numerous concerns with this method including the large effect of the culturing methodology on gene

expression as well as loss of unique differences in gene expression when averaging from a biofilm sample (5). Heterogeneity in biofilms is important as it may explain why the biofilm-specific antibiotic resistance genes may be expressed at different levels within the same biofilm, which is the focus of study in this chapter (11).

The creation of promoter-fluorescent protein constructs presents an alternative approach to study spatial and temporal gene expression in biofilms. This technique can be paired with the use of new technologies that can isolate certain components of the biofilm. Laser-capture microdissection microscopy is one of those techniques used to both isolate small sections of a biofilm and analyze gene expression through PCR (31, 58). For example, within mature macrocolonies the fast growing areas can be isolated from the slow growing areas of the biofilm. Although this is a powerful technique that allows quantitative analysis of gene expression between areas within the same biofilm, it is limited in the amount of areas that can be compared within a single biofilm (102).

Although it is known that the six biofilm-specific antibiotic resistance genes studied in the Mah lab are expressed at a higher level in biofilms as compared to planktonic cells, it is unknown exactly how expression is distributed amongst individual cells within the biofilms (10, 56, 64, 72, 126, 127). Are there differences in gene expression between more rapidly dividing cells versus slower growing cells due to their location in the biofilm? The physiological heterogeneity of small regions of cells within a biofilm is the result of numerous factors that affect gene expression. One of the main factors that governs heterogeneity in biofilms is the presence of large chemical gradients in nutrients, signals and waste products

(67). In addition to chemical gradients, stochastic gene expression, and genotype differences due to mutations also affect gene expression in biofilms resulting in a very complex heterogeneous environment in biofilms (1, 38, 67). For example, small differences in oxygen concentration are further exacerbated as the biofilm develops and becomes more complex (28). Once these chemical gradients are established, the physiology of cells within the biofilm is uniquely affected depending on where they are located.

Analysis of spatial expression will reveal the locations in which biofilm-specific antibiotic resistance genes are expressed within a developed biofilm. This will be examined using promoter-fluorescent protein constructs. Analysis of temporal expression will reveal the stage in the biofilm development cycle in which biofilm-specific antibiotic resistance genes begin to be expressed. As discussed in the chapter 1, there is a well defined development cycle that characterizes *P. aeruginosa* biofilms (Figure 1) (76). Understanding the specific stages at which these genes are expressed will help with overall understanding of biofilm-specific antibiotic resistance.

3.1.2 Fluorescent-protein constructs

Promoter fluorescent-protein constructs are created by cloning the promoter of the gene of interest into a vector upstream of a fluorescent protein. Activators and repressors bind the promoter which either increases or decreases transcription of the gene encoding the fluorescent protein. Overall transcription from that promoter can be visualized through fluorescence microscopy. Thus, fluorescence is a reporter for gene expression within each cell.

In addition to spatial differences, the fluorescent-protein constructs can be used to assay temporal differences in gene expression of groups of cells within the biofilm microenvironments keeping in mind that the maturation of the fluorescent protein is dependent upon factors that may not be consistent across all regions of the biofilm. Analysis of temporal differences will not only help to determine collectively whether or not the genes are expressed at a particular cell density, but also when the genes are active in specific regions of the biofilm. Biofilms containing the promoter-fluorescent protein constructs were grown and visualized at set time-points over the course of biofilm development to analyze expression of biofilm-specific antibiotic resistance genes in the different microenvironments. It is hypothesized that biofilm-specific antibiotic gene expression will differ temporally due to the heterogeneous nature of biofilms.

3.1.3 Yeast cloning to create promoter-fluorescent protein constructs

The creation of the promoter-fluorescent protein constructs was completed using homologous recombination in *Saccharomyces cerevisiae* (herein referred to as yeast). This is a unique method of cloning DNA that does not require restriction sites on each side of the insertion location. Homologous recombination in yeast was first identified in 1979 (106). However, this technique was not used in molecular biology laboratories for cloning until the late 1990's when Oldenberg et al began harnessing the power of yeast to create new plasmid constructs (75). This method is very useful because multiple pieces of DNA can be cloned into a plasmid in one reaction as long as the primers for the PCR of each fragment include 15-20 bases on homology to the plasmid to the fragment on either side to allow for yeast to perform homologous recombination of the PCR amplicon into the plasmid (97).

Recently, Shanks et al have developed numerous yeast-*Escherichia coli-Pseudomonas aeruginosa* shuttle vectors containing various features including inducible promoters that drive the expression of GFP. Some critical components of these inducible plasmids include URA3 which allows for the synthesis of uracil and *aaC1* which provides gentamicin resistance. These genes allowed for plasmid selection in yeast and bacteria respectively. Following the creation of novel constructs in yeast, they can be easily transformed into *E.coli* and subsequently conjugated to *P.aeruginosa.*

The first promoter-fluorescent protein construct created in the lab was made by Sarah Copeland (former technician). Sarah created an *ndvBp-GFP* construct by replacing the endogenous *araC*-inducible promoter P_{Bad}, with the *ndvB* promoter region thereby creating pSC01 (Figure 19) (74, 97). Normally, the P_{Bad} promoter is positively regulated by AraC protein in the presence of arabinose, whereas AraC binds the promoter and blocks transcription when arabinose is not present (74). However, P_{Bad} was removed during homologous recombination in the creation of pSC01 and thus GFP expression is solely under the control of the newly cloned *ndvB* promoter region. pSC01 was used to analyze activity of the *ndvB* promoter and also acted as the basis for the cloning of promoters and fluorescent proteins to create novel constructs including the design for a PA1874-77p-mCherry construct. *ndvB* and PA1874-77 were both chosen as the first genetic loci to study spatially and temporally due to their well characterized biofilm-specific antibiotic resistance phenotypes (64, 127).

mCherry was chosen as a second fluorescent protein to be used in our system due to its minimal excitation (587 nm) and emission (610 nm) peak spectrum overlap with GFP (95). It was also chosen due to its low half-life of 45 minutes, making it ideal for real-time analysis of spatial and temporal gene expression as well as it being ten times more photo-stable as compared to its parent, RFP (95). Additionally, mCherry has been shown to be expressed successfully in *Pseudomonas aeruginosa* (57).

The original goal of this project was to use the differences in absorption between GFP and mCherry to our advantage by growing mixed biofilms (both constructs together in one biofilm) in order to compare spatial and temporal expression of these two genes. However as the project progressed this approach was revised to encompass only individual assessment of spatial and temporal expression of biofilm-specific antibiotic resistance genes due to the recognition of complicating factors most notably the difference in the maturation between mCherry and GFP that will be discussed throughout this chapter.

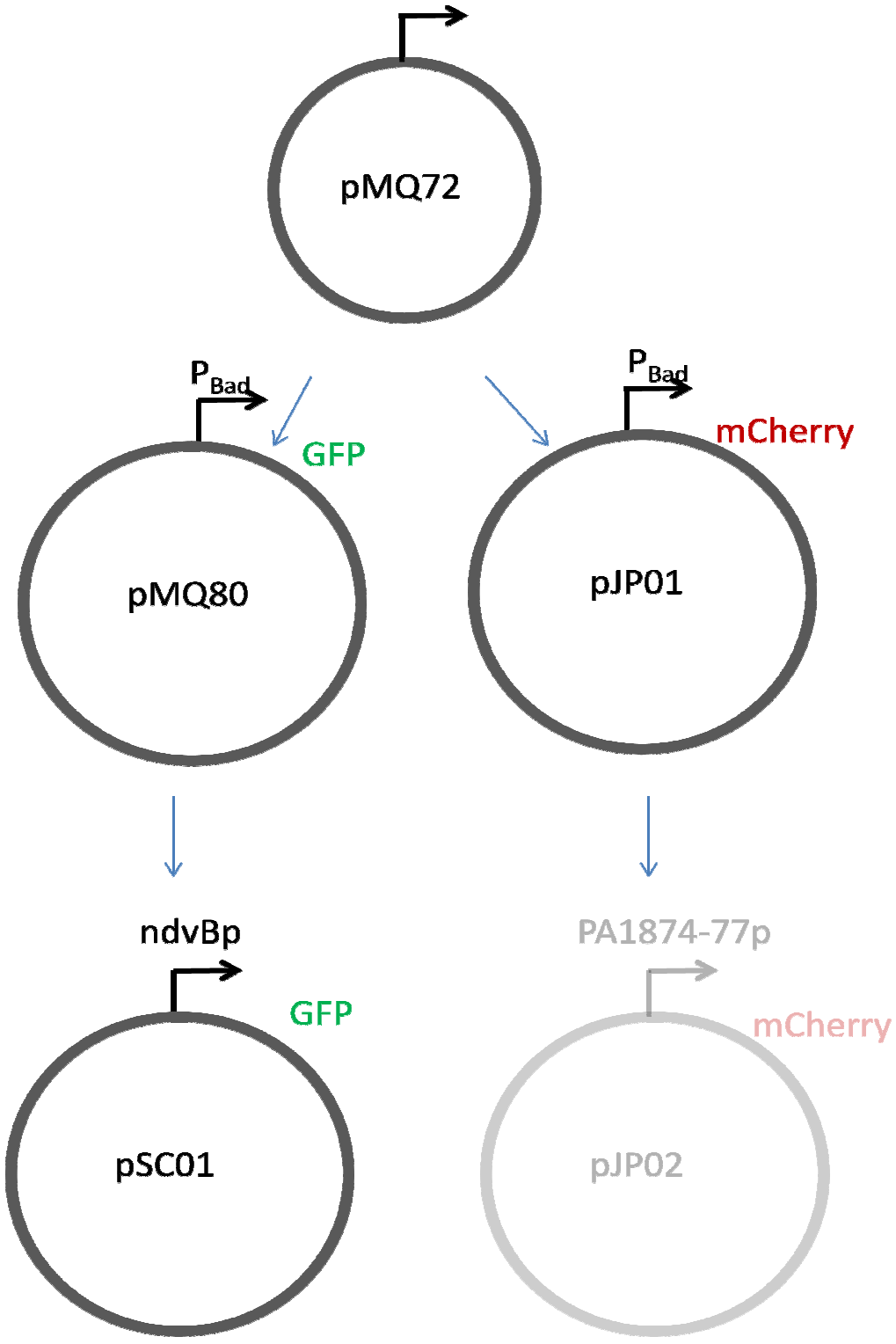

Figure 19: Plasmid Organization for chapter 3

3.1.4 Biofilm-specific antibiotic resistance genes

The biofilm-specific antibiotic resistance genes that are studied in the lab are ideal candidates for study of spatial and temporal variations. Individually, biofilm formation and antibiotic resistance genes are believed to be controlled by some of the more complex regulatory networks in the *Pseudomonas* genome although the details of these networks remains vague (8). Numerous regulators have been identified that play a role in both biofilm formation and antibiotic resistance and are described in Balasubramaniam et al (8). As a result, it is likely that expression of biofilm-specific antibiotic resistance genes will be influenced by the diverse heterogeneity that is found in biofilms due to the complexity of regulatory networks found. Furthermore, the 22bp motif that was analyzed in chapter 2 is part of the promoter region of all six biofilm-specific antibiotic resistance genes. The results from the analysis of promoter-fluorescent constructs and the discovery of regulators binding the 22bp motif can be used together to better understand regulation of expression of biofilm-specific antibiotic resistance genes in biofilms.

Together the results presented in this chapter both describe temporal expression of *ndvB* using pSC01 (*ndvB*p-GFP) as well as provide the framework for the more general use of promoter-fluorescent protein fusions for the study of biofilm-specific antibiotic resistance genes in the lab in the future.

3.2 Materials and methods

3.2.1 Bacterial strains and growth conditions

Bacterial strains (Table 6) were grown in Luria-Bertani [LB] or minimal medium at 37°C. The minimal medium consisted of M63 salts supplemented with arginine (0.4%) and $MgSO_4$ (1mM). *Saccharomyces cerevisiae* was grown in YPD (1% yeast extract, 2% peptone, 2% dextrose) or in uracil dropout medium (synthetic complete amino acids and nucleic acids without uracil) at 30°C. 100mM of L-arabinose was added as an inducer for plasmids containing the P_{Bad} promoter. Plasmids used in this chapter are listed in Table 7. Since plasmid selection using antibiotics was an important aspect of many of the experiments presented in this thesis, the concentration of antibiotics that were used for each strain are listed in Table 8.

Table 6: Bacterial strains used in Chapter 3

Strains	Relevant Characteristics	Strain I.D	Origin
E.coli			
DH5α		JPP5	TFM225
S17-1 λ pir		JPP6	TFM224
P. aeruginosa PA14		JPP1	TFM53
S.cerevisiae WTα	Ura- Gm^R	TFM172/JPP4	Baetz Lab, BMI

Table 7: Plasmids used in Chapter 3

Plasmid	Relevant Characteristic	Origin
pMQ80	P_{Bad}_GFP, Gm^R	O'Toole Lab (97)
pSC01	*ndvB*p_GFP, Gm^R	Mah Lab
pMQ72	Gm^R	O'Toole Lab (97)
pJP01	P_{Bad}_mCherry, Gm^R	Mah Lab
pLink	mCherry	Copeland Lab, CMM, University of Ottawa

Table 8: Final drug concentrations used for antibiotic selection of plasmids in *P.aeruginosa*, *E.coli* and *S.cerevisiae*

Strain	Final drug concentration (μg/mL)			
	Kanamycin (Kn)	Chloramphenicol (Chlor)	Gentamycin (Gm)	Ciprofloxacin (Cipro)
P. aeruginosa PA14	100	N/A	75-100	N/A
E.coli (all strains)	50	50	20	0.1
S. cerevisiae WT	N/A	N/A	15	N/A

3.2.2 Construction of pJP01

Yeast cloning was used to clone mCherry into pMQ72, a suitable vector for future cloning of promoters to create the promoter-fluorescent protein constructs. pJP01 was created in order to clone the PA1874-1877 promoter upstream of mCherry to create a promoter-mCherry construct. The constructs were created using the yeast transformation (30) and yeast smash n' grab miniprep (48) protocols as adapted by Shanks et al (97) and described below.

3.2.2.1 PCR of mCherry

PCR was performed with mCher-F/R-1 primers (Table 9) which not only amplified mCherry, but created regions of homology to the cloning vector pMQ72 needed for yeast homologous recombination. mCherry was amplified out of pLink, a mammalian vector that was obtained from the Copeland lab (Department of Cellular and Molecular Medicine, University of Ottawa). The PCR master mix consisted of the following components in 50 µL final reaction volume; 2 µL pLink, 8 µL Band Sharpener, 2 µL 10mM dNTPs, 1 µL forward primer (10pmol/ µL), 1 µL reverse primer (10pmol/ µL), 5 µL 10X buffer and 1.5µL Taq polymerase. All PCR components were from Feldan. The PCR was run in the MyCycler thermocycler from Bio-Rad with the following reaction conditions: an initial denaturation at 95°C for 3 minutes followed by 15 cycles of denaturation at 95°C for 10 seconds, annealing at 52°C for 30 seconds and extension at 70°C for 30 seconds. 35 more cycles of denaturation at 95°C and extension at 70°C then occurred followed by a final extension for 10 minutes to end the PCR. PCR products were run on a 1.0% DNA agarose gel to verify amplicon size. PCR products were purified using a PCR purification kit (Invitrogen).

3.2.2.2 Digest

pMQ72 vector was digested with SmaI (NEB) at 37°C for 1.5 hours. Digests were performed in duplicate in a final volume of 50 µL consisting of 5µL buffer, 2µL SmaI, and 8µL plasmid DNA. Digests were confirmed by running both digested and undigested pMQ72 on a gel and comparing band size between the digested and undigested samples.

3.2.2.3 Yeast Transformation

As per the Shanks et al yeast transformation protocol, wild-type *S.cerevisiae* was inoculated into liquid YPD and grown for 24 hours at 30°C in order to prepare a culture for transformation. Following growth, 0.5mL of the 24 hour culture was spun down and rinsed with TE buffer. The cells were spun down again and mixed with 0.5mL lazy bones solution (97), 1µL restriction-digested plasmid, 2µL salmon sperm DNA at 2mg/mL (Sigma) and 3µL mCherry PCR product. The cells were vortexed for 1 minute and then incubated at room temperature for 20 hours. The cells were then heat shocked for 12 minutes at 42°C and then centrifuged at 10,000g. Pelleted cells were resuspended in 150µL TE buffer and plated on ura^- plates to select for transformants. Ura^- plates were incubated for a minimum of 72 hours.

3.2.2.4 Yeast Miniprep

A toothpick was used to collect one large colony from the ura^- plate and transfer it to 100µL TE buffer. The colony was vortexed into the buffer and then spun down at 10,000 rpm for 10 seconds. 200µL smash n' grab buffer (1% SDS, 2% Triton X-100, 100mM NaCl, 10mM Tris-HCl pH8, 1mM EDTA) was then added to the pellet. 0.3g of 0.5mm glass beads were

added to the tubes as well as 200µL of a 1:1 phenol: chloroform mix. The tubes were then vortexed continuously for 2 minutes on full speed to break open the cells and then centrifuged for 5 minutes at 13,000 rpm. The supernatant was recovered and purified using a PCR purification kit (Invitrogen).

3.2.2.5 Transformation of pJP01 into *E.coli* (DH5α and S17-1)

Miniprepped DNA isolated from the yeast cells was transformed into *E.coli* DH5α. Competent DH5α cells were made using the ultra-competent Inoue method (Inoue et al 1990). 10µL of yeast DNA was added to 100µL competent DH5α cells for 30 minutes on ice. The cells were heat shocked for 90 seconds at 42 °C and then put back on ice. The cells were added to 800µL LB and incubated on a shaker at 37 °C for 75 minutes. 150µL of the incubated broth was plated on 20µg/mL gentamycin selection plates and incubated overnight. Screening of transformants was done by picking 10 colonies from these plates and growing overnight cultures under antibiotic selection followed by a plasmid miniprep and PCR of mCherry from the miniprep. A successful clone was chosen and stored in DH5α, and was also transformed into S17-1 using the same protocol that was used for transformation into DH5α. Competent S17-1 cells were made using the calcium-chloride method (92). Successful S17-1 transformants were used to conjugate pJP01 into *P.aeruginosa.*

3.2.2.6 Conjugation of pJP01 into PA14

An overnight culture of the recipient strain (PA14) was grown at 42 °C, while an overnight of the donor strain (*E.coli* S17-1 + pJP01) was grown at 37 °C. These cultures were mixed together in a 1:1 ratio following overnight growth. The mixed culture was spun down

at a speed of 12,000 rpm for 1 minute and the pellet was resuspended in 30µL of LB. The resuspended cells were dispensed onto an LB plate for overnight growth at 37 °C. Following growth, the bacterial lawn was scraped off the plate using the tip of a pipette and resuspended into 500µL of LB. The cells were fully resuspended in this LB before being plated on gentamycin and ciprofloxacin counter selection plates. *P. aeruginosa* colonies were then screened for pJP01 by miniprep and PCR as was done following transformation into DH5α.

3.2.3 Fluorescence microscopy

Both planktonic and biofilm cells were visualized using the Leica DMI6000B phase-contrast microscope with GFP and TX2 filter cubes.

3.2.3.1 Coverslip biofilm assay

The wells of a 6-well plate (Corning) were filled with 4 mL of 1xM63. The wells were inoculated with the appropriate strain of bacteria (1:75 dilution of an overnight culture) and antibiotics (Table 8) if necessary. An autoclaved, cut pipette tip was placed into each of the wells using sterile tweezers. The tip was used to anchor a coverslip inside the well in order to create an air liquid interface as is seen in Figure 20. No 2 coverslips (Fisher) were sterilized by immersing in 95% ethanol and flaming before placing them against the pipette tip in the well. The plates were incubated at 37 °C for 24 hours. Upon collection, coverslips were rinsed with 1XM63 in order to remove planktonic cells before being transferred to a microscopy slide for visualization. 5µL of media was added on the slide before placing the coverslip down for visualization. This was done to reduce the chances that the bacteria would filament in

response to being removed from liquid prior to taking pictures. A small amount of clear nail polish was added around the edge of the coverslip to keep it in place during visualization.

3.2.3.2 Visualization of planktonic cells

LB agarose was prepared in a 250 mL glass Erlenmeyer flask by adding 0.3g agarose to 40mL LB and heating for approximately 1 minute in a microwave. LB agarose was kept warm in a water bath set at around 65 °C to prevent it from solidifying. Slides were prepared by diluting overnight culture with LB (dilution varied with OD_{600} of the culture). Diluted cultures were mixed 1:1 with the warm LB-agarose. 3µL of this mixture was added to a slide and quickly covered with a coverslip and visualized. Agarose was needed to immobilize the individual planktonic cells. This provided the opportunity for phase contrast and fluorescence images to be taken.

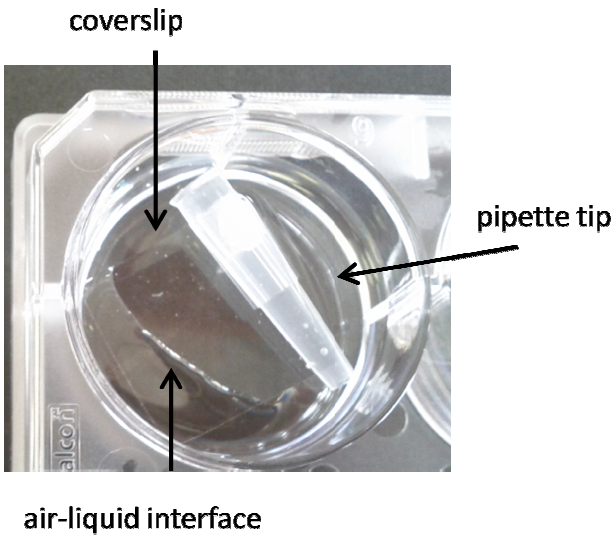

Figure 20: Coverslip biofilm assay

3.2.4 Western blot

10% SDS-PAGE gels were poured and polymerized (Section 2.2.1.5) and run at 110V until the dye front reached the end of the gel. The gels were then transferred to a nitrocellulose membrane, using a transfer cassette, and ran at 110V for one hour. The gels were incubated with ponceau stain to check for protein concentration. The gels were then rinsed of the ponceau stain and blocked with 1X PBS- 5%-milk- 0.1% Tween-20 solution. Following blocking, the gels were incubated with the primary antibody (goat anti-GFP) (Roche) at a 1:1000 dilution (Roche) for one hour, and then washed three times with a PBS-Tween solution. The gels were then incubated with the secondary antibody (rabbit anti-goat HRP) at a 1:5000 dilution for one hour. Following three washes in PBS-Tween, the gels were visualized using electrochemiluminescence.

Table 9: Primers used in Chapter 3

Name	Sequence (5' to 3')	Direction	Use
mCher-R-1	AATCTTCTCTCATCCGCCAAAACAGCCAAGCTTGCATGCCTGCAGACTAGCCTACTTGTACAGCTCGTCC	Reverse	Cloning mCherry into pMQ70 (yeast homologous recombination)
mCher-F-1	ACCCGTTTTTTTGGGCTAGCGAATTCGAGCTCGGTACCCGGGGAAGGAGATATACATATGGTGAGCAAGGGCCAG	Forward	Cloning mCherry into mPQ70 (yeast homologous recombination)
mCherSEQ-F	CAAGGATGCCTGGCAGTTTAT	Forward	Confirm yeast cloning of mCherry into pMQ70 (to create pJP01)
mCherSEQ-R	TCTGTAACAAAGCGGGACCAA	Reverse	Confirm yeast cloning of mCherry into mPQ70 (to create pJP01)
PA1874-1877-R-1	CTTGCTCACCATATGTATATCTCCTTCTTCCGACATTCCTCTTGTCAA	Forward	Cloning PA1874-1877 into pJP01
PA1874-1877-R-1	CCATGACAAAAACGCGTAACAAAAGTGTCTATAATCAGAGAGGATCGGTTGGATA	Reverse	Cloning PA1874-1877 into pJP01
PA1874-1877SEQ-F	CGCCATTCAGAGAAGAAACC	Forward	Confirm yeast cloning of PA1874-1877 into pJP01
PA1874-1877-SEQ-R	AAGCGCATGAACTCCTTGAT	Reverse	Confirm yeast cloning of PA1874-1877 into pJP01

3.3 Results

3.3.1 Creation of pJP01 (pMQ72_mCherry)

In order to examine spatial and temporal expression of biofilm-specific antibiotic resistance genes, pMQ72 was used as the template plasmid for the creation of promoter-fluorescent protein constructs. This plasmid was chosen not only for its ability to be maintained and expressed in *E.coli, P. aeruginosa* and yeast, but also because it was previously used to create an *ndvB*p_GFP construct (pSC01) that displayed biofilm-specific expression. pMQ72 was used to clone in mCherry, as we wanted to replicate exactly what was done by Shanks *et al* to create pMQ80 (P_{Bad}-GFP) (Table 10) (97). In the end, equivalent constructs containing fluorescent proteins that differ only in the promoters that drive expression of each fluorescent protein were created (Figure 19).

The first step was to clone mCherry into pMQ72 at the exact same location where GFP had been cloned into pMQ72. This was done using homologous recombination in yeast (Section 3.2.2.3). Briefly, PCR amplified mCherry and digested pMQ70 were transformed into yeast. Homologous combination occurred in the yeast resulting in the creation of the P_{Bad}-mCherry (pJP01) construct. The cloning of mCherry into pJP01 was confirmed via sequencing.

3.3.2 Visualizing pJP01 in biofilms

P. aeruginosa biofilms with (Figure 21C) and without (Figure 21A) pJP01 were visualized by fluorescence microscopy in order to confirm successful cloning of pJP01. Fluorescence was captured from *P. aeruginosa* biofilms containing pJP01 when visualized through the TX2 filter cube (Figure 21D), whereas no fluorescence was captured in *P.*

aeruginosa wild-type cells without pJP01 (Figure 21B), demonstrating successful expression of mCherry in *P.aeruginosa*.

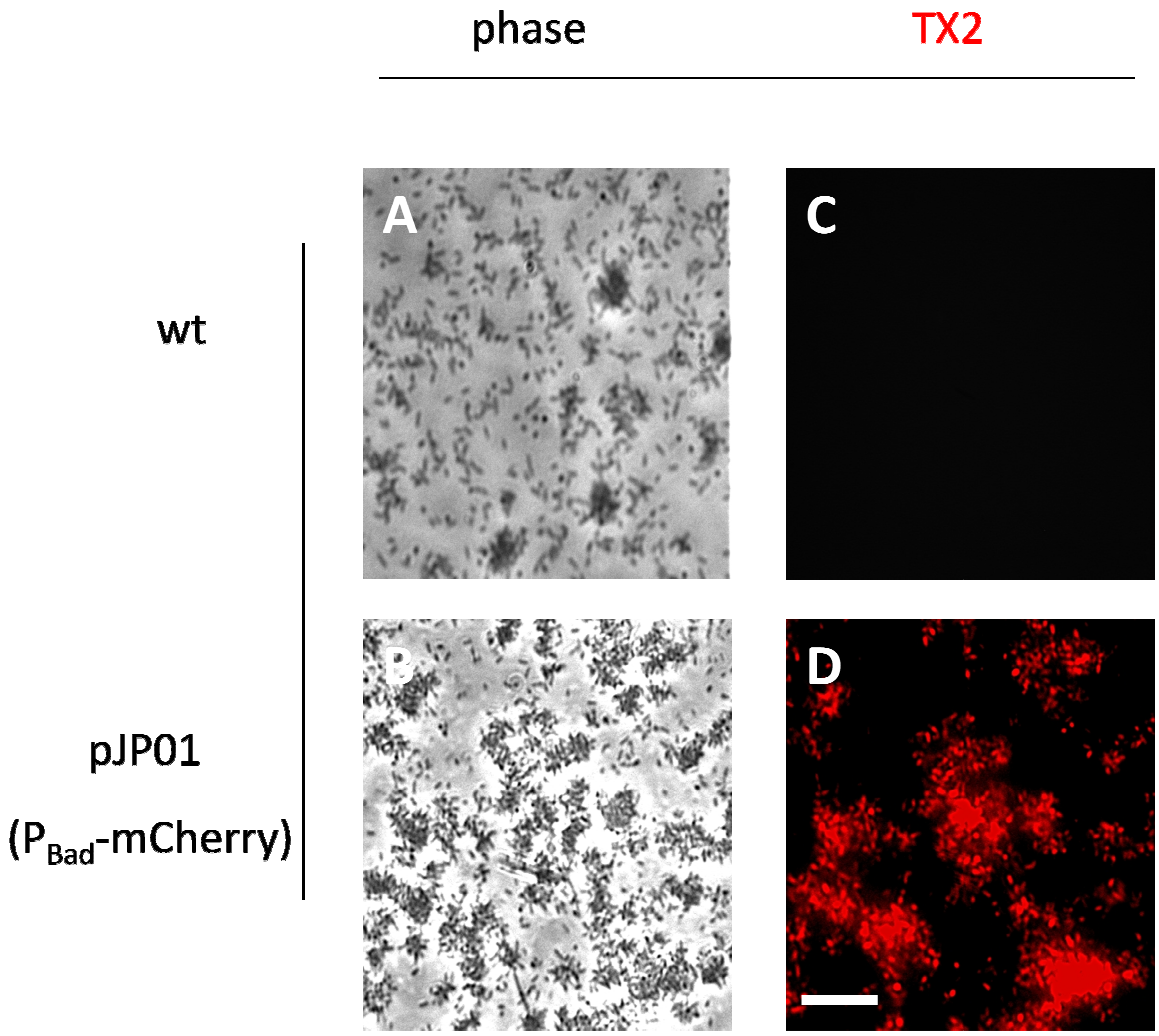

Figure 21: Phase-contrast microscopy demonstrates successful cloning of mCherry in pJP01 and expression in *P.aeruginosa*. Images were taken after 24 hours of growth using the coverlip-biofilm assay (Section 3.2.3.1) and show fluorescence in *P. aeruginosa* cells containing pJP01 confirming the presence of mCherry in this construct. The 40x objective was used. Scale bar, 15µm.

The results presented in Figure 21 confirmed that pJP01 can be used as a basic construct for the cloning of promoters that can drive expression of mCherry in order to investigate spatial and temporal expression of biofilm-specific antibiotic resistance genes.

3.3.3 *ndvB* expression in biofilms

In addition to creating novel fluorescent protein constructs, use of a previously created construct was done in order to learn more about its expression in biofilms. The previous creation of an *ndvB*p-GFP construct provided an opportunity to both study expression of *ndvB* as well as optimize the use of promoter-fluorescent protein constructs in the lab. Temporal expression of *ndvB* was the focus of this chapter and was determined by monitoring fluorescence driven by the *ndvB* promoter in pSC01 (*ndvB*p-GFP). The goal of this experiment was to determine at which point in the biofilm development cycle *ndvB* began to be expressed by growing biofilms containing pSC01. Negative controls included planktonic cells carrying pSC01 (*ndvB*p-GFP) construct and biofilm cells carrying pMQ80 (P_{bad}-GFP).

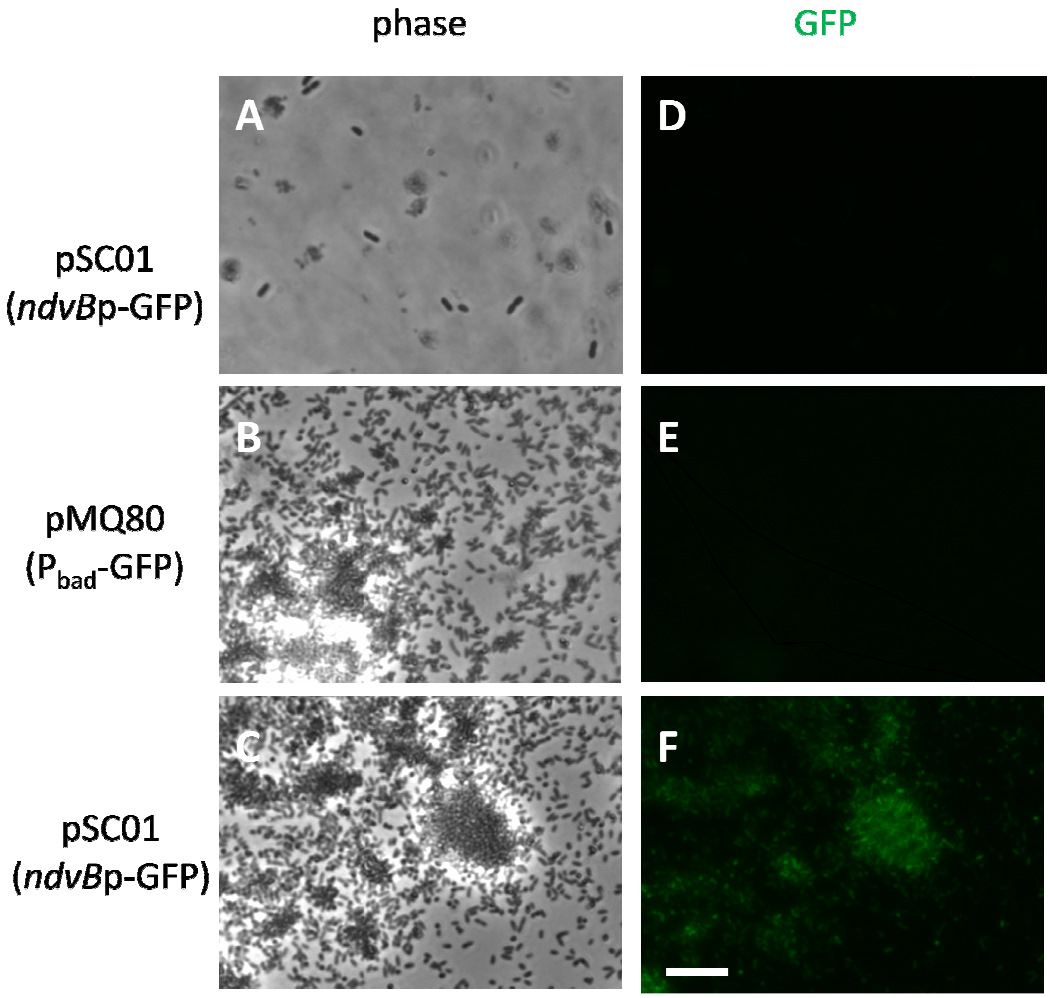

Figure 22: The *ndvB* promoter is important for biofilm-specific expression of *ndvB* in *P.aeruginosa*. (A,D) Planktonic cells containing pSC01 (*ndvB*p-GFP) after 16 hours of growth. (B,E) Biofilm cells containing pMQ80 (P_{Bad}-GFP) after 24 hours of growth. (C,F) Biofilm cells containing pSC01 (*ndvB*p-GFP) after 24 hours of growth. Biofilms were grown using the coverslip biofilm assay. The 40x objective was used. Scale bar, 15µm.

GFP expression was not captured in logarithmic-phase planktonic cells as *ndvB* is only expressed in biofilm and stationary-phase planktonic cells (Figure 22D) (64, 127). Fluorescence was also not captured in biofilms containing pMQ80 (P_{Bad}-GFP) (Figure 22E). However, fluorescence was captured in biofilms containing pSC01 (*ndvB*p-GFP) (Figure 22F). These results showed that the *ndvB* promoter was active in biofilms but not in logarithmic phase planktonic cells.

Once detection of fluorescence using our microscopic parameters was optimized, and expression of *ndvB* in biofilms was confirmed, the focus of the investigation shifted towards examining when *ndvB* became active in biofilms. This was done by growing biofilms carrying pSC01 (*ndvB*p-GFP) and monitoring fluorescence over time. Biofilms were inoculated from a frozen stock of PA14 carrying pSC01 (*ndvB*p-GFP) since cells grown to stationary phase (typical method to inoculate biofilm cultures) express GFP. Once the absence of GFP expression in the frozen stock was confirmed (data not shown), these cells were used to inoculate coverslip biofilms and fluorescence was monitored over the course of biofilm development. Over the course of 12 hours, captured fluorescence gradually increased from no capture at 4 hours (Figure 23A) to significant capture at 12 hours (Figure 23D). Interestingly, the amount of fluorescence captured at 12 hours was localized compared to 8 hours suggesting that *ndvB* was expressed within the biofilm microcolonies (Figure 23D).

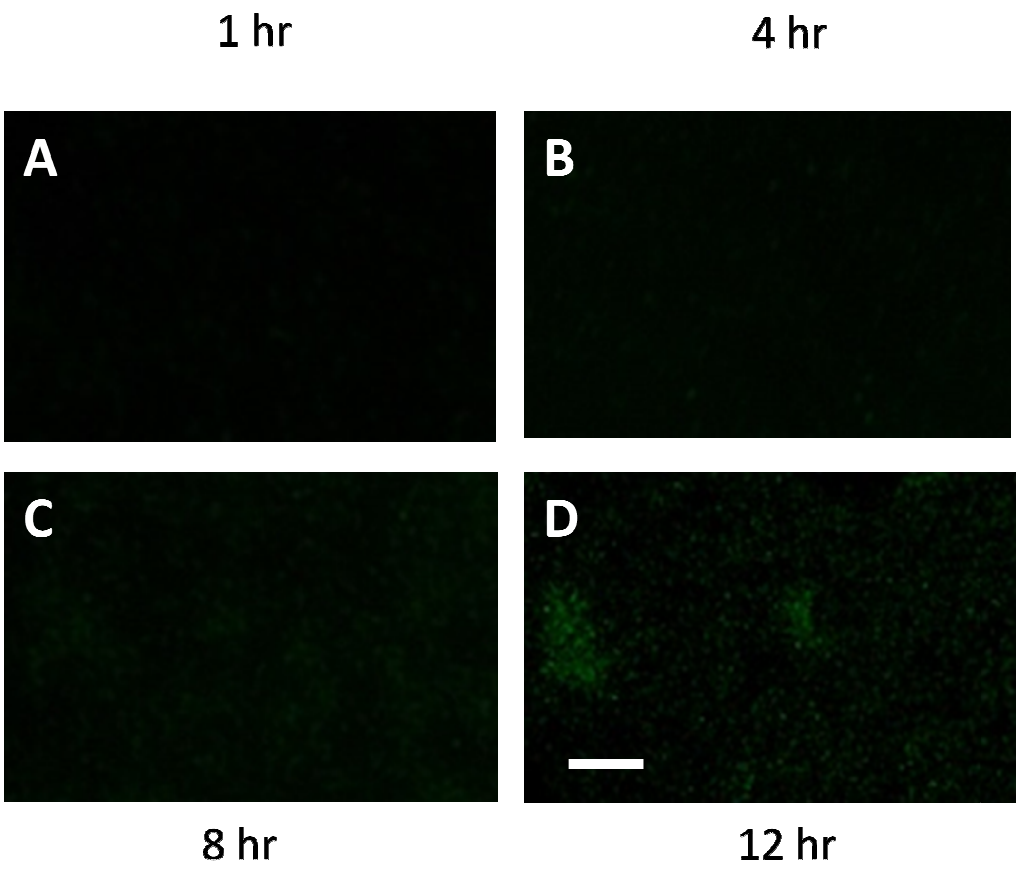

Figure 23: ndvB expression is localized in biofilm microcolonies in *P.aeruginosa*. Biofilms were grown using the coverslip assay and representative images from 1 hr (A), 4 hr (B), 8 hr (C) and 12 hr (D) post-inoculation are shown below. The 40x objective was used. Scale bar, 15µm.

In order to more accurately pinpoint when the *ndvB* promoter becomes active during biofilm development, this experiment was repeated with a few changes. Firstly, the amount of viable cells in the freezer stock prior to inoculation was measured in order to set a standard for the inoculum amount. In addition, phase images were taken alongside fluorescence images in order to monitor the progression of biofilm development and compare *ndvB* promoter activity with the biofilm development cycle. Coverslip biofilms were inoculated with a freezer stock containing a standard amount of cells (10^5 CFU's/µL). Fluorescence was monitored over the course of 12 hours. Representative images coinciding with the stages of biofilm development as described by O'Toole et al (Figure 1) (76) showed that the *ndvB* promoter became active following monolayer formation (Figure 24B and E) but before the formation of microcolonies (Figure 24C and F). The status of attachment of the cells was confirmed by rinsing the coverslips and using microscopy to assess the relative numbers of cells still attached to the surface following the rinse (data not shown).

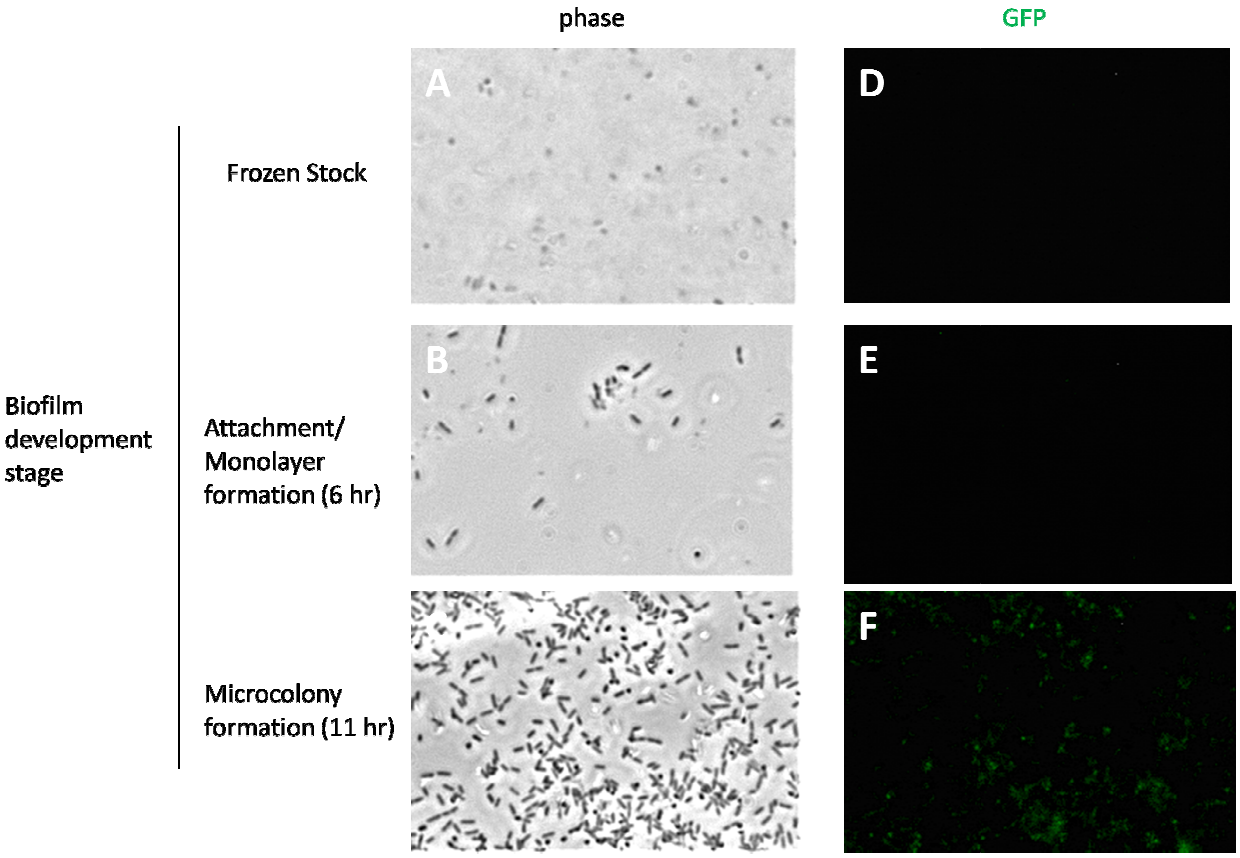

Figure 24: ndvB is expressed in a monolayer *P. aeruginosa* biofilm. Biofilms were grown using the coverslip biofilm assay and representative images from prior to inoculation (A,D), after 6 hours of biofilm growth (monolayer formation) (B,E), and after 11 hours of biofilm growth (microcolony formation) (C,F) are shown. The 40x objective was used. Scale bar, 15µm.

3.3.4 Temporal expression of *ndvB* in planktonic cells

Although *ndvB* is not expressed in logarithmic phase planktonic cells, it is expressed in stationary phase planktonic cells as determined by qPCR (unpublished data- Li Zhang). In order to determine at which point the *ndvB* promoter became active in a planktonic cells, a culture carrying pSC01 (*ndvB*p-GFP) was inoculated from set amount of frozen stock cells and monitored for the presence of GFP using fluorescence microscopy over time. No fluorescence was captured 8 hours following inoculation; however fluorescence was captured 16 hours later (Figure 25). This suggested that the *ndvB* promoter became active between 8 and 24 hours following inoculation in planktonic cells.

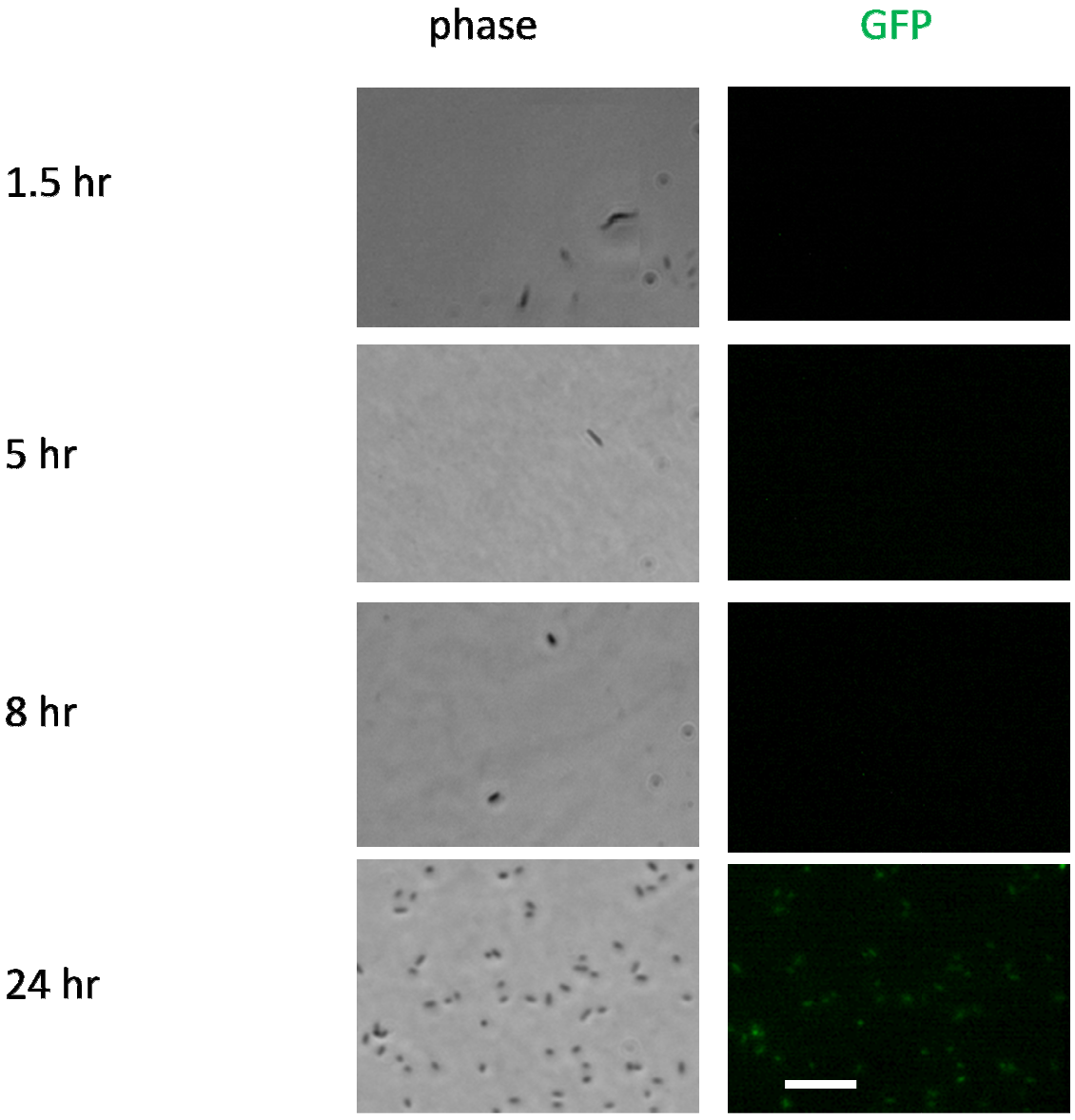

Figure 25: *ndvB* expression in *P. aeruginosa* planktonic cells. Cells were grown from frozen stock and representative images were taken at 1.5 hr, 5hr, 8hr and 24 hours post inoculation. Fluorescence was captured in cells at 24 hours of growth but not at 8 hours of growth. The 40x objective was used. Scale bar, 15µm.

This experiment was repeated with a few changes in order to better understand when *ndvB* becomes active in planktonic cells. OD_{600} was measured as opposed to time which can be better used to compare the data to growth stages as well as the inclusion of additional time points. *ndvB* promoter activity began when the planktonic cultures reached an OD_{600} of 1.7-2.0 (Figure 26). This particular OD_{600} coincides with early stationary phase as determined by analysis of growth curves using frozen stock cultures as the inoculum (Figure 27, A and B).

Western blots were performed on total protein extracted from these planktonic cultures at OD_{600} of 0.05, 0.5, 0.9, 1.4, 1.9 and 2.9, in order to examine GFP levels quantitatively. The western blot showed that there was a large increase in GFP levels between OD_{600} 1.9 and 2.9. (Figure 28 A). Combined, the fluorescence microscopy (Figure 26) and western blot (Figure 28) data suggests that *ndvB* began to be expressed at OD_{600} of approximately 2.0, consistent with early stationary phase (Figure 27).

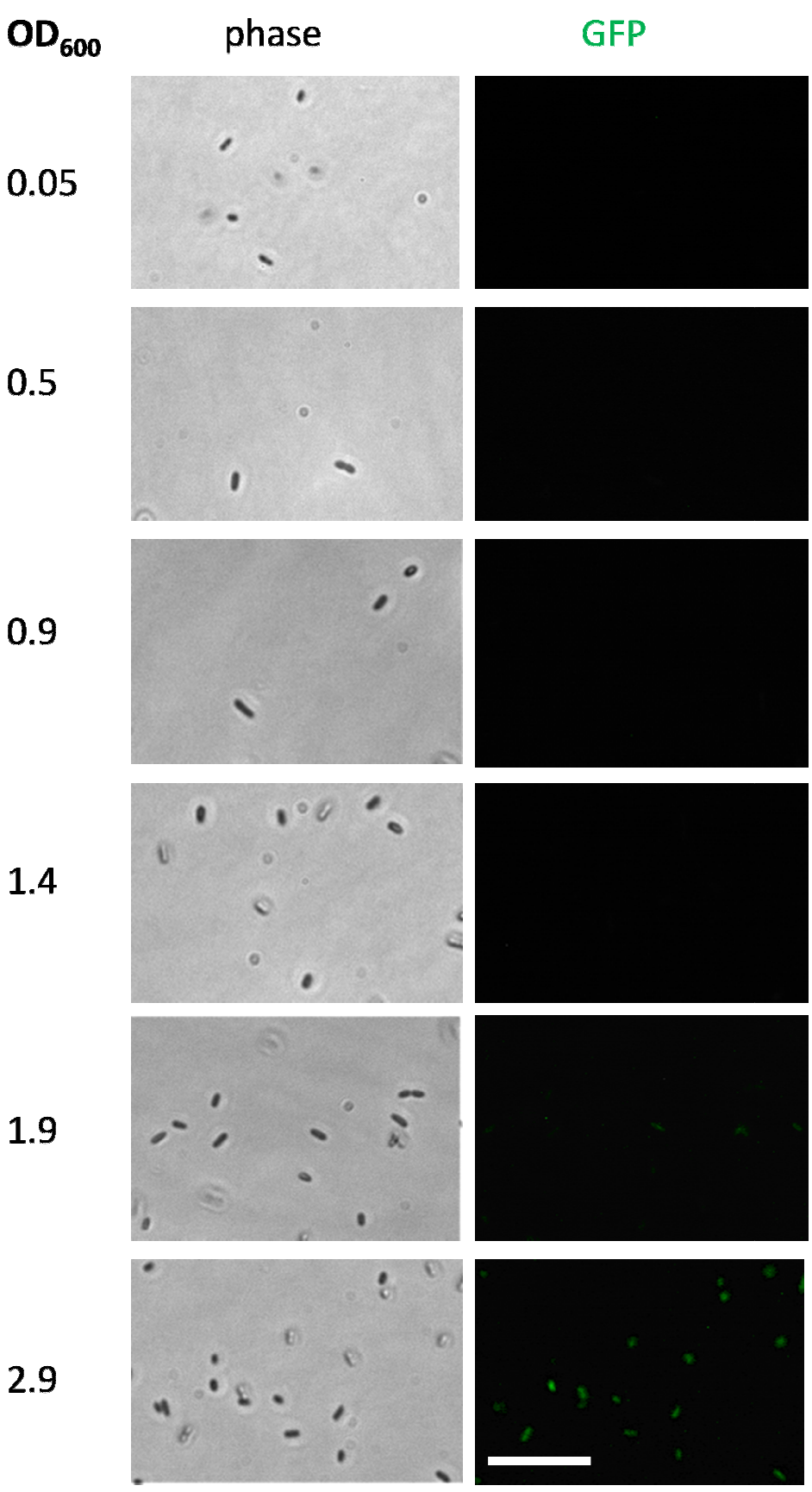
OD600
phase
GFP
0.05
0.5
0.9
1.4
1.9
2.9

Figure 26: ndvB begins to be expressed in early stationary phase planktonic cells in *P.aeruginosa*. Cells were grown from frozen stock and representative images were taken at an OD_{600} of 0.05, 0.5, 0.9, 1.4, 1.9, and 2.9 post inoculation. Fluorescence was captured in cells at OD_{600} of 1.9 but not at 1.4. The 63x objective was used. Scale bar, 15µm.

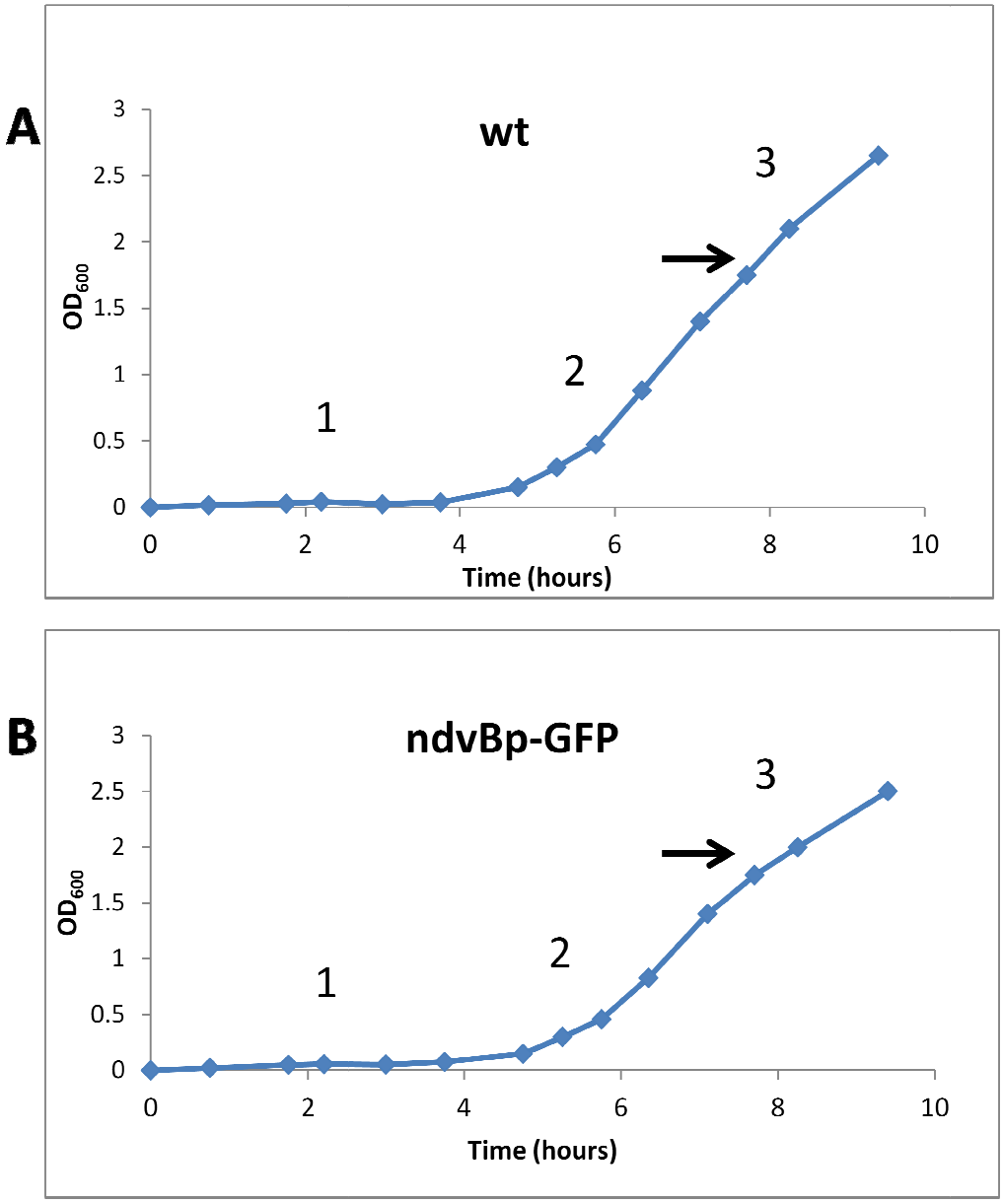

Figure 27: Growth curves of *P. aeruginosa* showing the stages of microbial development following inoculation from frozen stock. Wild type (A), and PA14 containing pSC01 (*ndvB*p-GFP) (B) frozen stocks were used to inoculate LB cultures and the OD_{600} of these cultures was monitored over 10 hours of growth. The stages of the growth curve are shown on the graph. 1-lag phase, 2- logarithmic phase and 3- early stationary phase. The arrow indicates the OD_{600} at which *ndvB* is hypothesized to become active based on the result in Figure 26.

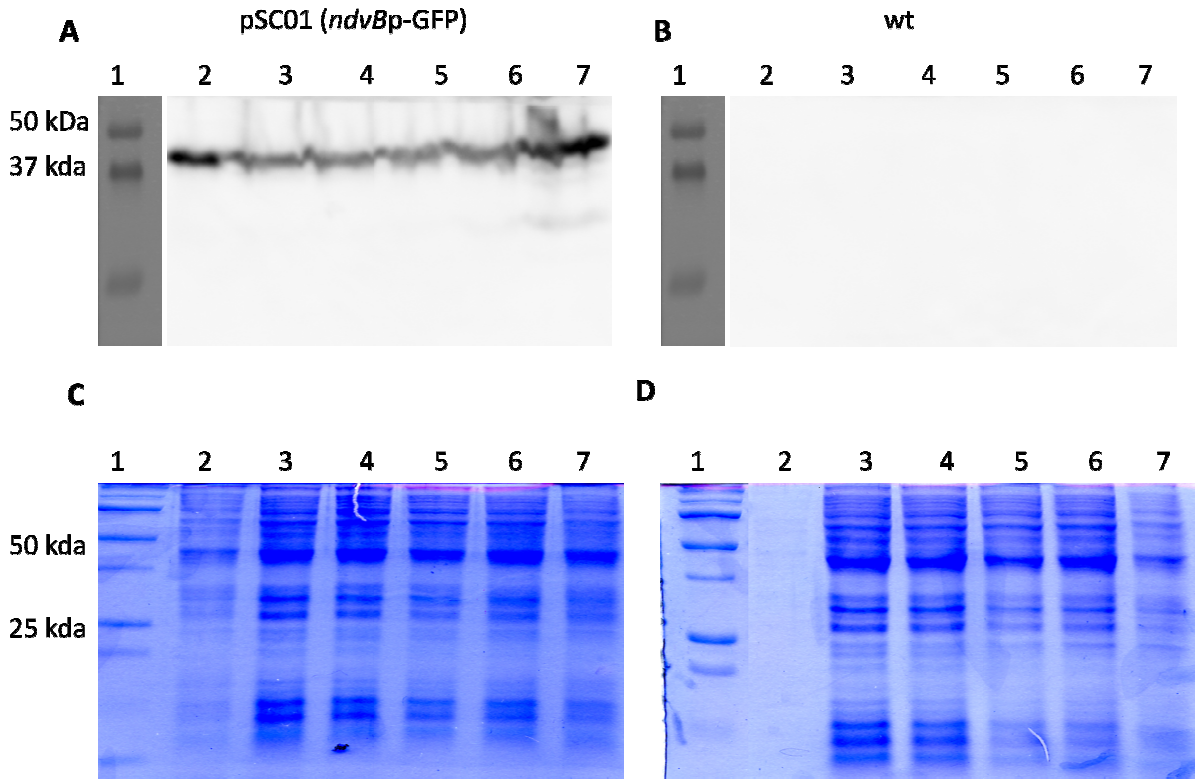

Figure 28: GFP is more highly expressed at OD_{600} of 2.9 than at earlier timepoints in planktonic cultures of *P.aeruginosa*. Western blots were performed on whole cell extracts from *P. aeruginosa* planktonic cells grown from frozen stock at an OD_{600} of 0.05 (lane 2), 0.5 (lane 3), 0.9 (lane 4), 1.4 (lane 5), 1.9 (lane 6) and 2.9 (lane 7). (A) pSC01 (*ndvB*p-GFP) (B) wt. Control of loading was done by running the extracts on a Coomassie stained SDS-PAGE gel (C) pSC01 (*ndvB*p-GFP), (D) wt.

In addition to determining the OD_{600} at which *ndvB* is expressed in planktonic cells, tobramycin was added to the planktonic cells to determine if the presence of an antibiotic increased *ndvB* expression (Figure 29) shows that following incubation with sub-minimal inhibitory concentration (MIC) values of tobramycin overnight, expression of *ndvB* remained unchanged (Figure 29 D,E and F). This was determined by comparing the relative fluorescence driven by *ndvB* promoter activity under 0.25 µg/mL, 0.5 µg/mL tobramycin and a no tobramycin control.

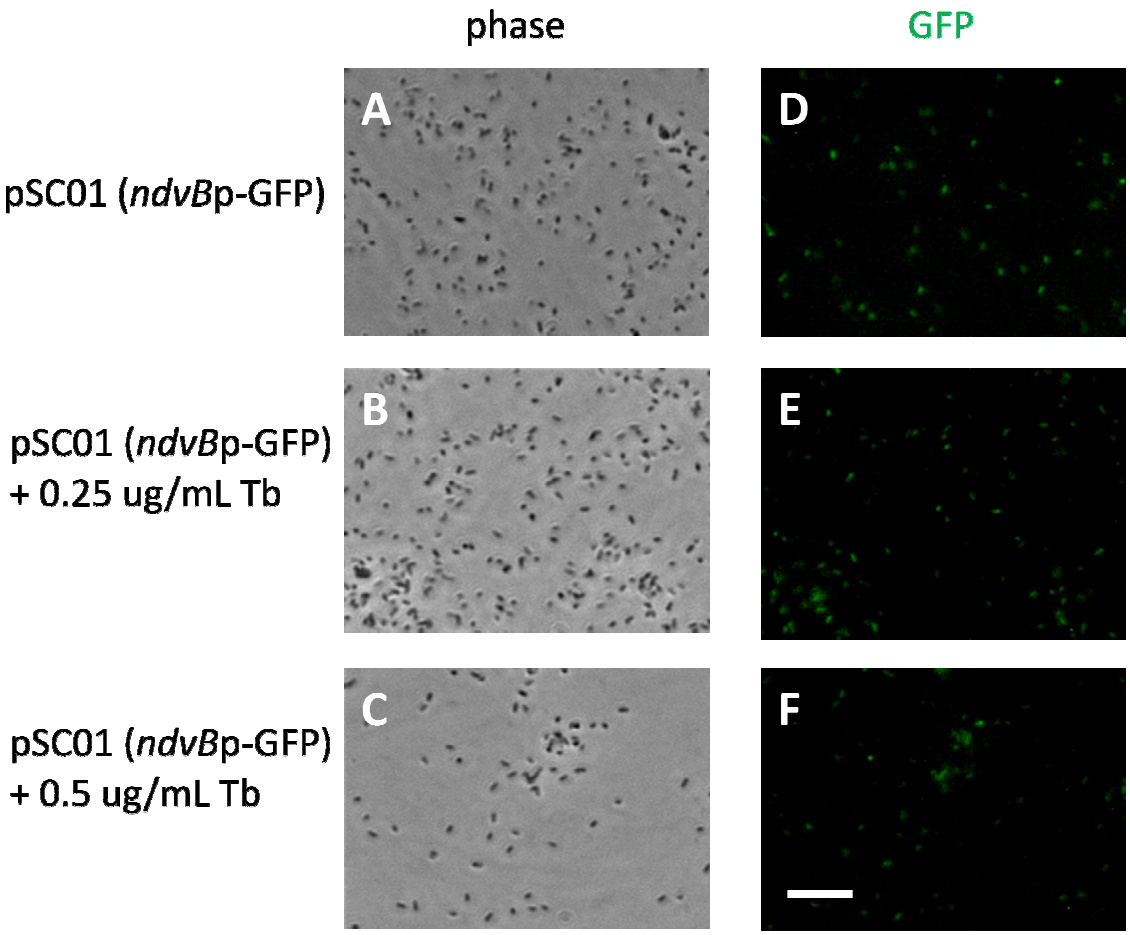

Figure 29: The addition of sub-inhibitory concentrations of tobramycin does not increase ndvB expression. Tobramycin was added to the overnight cultures at the time of inoculation. Cells were grown for 16 hours and visualized under fluorescence microscopy using the 40x objective. Scale bar, 15µm.

3.4 Discussion

The use of promoter-fluorescent protein constructs in the analysis of gene expression of biofilm-specific antibiotic resistance genes in this chapter has revealed some interesting results but these did not come without some difficulties that altered the initial goal of the chapter and also made it difficult to work with what was available. These difficulties will be analyzed and some future experiments will be discussed. In summary, a previously constructed *ndvB*p-GFP construct was successfully used to study temporal expression of *ndvB* in both stationary-phase planktonic and biofilm cells. It was found that *ndvB* began to be expressed following monolayer formation in biofilms. Planktonically, *ndvB* began to be expressed near an OD_{600} of 2.0, in early stationary phases. The discovery of the temporal expression of *ndvB* using this method has also facilitated the future study of expression of biofilm-specific antibiotic resistance genes using this method. In addition, a novel promoter-fluorescent protein construct with a different fluorescent protein (mCherry) was created.

As stated above, the initial overall goal of this project was to create a series of promoter-fluorescent protein constructs that would allow analysis of the expression of six biofilm-specific antibiotic resistance genes. The project was initially designed so that each of the six promoters drove expression of a different fluorescent protein. Biofilms with cells containing these constructs would be grown together to compare spatial and temporal expression of biofilm-specific antibiotic resistance genes. Expression of biofilm-specific antibiotic resistance genes has not been studied, and thus any results concerning temporal and spatial expression would be novel research. In order to not be overwhelmed by its large scope, the project was narrowed down to solely study temporal expression of only one of

the biofilm-specific antibiotic resistance genes, *ndvB.* This was decided not only because of time constraints, but also due to difficulties that arose over the course of the thesis.

pSC01 (*ndvB*p-GFP) contains GFPmut3, a very stable variant of GFP with a half-life of 20 hours (110). This long half life made analysis of real-time temporal expression difficult, as once enough GFP was translated and could be detected through microscopy, it would remain detectable for 24 hours. Therefore, this construct could not be used to study when *ndvB* expression was turned on versus turned off. In order to successfully use this construct, initial *ndvB* expression in both stationary phase planktonic as well as biofilm cells was the focus of this chapter.

It was additionally difficult to study temporal expression in biofilms as the standard method of inoculating biofilms could not be used. Typically, biofilms are inoculated by growing a stationary-phase planktonic culture followed by a subculture into media with a surface. As stationary-phase cultures are already expressing *ndvB*, GFP was present in these cultures (Li Zhang- unpublished data). In order to successfully use this construct, frozen stock cells containing pSC01 (*ndvB*p-GFP) that were not expressing GFP after being left at room temperature for 24 hours were used to inoculate planktonic and biofilm experiments. The frozen stocks did not express GFP because of full turnover that occurred after 24 hours. Under low nutrient and high waste conditions, the transition of *P. aeruginosa* cells from the typical rod shape to a much smaller ultramicrobacteria as described by Kjelleberg *et al* (55). This starvation response found throughout the bacterial kingdom when cells experience

unfavorable conditions may also explain why frozen stock cells did not express GFP prior to inoculation.

One interesting potential application of the use of these promoter-fluorescent protein constructs is to grow mixed biofilms and simultaneously monitor the expression of two or more biofilm-specific antibiotic resistance genes. This possibility was what led the lab to begin the cloning to create these promoter-fluorescent protein constructs. Upon further investigation, it was determined that experiments involving more than one fluorescent protein at once would not be ideal. Although recent studies have successfully grown mixed biofilms containing two different fluorescent proteins (mCherry and GFP) in *P.aeruginosa,* it was not possible to use this approach with promoter- fluorescent protein constructs (37, 57). In studies that successfully were able to create mixed-species biofilms, fluorescent proteins were used simply to tag proteins. For example, in the Lagendijk et al study, two strains of *Pseudomonas putida* were differentiated by the fluorescent protein they were expressing. In this case fluorescence was used in order to contrast biofilm formation between the two strains (57). Although this paper successfully provides the background for many of the tasks we set out to complete including visualizing mixed species biofilms with two different fluorescent proteins, it is different in that it took a more simplistic approach in that the fluorescent proteins were simply used to tag proteins.

This is in contrast to the goal in our analysis where promoters drive fluorescent protein expression. Thus, differences in half life as well as maturation requirements between the two proteins may account for differences in expression of the two proteins in addition to

promoter activity. For example, mCherry and GFP require different amounts of oxygen to mature (29). With this is mind, our system would not portray an accurate representation of real-time gene expression where differences in expression of the fluorescent protein is based solely on promoter activity (88, 95). As a result our original idea of using *ndvB*p-GFP and PA1874-77p-mCherry in the same biofilm to compare expression of these promoters may not be useful. It was due to these reasons that the focus of my thesis was narrowed to only study when *ndvB* became active using pSC01 (*ndvB*p-GFP).

Although the mCherry and GFP constructs could not be used together in a mixed species biofilm, the use of both GFP and mCherry constructs individually to assess real time gene expression remained as a viable option and was used successfully to analyze *ndvB* expression in planktonic and biofilm cells. Some important considerations that affect fluorescence include brightness and photostability of the protein. These properties are not only inherent in the protein structure itself but also depend on the conditions in which they are expressed as well as the strain in which they are translated in (96).

In order to fully characterize temporal *ndvB* expression, the first experiment was to confirm that expression of *ndvB* occurred in biofilms but not in logarithmic phase planktonic cells. Fluorescence microscopy with pSC01 (*ndvB*p-GFP) confirmed activity of the *ndvB* promoter in biofilm cells but not in logarithmic phase planktonic cells. This coincided with previous observations that *ndvB* expression is very low in logarithmic phase cells and high in stationary phase cells (64). It was interesting to note the increased amount of fluorescence in the macrocolonies that occurred at 12 hours (Figure 22). Although there are more cells

present in macrocolonies and thus there would be increased fluorescence due to the overlap of cells, it may also indicate increased *ndvB* promoter activity in this area of the biofilm. This idea that would agree with the widespread knowledge that the outer most parts of the macrocolonies are more metabolically active than other parts of the biofilm and therefore might be expressing *ndvB* at a higher level (101, 103). In addition to being more metabolically active, these outer areas of the biofilm are more likely to encounter antibiotics and as a result may also be a trigger for the transcription of ndvB (3, 109). However, the results in Figure 29 showed that the presence of tobramycin (shown to interact with *ndvB*-derived glucans) did not increase *ndvB* expression in biofilms.

After confirming higher *ndvB* expression in biofilms, expression was more precisely studied by comparing fluorescence alongside the biofilm development cycle. This more detailed look at temporal expression in biofilms revealed that *ndvB* promoter activity began following initial attachment and monolayer formation but before the formation of microcolonies (Figure 24). In addition, this result confirms what was seen in Figure 22: a higher level of fluorescence in microcolonies. However, results obtained from the study of promoter-fluorescent protein constructs in biofilms needs to be interpreted carefully. Fluorescent protein maturation is affected by the concentration of certain compounds including oxygen (28, 122) which as described above is subject to large gradients in biofilms. This oxygen concentration gradient may explain some of the differences in fluorescence between adjacent regions in the biofilm in addition to differences in promoter activity.

The main goal of monitoring planktonic *ndvB* expression was to focus on *e*xpression over early timepoints in order to pinpoint the exact time at which expression begins and correlate this with planktonic growth phase. Firstly, it was found using pSC01 that *ndvB* promoter activity began around OD600 of 1.7-2.0 (Figure 26).

In addition, an alternative method was used to support the fluorescence data that the *ndvB* promoter became active around OD_{600} 1.7-2.0. It was important to use a second method to confirm GFP levels due to the fact that the cells had to be suspended in agarose during fluorescence microscopy to immobilize the cells and allow for them to be exposed to fluorescence in a still state. Agarose slightly reduces the refractive index of the medium which could have interfered with the microscopy (82).

For this second method, whole cell extracts were removed from the same time points that were examined in Figure 26 and collected. GFP was then detected using an anti-GFP antibody using western blot. Instead of using a loading control, coomassie and ponceau staining were used to compare the amount of protein loaded in each well. GFP was detected from the western blot beginning at OD_{600} 0.05. This level was especially high as less total protein was loaded from this fraction. This can be explained by the expression of GFP by the cells in the frozen stock as inoculation of this experiment was done using frozen stock cells that were not left at room temperature for 24 hours to allow for GFP to turnover (110). The detection of GFP from all samples, although not ideal, was most likely due to small levels of *ndvB* promoter activity due to the binding and disassociation of proteins with affinity to the

promoter. The detection of small levels of GFP occurred due to the low dilution of GFP antibody that was used because of uncertainty in the levels of GFP that would be detected.

Together, fluorescence microscopy and western blots results found that *ndvB* expression began around an OD_{600} of 2.0 (Figure 25, Figure 26 and Figure 28). This corresponds to early stationary phase as confirmed by growth curves that were created using frozen stocks for inoculation (Figure 27). Expression of *ndvB* in stationary-phase planktonic cells shows density dependence, and correlates with previous qPCR results (Li Zhang). This result suggests that there may be a well defined cell density at which *ndvB* begins to be expressed. Whether or not this is due to quorum sensing remains unclear. However, *ndvB* has yet to be identified in quorum sensing screens and thus it is unlikely that *ndvB* is controlled by quorum sensing (47). This experiment would need to be repeated with a strain deficient in QS in order to determine whether or not *ndvB* expression is affected.

The results from this study suggest that *ndvB* is expressed once a certain biofilm development stage is reached (microcolonies) whereas density dependence is important in planktonic cells. In the future, *ndvB* expression needs to be more fully investigated in both biofilm and planktonic cells in order to learn more about the details of expression. Tobramycin was added during planktonic growth in order to assess whether adding antibiotics to the cultures might be a trigger for increased *ndvB* promoter activity. *ndvB* encodes a glucosyltransferase that is responsible for the production of cyclic glucans that have been shown to bind and sequester tobramycin in the periplasm (64). Thus, it would make sense if adding tobramycin to the cultures resulted in upregulation of *ndvB.* However,

there was no increase in *ndvB* expression when tobramycin was added to cultures expression pSC01 (Figure 29). This suggests that the presence of tobramycin does not affect *ndvB* promoter activity.

In an attempt to make pSC01 more useful for real-time analysis of gene expression, an honours student in the lab has recently added a degradation tag to the N-terminus of GFP in order to significantly decrease its half life as per Anderson et al (6).The introduction of a degradation tag will reduce the half-life of the GFP from 24 hours to between 1 and 2 hours, making the resulting short-lived GFP molecule ideal for real-time analysis (6). The shorter half-life GFP will allow us to focus on spatial activity of the *ndvB* promoter. We will be able to analyze whether or not the *ndvB* promoter activity fluctuates during the course of biofilm development, a feat that was not possible to do with the stable GFP expressed from pSC01.

Once completed, the collection of promoter-fluorescent proteins can be used in a flowing system to accurately analyze not only temporal, but spatial gene expression of regions of cells within biofilms. In addition, the chemical environment in which the cell is growing can be measured thereby providing clues to potential triggers of biofilm-specific expression. Some parameters that are able to be measured include oxygen, carbon dioxide and many different metabolites (12, 122). The use of these constructs in conjunction with these measuring devices has helped unravel potential triggers for modulation of gene expression at the individual cell level, something that was not possible when assessing expression in bulk. This can be used to measure microenvironments in conjunction with expression of biofilm-specific antibiotic resistance genes.

In conclusion, the work presented in this chapter has presented some initial results concerning analysis of spatial and temporal expression of biofilm-specific antibiotic resistance genes. More specifically, pSC01 (*ndvB*p-GFP) was used to determine that the *ndvB* promoter is active in biofilms and not in logarithmic phase planktonic cells through visualizing the *ndvB*p-GFP construct in biofilms. It was determined that *ndvB* begins to be expressed in biofilms following monolayer formation and before the presence of macrocolonies. In planktonic cells, *ndvB* expression began in early stationary phase. In addition, through initial experiments it was found that a shorter half-life GFP is crucial for real-time expression studies and thus a degradation tag was added to the *ndvB*p-GFP construct.

The next step is to identify the triggers of expression of *ndvB* and to determine why expression begins at such a well-defined timepoint in both biofilms and logarithmic phase planktonic cells. The concepts discussed from chapter 2 suggest that regulation of the biofilm-specific antibiotic resistance genes might be through the discovery of a novel proximal control element. Proteins with affinity for the 22bp motif that may affect regulation of biofilm-specific antibiotic resistance genes is currently one area of focus in the lab and might help explain the expression pattern of *ndvB* that was found in this chapter. Understanding the regulation of expression of biofilm-specific antibiotic resistance genes will open the door to the study of approaches to decrease expression of these genes, which will reduce antibiotic resistance in *P. aeruginosa* biofilms and contribute towards the understanding of the treatment of biofilm-based diseases as a whole.

LIST OF REFERENCES

1. **Allegrucci, M, Sauer, K.** 2007. Characterization of colony morphology variants isolated from *Streptococcus pneumoniae* biofilms. J. Bacteriol. **189:**2030-2038.

2. **Allesen-Holm, M, Barken, KB, Yang, L, Klausen, M, Webb, JS, Kjelleberg, S, Molin, S, Givskov, M, Tolker-Nielsen, T.** 2006. A characterization of DNA release in *Pseudomonas aeruginosa* cultures and biofilms. Mol. Microbiol. **59:**1114-1128.

3. **Allison, DG.** 2003. The biofilm matrix. Biofouling. **19:**139-150.

4. **Allison, DG, Ruiz, B, Sanjose, C, Jaspe, A, Gilbert, P.** 1998. Extracellular products as mediators of the formation and detachment of *Pseudomonas fluorescens* biofilms. FEMS Microbiol. Lett. **167:**179-184.

5. **An, D, Parsek, MR.** 2007. The promise and peril of transcriptional profiling in biofilm communities. Curr. Opin. Microbiol. **10:**292-296.

6. **Andersen, JB, Sternberg, C, Poulsen, LK, Bjørn, SP, Givskov, M, Molin, S.** 1998. New unstable variants of green fluorescent protein for studies of transient gene expression in bacteria. Appl. Environ. Microbiol. **64:**2240-2246.

7. **Bailey, TL, Williams, N, Misleh, C, Li, WW.** 2006. MEME: Discovering and analyzing DNA and protein sequence motifs. Nucleic Acids Res. **34:**W369-W373.

8. **Balasubramanian, D, Schneper, L, Kumari, H, Mathee, K.** 2013. A dynamic and intricate regulatory network determines *Pseudomonas aeruginos*a virulence. Nucleic Acids Res. **41:**1-20.

9. **Baty III, AM, Eastburn, CC, Techkarnjanaruk, S, Goodman, AE, Geesey, GG.** 2000. Spatial and temporal variations in chitinolytic gene expression and bacterial biomass production during chitin degradation. Appl. Environ. Microbiol. **66:**3574-3585.

10. **Beaudoin, T, Zhang, L, Hinz, AJ, Parr, CJ, Mah, T-.** 2012. The biofilm-specific antibiotic resistance gene ndvB is important for expression of ethanol oxidation genes in Pseudomonas aeruginosa biofilms. J. Bacteriol. **194:**3128-3136.

11. **Beloin, C, Ghigo, J-.** 2005. Finding gene-expression patterns in bacterial biofilms. Trends Microbiol. **13:**16-19.

12. **Beyenal, H, Davis, CC, Lewandowski, Z.** 2004. An improved Severinghaus-type carbon dioxide microelectrode for use in biofilms. Sensors and Actuators, B: Chemical. **97:**202-210.

13. **Blatter, EE, Ross, W, Tang, H, Gourse, RL, Ebright, RH.** 1994. Domain organization of RNA polymerase α subunit: C-terminal 85 amino acids constitute a domain capable of dimerization and DNA binding. Cell. **78:**889-896.

14. **Bolister, N, Basker, M, Hodges, NA, Marriott, C.** 1991. The diffusion of β-lactam antibiotics through mixed gels of cystic fibrosis-derived mucin and Pseudomonas aeruginosa alginate. J. Antimicrob. Chemother. **27:**285-293.

15. **Brooun, A, Liu, S, Lewis, K.** 2000. A dose-response study of antibiotic resistance in Pseudomonas aeruginosa biofilms. Antimicrobial Agents Chemother. **44:**640-646.

16. **Byrd, MS, Sadovskaya, I, Vinogradov, E, Lu, H, Sprinkle, AB, Richardson, SH, Ma, L, Ralston, B, Parsek, MR, Anderson, EM, Lam, JS, Wozniak, DJ.** 2009. Genetic and biochemical analyses of the *Pseudomonas aeruginosa* Psl exopolysaccharide reveal overlapping roles for polysaccharide synthesis enzymes in Psl and LPS production. Mol. Microbiol. **73:**622-638.

17. **Caiazza, NC, O'Toole, GA.** 2004. **SadB is required for the transition from reversible to irreversible attachment during biofilm formation by Pseudomonas aeruginosa PA14**. J. Bacteriol. **186(14):**4476.

18. **Chodosh, LA.** 2001. Purification of DNA-binding proteins using biotin/streptavidin affinity systems. Current Protocols in Molecular Biology / Edited by Frederick M.Ausubel ...[Et Al.]. **Chapter 12:**.

19. **ClonTech Laboratories Inc.** 2007.
TALON Metal Affinity Resins
User Manual **PT1320-1 (PR7Y2405):**April 15, 2013.

20. **Colvin, KM, Gordon, VD, Murakami, K, Borlee, BR, Wozniak, DJ, Wong, GCL, Parsek, MR.** 2011. The pel polysaccharide can serve a structural and protective role in the biofilm matrix of Pseudomonas aeruginosa. PLoS Pathogens. **7:**.

21. **Costerton, JW, Cheng, KJ, Geesey, GG, Ladd, TI, Nickel, JC, Dasgupta, M, Marrie, TJ.** 1987. Bacterial biofilms in nature and disease. Annu. Rev. Microbiol. **41:**435-464.

22. **Costerton, JW, Geesey, GG, Cheng, KJ.** 1978. How bacteria stick. Sci. Am. **238:**86-95.

23. **Costerton, JW, Lewandowski, Z, Caldwell, DE, Korber, DR, Lappin-Scott, HM.** 1995. Microbial biofilms. Annu. Rev. Microbiol. **49:**711-745.

24. **Costerton, JW, Stewart, PS, Greenberg, EP.** 1999. Bacterial biofilms: A common cause of persistent infections. Science. **284:**1318-1322.

25. **De Beer, D, Glud, A, Epping, E, Kühl, M.** 1997. A fast-responding CO2 microelectrode for profiling sediments, microbial mats, and biofilms. Limnol. Oceanogr. **42:**1590-1600.

26. **De Beer, D, Huisman, JW, Van den Heuvel, JC, Ottengraf, SPP.** 1992. The effect of pH profiles in methanogenic aggregates on the kinetics of acetate conversion. Water Res. **26:**1329-1336.

27. **De Beer, D, Srinivasan, R, Stewart, PS.** 1994. Direct measurement of chlorine penetration into biofilms during disinfection. Appl. Environ. Microbiol. **60:**4339-4344.

28. **De Beer, D, Stoodley, P, Roe, F, Lewandowski, Z.** 1994. Effects of biofilm structures on oxygen distribution and mass transport. Biotechnol. Bioeng. **43:**1131-1138.

29. **Doherty, GP, Bailey, K, Lewis, PJ.** 2010. Stage-specific fluorescence intensity of GFP and mCherry during sporulation in *Bacillus Subtilis*. BMC Research Notes. **3:**.

30. **Elble, R.** 1992. A simple and efficient procedure for transformation of yeasts. BioTechniques. **13:**18-20.

31. **Emmert-Buck, MR, Bonner, RF, Smith, PD, Chuaqui, RF, Zhuang, Z, Goldstein, SR, Weiss, RA, Liotta, LA.** 1996. Laser capture microdissection. Science. **274:**998-1001.

32. **Estrem, ST, Gaal, T, Ross, W, Gourse, RL.** 1998. Identification of an UP element consensus sequence for bacterial promoters. Proc. Natl. Acad. Sci. U. S. A. **95:**9761-9766.

33. **Evans, DJ, Allison, DG, Brown, MRW, Gilbert, P.** 1991. Susceptibility of Pseudomonas aeruginosa and *Escherichia coli* biofilms towards ciprofloxacin: effect of specific growth rate. J. Antimicrob. Chemother. **27:**177-184.

34. **Evans, LR, Linker, A.** 1973. Production and characterization of the slime polysaccharide of *Pseudomonas aeruginosa.* J. Bacteriol. **116:**915-924.

35. **Flemming, H-, Neu, TR, Wozniak, DJ.** 2007. The EPS matrix: The "House of Biofilm Cells". J. Bacteriol. **189:**7945-7947.

36. **Friedman, L, Kolter, R.** 2004. Two genetic loci produce distinct carbohydrate-rich structural components of the *Pseudomonas aeruginosa* biofilm matrix. J. Bacteriol. **186:**4457-4465.

37. **García-Cayuela, T, De Cadiñanos, LPG, Mohedano, ML, De Palencia, PF, Boden, D, Wells, J, Peláez, C, López, P, Requena, T.** 2012. Fluorescent protein vectors for promoter analysis in lactic acid bacteria and *Escherichia coli.* Appl. Microbiol. Biotechnol. **96:**171-181.

38. **Glud, RN, Ramsing, NB, Revsbech, NP.** 1992. Photosynthesis and photosynthesis-coupled respiration in natural biofilms quantified with oxygen microsensors. J. Phycol. **28:**51-60.

39. **González-Pastor, JE, Hobbs, EC, Losick, R.** 2003. Cannibalism by sporulating bacteria. Science. **301:**510-513.

40. **Govan, JRW, Deretic, V.** 1996. Microbial pathogenesis in cystic fibrosis: Mucoid Pseudomonas aeruginosa and *Burkholderia cepaci*a. Microbiol. Rev. **60:**539-574.

41. **Greenberg, EP.** 2000. Pump up the versatility. Nature. **406:**947-948.

42. **Harrison, JJ, Ceri, H, Roper, NJ, Badry, EA, Sproule, KM, Turner, RJ.** 2005. Persister cells mediate tolerance to metal oxyanions in Escherichia coli. Microbiology. **151:**3181-3195.

43. **Hartzell, PL, Millstein, J, Lapaglia, C.** 1999. Biofilm formation in hyperthermophilic archaea. Methods in Enzymology. **310:**335-349.

44. **Hawley, DK, Mcclure, WR.** 1983. Compilation and analysis of *Escherichia coli* promoter DNA sequences. Nucleic Acids Res. **11:**2237-2255.

45. **He, J, Baldini, RL, Deziel, E, Saucier, M, Zhang, Q, Liberati, NT, Lee, D, Urbach, J, Goodman, HM, Rahme, LG.** 2004. The broad host range pathogen *Pseudomonas aeruginosa* strain PA14 carries two pathogenicity islands harboring plant and animal virulence genes. Proc. Natl. Acad. Sci. U. S. A. **101:**2530-2535.

46. **Hentzer, M, Teitzel, GM, Balzer, GJ, Heydorn, A, Molin, S, Givskov, M, Parsek, MR.** 2001. Alginate overproduction affects *pseudomonas aeruginosa* biofilm structure and function. J. Bacteriol. **183:**5395-5401.

47. **Hentzer, M, Wu, H, Andersen, JB, Riedel, K, Rasmussen, TB, Bagge, N, Kumar, N, Schembri, MA, Song, Z, Kristoffersen, P, Manefield, M, Costerton, JW, Molin, S, Eberl, L, Steinberg, P, Kjelleberg, S, Høiby, N, Givskov, M.** 2003. Attenuation of *Pseudomonas aeruginosa* virulence by quorum sensing inhibitors. EMBO J. **22:**3803-3815.

48. **Hoffman, CS, Winston, F.** 1987. A ten-minute DNA preparation from yeast efficiently releases automomous plasmids for transformation of *Escherichia coli*. Gene. **57:**267-272.

49. **Hogardt, M, Heesemann, J.** 2010. Adaptation of *Pseudomonas aeruginosa* during persistence in the cystic fibrosis lung. International Journal of Medical Microbiology. **300:**557-562.

50. **Hoyle, BD, Alcantara, J, Costerton, JW.** 1992. *Pseudomonas aeruginosa* biofilm as a diffusion barrier to piperacillin. Antimicrobial Agents Chemother. **36:**2054-2056.

51. **Huang, K-, Schieberl, JL, Igo, MM.** 1994. A distant upstream site involved in the negative regulation of the *Escherichia coli* ompF gene. J. Bacteriol. **176:**1309-1315.

52. **Kadonaga, JT, Tjian, R.** 1986. Affinity purification of sequence-specific DNA binding proteins. Proc. Natl. Acad. Sci. U. S. A. **83:**5889-5893.

53. **Keren, I, Kaldalu, N, Spoering, A, Wang, Y, Lewis, K.** 2004. Persister cells and tolerance to antimicrobials. FEMS Microbiol. Lett. **230:**13-18.

54. **King, JM, Brutinel, ED, Marsden, AE, Schubot, FD, Yahr, TL.** 2012. Orientation of Pseudomonas aeruginosa ExsA monomers bound to promoter DNA and base-specific contacts with the P exoT promoter. J. Bacteriol. **194:**2573-2585.

55. **Kjelleberg, S.** 1984. Starvation-Induced Effects on Bacterial Surface Characteristics. Appl Environ Microbiol. **48(3):**497–503.

56. **La Tourette Prosser, B, Taylor, D, Dix, BA, Cleeland, R.** 1987. Method of evaluating effects of antibiotics on bacterial biofilm. Antimicrobial Agents Chemother. **31:**1502-1506.

57. **Lagendijk, EL, Validov, S, Lamers, GEM, De Weert, S, Bloemberg, GV.** 2010. Genetic tools for tagging Gram-negative bacteria with mCherry for visualization in vitro and in natural habitats, biofilm and pathogenicity studies. FEMS Microbiol. Lett. **305:**81-90.

58. **Lenz, AP, Williamson, KS, Pitts, B, Stewart, PS, Franklin, MJ.** 2008. Localized gene expression in *Pseudomonas aeruginosa* biofilms. Appl. Environ. Microbiol. **74:**4463-4471.

59. **Levin, BR, Rozen, DE.** 2006. Non-inherited antibiotic resistance. Nature Reviews Microbiology. **4:**556-562.

60. **Li, X-, Nikaido, H.** 2004. Efflux-Mediated Drug Resistance in Bacteria. Drugs. **64:**159-204.

61. **Liu, X, Roe, F, Jesaitis, A, Lewandowski, Z.** 1998. Resistance of biofilms to the catalase inhibitor 3-amino-1,2,4-triazole. Biotechnol. Bioeng. **59:**156-162.

62. **Mah, T.** 2012. **B**iofilm-specific antibiotic resistance. Future Microbiology. **7(9):**1061.

63. **Mah, T-F, Kuznedelov, K, Mushegian, A, Severinov, K, Greenblatt, J.** 2000. The Î± subunit of E. coli RNA polymerase activates RNA binding by NusA. Genes and Development. **14:**2664-2675.

64. **Mah, T-F, Pitts, B, Pellock, B, Walker, GC, Stewart, PS, O'Toole, GA.** 2003. A genetic basis for P*seudomonas aeruginos*a biofilm antibiotic resistance. Nature. **426:**306-310.

65. **Mah, T-F, O'Toole, GA.** 2001. Mechanisms of biofilm resistance to antimicrobial agents. Trends Microbiol. **9:**34-39.

66. **Martin, RG, Rosner, JL.** 2001. The AraC transcriptional activators. Curr. Opin. Microbiol. **4:**132-137.

67. **Mcadams, HH, Arkin, A.** 1997. Stochastic mechanisms in gene expression. Proc. Natl. Acad. Sci. U. S. A. **94:**814-819.

68. **Merritt, JH, Brothers, KM, Kuchma, SL, O'Toole, GA.** 2007. SadC reciprocally influences biofilm formation and swarming motility via modulation of exopolysaccharide production and flagellar function. J. Bacteriol. **189:**8154-8164.

69. **Miroux, B, Walker, JE.** 1996. Over-production of proteins in Escherichia coli: Mutant hosts that allow synthesis of some membrane proteins and globular proteins at high levels. J. Mol. Biol. **260:**289-298.

70. **Mishra, M, Byrd, MS, Sergeant, S, Azad, AK, Parsek, MR, McPhail, L, Schlesinger, LS, Wozniak, DJ.** 2012. P*seudomonas aeruginosa* Psl polysaccharide reduces neutrophil phagocytosis and the oxidative response by limiting complement-mediated opsonization. Cell. Microbiol. **14:**95-106.

71. **Mulcahy, H, Charron-Mazenod, L, Lewenza, S.** 2008. Extracellular DNA chelates cations and induces antibiotic resistance in Pseudomonas aeruginosa biofilms. PLoS Pathogens. **4:**.

72. **Nickel, JC, Ruseska, I, Wright, JB, Costerton, JW.** 1985. Tobramycin resistance of *Pseudomonas aeruginosa* cells growing as a biofilm on urinary catheter material. Antimicrobial Agents Chemother. **27:**619-624.

73. **Nickel, JC, Wright, JB, Ruseska, I, Marrie, TJ, Whitfield, C, Costerton, JW.** 1985. Antibiotic resistance of P*seudomonas aeruginosa* colonizing a urinary catheter in vitro. Eur. J. Clin. Microbiol. **4:**213-218.

74. **Ogden, S, Haggerty, D, Stoner, CM.** 1980. The *Escherichia coli* L-arabinose operon: Binding sites of the regulatory proteins and a mechanism of positive and negative regulation. Proc. Natl. Acad. Sci. U. S. A. **77:**3346-3350.

75. **Oldenburg, KR, Vo, KT, Michaelis, S, Paddon, C.** 1997. Recombination-mediated PCR-directed plasmid construction in vivo in yeast. Nucleic Acids Res. **25:**451-452.

76. **O'Toole, G, Kaplan, HB, Kolter, R.** 2000. Biofilm formation as microbial development. Annual Review of Microbiology. **54:**49-79.

77. **O'Toole, GA, Kolter, R.** 1998. Initiation of biofilm formation in *Pseudomonas fluorescens* WCS365 proceeds via multiple, convergent signalling pathways: A genetic analysis. Mol. Microbiol. **28:**449-461.

78. **Pan, G, Aso, T, Greenblatt, J.** 1997. Interaction of elongation factors TFIIS and Elongin A with a human RNA polymerase II holoenzyme capable of promoter-specific initiation and responsive to transcriptional activators. J. Biol. Chem. **272:**24563-24571.

79. **Park, S-, Ko, BJ, Kim, B-.** 2005. Mass spectrometric screening of transcriptional regulators using DNA affinity capture assay. Anal. Biochem. **344:**152-154.

80. **Park, S-, Yang, Y-, Song, E, Kim, E-, Kim, WS, Sohng, JK, Lee, HC, Liou, KK, Kim, B-.** 2009. Mass spectrometric screening of transcriptional regulators involved in antibiotic biosynthesis in *streptomyces coelicolor* A3(2). Journal of Industrial Microbiology and Biotechnology. **36:**1073-1083.

81. **Phillips, TA, VanBogelen, RA, Neidhardt, FC.** 1984. Lon gene product of Escherichia coli is a heat-shock protein. J. Bacteriol. **159:**283-287.

82. **Pierscionek, B.** 1994. Refractive index of the human lens surface measured with an optic fibre sensor. Ophthalmic Res. **26(1):**32.

83. **Plano, GV.** 2004. Modulation of AraC family member activity by protein ligands. Mol. Microbiol. **54:**287-290.

84. **Plotnikova, JM, Rahme, LG, Ausubel, FM.** 2000. Pathogenesis of the human opportunistic pathogen *Pseudomonas aeruginosa* PA14 in Arabidopsis. Plant Physiol. **124:**1766-1774.

85. **Pollock, R, Treisman, R.** 1990. A sensitive method for the determination of protein-DNA binding specificities. Nucleic Acids Res. **18:**6197-6204.

86. **Ramsing, NB, Kuhl, M, Jorgensen, BB.** 1993. Distribution of sulfate-reducing bacteria, O2, and H2S in photosynthetic biofilms determined by oligonucleotide probes and microelectrodes. Appl. Environ. Microbiol. **59:**3840-3849.

87. **Records, AR, Gross, DC.** 2010. Sensor kinases RetS and LadS regulate Pseudomonas syringae Type VI secretion and virulence factors. J. Bacteriol. **192:**3584-3596.

88. **Remington, SJ.** 2006. Fluorescent proteins: maturation, photochemistry and photophysics. Curr. Opin. Struct. Biol. **16:**714-721.

89. **Rippe, K.** 1998. Analysis of protein-DNA binding at equilibrium. B. I. F Futura. **12:**20.

90. **Ross, W, Gosink, KK, Salomon, J, Igarashi, K, Zou, C, Ishihama, A, Severinov, K, Gourse, RL.** 1993. A third recognition element in bacterial promoters: DNA binding by the α subunit of RNA polymerase. Science. **262:**1407-1413.

91. **Sadovskaya, I, Vinogradov, E, Li, J, Hachani, A, Kowalska, K, Filloux, A.** 2010. High-level antibiotic resistance in *Pseudomonas aeruginos*a biofilm: the ndvB gene is involved in the production of highly glycerol-phosphorylated beta-(1->3)-glucans, which bind aminoglycosides. Glycobiology. **20:**895-904.

92. **Sambrook, J, Russel, D.** 2001. Calcium-chloride method to create competent cells-variation of Cohen et al 1972*In* Anonymous Molecular cloning: a laboratory manual. Vol. 2, 3rd ed., vol. 2. Cold Spring Harbor Laboratory Press, 2001.

93. **Sauer, K, Camper, AK, Ehrlich, GD, Costerton, JW, Davies, DG.** 2002. *Pseudomonas aeruginosa* displays multiple phenotypes during development as a biofilm. J. Bacteriol. **184:**1140-1154.

94. **Schuster, M, Lostroh, CP, Ogi, T, Greenberg, EP.** 2003. Identification, timing, and signal specificity of *Pseudomonas aeruginosa* quorum-controlled genes: A transcriptome analysis. J. Bacteriol. **185:**2066-2079.

95. **Shaner, NC, Campbell, RE, Steinbach, PA, Giepmans, BNG, Palmer, AE, Tsien, RY.** 2004. Improved monomeric red, orange and yellow fluorescent proteins derived from Discosoma sp. red fluorescent protein. Nat. Biotechnol. **22:**1567-1572.

96. **Shaner, NC, Steinbach, PA, Tsien, RY.** 2005. A guide to choosing fluorescent proteins. Nature Methods. **2:**905-909.

97. **Shanks, RMQ, Caiazza, NC, Hinsa, SM, Toutain, CM, O'Toole, GA.** 2006. Saccharomyces cerevisiae-based molecular tool kit for manipulation of genes from gram-negative bacteria. Appl. Environ. Microbiol. **72:**5027-5036.

98. **Shanks, RMQ, Kadouri, DE, MacEachran, DP, O'Toole, GA.** 2009. New yeast recombineering tools for bacteria. Plasmid. **62:**88-97. doi: DOI: 10.1016/j.plasmid.2009.05.002.

99. **Song, E, Yang, Y-, Lee, B-, Kim, E-, Kim, J-, Park, S-, Lee, K, Kim, W-, You, S, Hwang, D, Kim, B-.** 2010. An integrative approach for high-throughput screening and characterization of transcriptional regulators in Streptomyces coelicolor. Pure and Applied Chemistry. **82:**57-67.

100. **Southey-Pillig, CJ, Davies, DG, Sauer, K.** 2005. Characterization of temporal protein production in *Pseudomonas aeruginosa* biofilms. J. Bacteriol. **187:**8114-8126.

101. **Sternberg, C, Christensen, BB, Johansen, T, Nielsen, AT, Andersen, JB, Givskov, M, Molin, S.** 1999. Distribution of bacterial growth activity in flow-chamber biofilms. Appl. Environ. Microbiol. **65:**4108-4117.

102. **Stewart, P, Franklin, M.** 2008. Physiological hetereogeneity in biofilms. Nat. Rev. Microbiol. **6(3):**199.

103. **Stewart, PS.** 2003. Diffusion in biofilms. J. Bacteriol. **185:**1485-1491.

104. **Stoodley, P, Boyle, JD, Debeer, D, Lappin-Scott, HM.** 1999. Evolving perspectives of biofilm structure. Biofouling. **14:**75-90.

105. **Stover, CK, Pham, XQ, Erwin, AL, Mizoguchi, SD, Warrener, P, Hickey, MJ, Brinkman, FSL, Hufnagle, WO, Kowallk, DJ, Lagrou, M, Garber, RL, Goltry, L, Tolentino, E, Westbrock-Wadman, S, Yuan, Y, Brody, LL, Coulter, SN, Folger, KR, Kas, A, Larbig, K, Lim, R, Smith, K, Spencer, D, Wong, GK-, Wu, Z, Paulsen, IT, Relzer, J, Saler, MH, Hancock, REW, Lory, S, Olson, MV.** 2000. Complete genome sequence of *Pseudomonas aeruginosa* PAO1, an opportunistic pathogen. Nature. **406:**959-964.

106. **Struhl, K, Stinchcomb, DT, Scherer, S, Davis, RW.** 1979. High-frequency transformation of yeast: autonomous replication of hybrid DNA molecules. Proc. Natl. Acad. Sci. U. S. A. **76:**1035-1039.

107. **Studier, FW.** 1991. Use of bacteriophage T7 lysozyme to improve an inducible T7 expression system. J. Mol. Biol. **219:**37-44.

108. **Suh, S-, Silo-Suh, L, Woods, DE, Hassett, DJ, West, SEH, Ohman, DE.** 1999. Effect of rpoS mutation on the stress response and expression of virulence factors in *Pseudomonas aeruginosa*. J. Bacteriol. **181:**3890-3897.

109. **Sutherland, IW.** 2001. The biofilm matrix - An immobilized but dynamic microbial environment. Trends Microbiol. **9:**222-227.

110. **Tombolini, R, Unge, A, Davey, ME, De Bruijn, FJ, Jansson, JK.** 1997. Flow cytometric and microscopic analysis of GFP-tagged *Pseudomonas fluorescen*s bacteria. FEMS Microbiol. Ecol. **22:**17-28.

111. **Wagner, VE, Bushnell, D, Passador, L, Brooks, AI, Iglewski, BH.** 2003. Microarray analysis of P*seudomonas aeruginosa* quorum-sensing regulons: Effects of growth phase and environment. J. Bacteriol. **185:**2080-2095.

112. **Walters III, MC, Roe, F, Bugnicourt, A, Franklin, MJ, Stewart, PS.** 2003. Contributions of antibiotic penetration, oxygen limitation, and low metabolic activity to tolerance of

Pseudomonas aeruginosa biofilms to ciprofloxacin and tobramycin. Antimicrobial Agents Chemother. **47:**317-323.

113. **Webb, JS, Thompson, LS, James, S, Charlton, T, Tolker-Nielsen, T, Koch, B, Givskov, M, Kjelleberg, S.** 2003. Cell death in *Pseudomonas aeruginos*a biofilm development. J. Bacteriol. **185:**4585-4592.

114. **Westall, F, De Wit, MJ, Dann, J, Van der Gaast, S, De Ronde, CEJ, Gerneke, D.** 2001. Early archean fossil bacteria and biofilms in hydrothermally-influenced sediments from the Barberton greenstone belt, South Africa. Precambrian Res. **106:**93-116.

115. **Whitchurch, CB, Tolker-Nielsen, T, Ragas, PC, Mattick, JS.** 2002. Extracellular DNA required for bacterial biofilm formation. Science. **295:**1487.

116. **Whiteley, M, Lee, KM, Greenberg, EP.** 1999. Identification of genes controlled by quorum sensing in *Pseudomonas aeruginosa*. Proc. Natl. Acad. Sci. U. S. A. **96:**13904-13909.

117. **Willey, JM, Sherwood, L, Woolverton, CJ, Prescott, LM, Willey, JM.** 2011. Prescott's microbiology. McGraw-Hill, New York.

118. **Winsor, GL, Lam, DKW, Fleming, L, Lo, R, Whiteside, MD, Yu, NY, Hancock, REW, Brinkman, FSL.** 2011. Pseudomonas Genome Database: Improved comparative analysis and population genomics capability fo*r Pseudomonas* genomes. Nucleic Acids Res. **39:**D596-D600.

119. **Winsor, GL, Lo, R, Ho Sui, SJ, Ung, KSE, Huang, S, Cheng, D, Ching, W-H, Hancock, REW, Brinkman, FSL.** 2005. *Pseudomonas aeruginosa* Genome Database and PseudoCAP: Facilitating community-based, continually updated, genome annotation. Nucleic Acids Res. **33:**D338-D343.

120. **Winsor, GL, Van Rossum, T, Lo, R, Khaira, B, Whiteside, MD, Hancock, REW, Brinkman, FSL.** 2009. *Pseudomona*s Genome Database: Facilitating user-friendly, comprehensive comparisons of microbial genomes. Nucleic Acids Res. **37:**D483-D488.

121. **Wu, KK.** 2006. Analysis of protein-DNA binding by streptavidin-agarose pulldown. Methods Mol. Biol. **338:**281-290.

122. **Xu, KD, Stewart, PS, Xia, F, Huang, C-, McFeters, GA.** 1998. Spatial physiological heterogeneity in *Pseudomonas aeruginosa* biofilm is determined by oxygen availability. Appl. Environ. Microbiol. **64:**4035-4039.

123. **Yahr, TL, Wolfgang, MC.** 2006. Transcriptional regulation of the *Pseudomonas aeruginosa* type III secretion system. Mol. Microbiol. **62:**631-640.

124. **Yaneva, M, Tempst, P.** 2003. Affinity Capture of Specific DNA-Binding Proteins for Mass Spectrometric Identification. Anal. Chem. **75:**6437-6448.

125. **Zhang, L, Fritsch, M, Hammond, L, Landreville, R, Mah, TF.** 2013. Identification of genes involved in *Pseudomonas aeruginosa* biofilm-specific antibiotic resistance. Proc. Natl. Acad. Sci. U. S. A. . doi: 10.1371/journal.pone.0061625.

126. **Zhang, L, Hinz, AJ, Nadeau, J-, Mah, T-.** 2011*. Pseudomonas aeruginosa t*ssC1 links type VI secretion and biofilm-specific antibiotic resistance. J. Bacteriol. **193:**5510-5513.

127. **Zhang, L, Mah, TF.** 2008. Involvement of a novel efflux system in biofilm-specific resistance to antibiotics. J. Bacteriol. **190:**4447-4452. doi: 10.1128/JB.01655-07.

128. **Zhang, X, Studier, FW.** 1997. Mechanism of inhibition of bacteriophage T7 RNA polymerase by T7 lysozyme. J. Mol. Biol. **269:**10-27.

CONTRIBUTION OF COLLABORATORS

- pSC01 (*ndvB*p-GFP) was created by Sarah Copeland (former technician in the lab). Sarah cloned the promoter region of *ndvB* in front of GFP to create the promoter-fluorescent protein construct that was used in this thesis.
- The 22bp motif was discovered by Sine Svenningsen (former post-doctoral fellow in the lab) using MEME.
- The western blot (Figure 28) was performed in the Trinkle-Mulchay lab (CMM) using their equipment and supplies. The experiment was performed jointly by me and Delphine Chamousset (technician, CMM).